Coordinate System Dependence of Muscle Forces Predicted using
Optimization Methods in Musculoskeletal Joints

by

Janine E. Pierce

B.S. Mechanical Engineering
University of California, Berkeley (2002)

Submitted to the Department of Mechanical Engineering in Partial Fulfillment of the
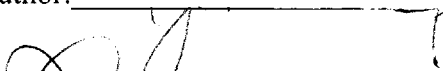Requirements for the Degree of

Master of Science in Mechanical Engineering
at the
Massachusetts Institute of Technology

June 2004

Signature of Author:_____

Department of Mechanical Engineering
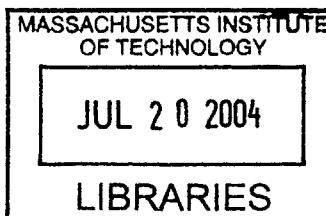May 7, 2004

Certified by:_

Guoan Li
Lecturer, Department of Mechanical Engineering, MIT
Assistant Professor of Orthopaedic Surgery, Harvard Medical School
Thesis Supervisor

Certified by:_____

Derek Rowell
Professor of Mechanical Engineering
Thesis Supervisor

Accepted by:__

Ain A. Sonin
Chairman, Department Committee on Graduate Students

Coordinate System Dependence of Muscle Forces Predicted using
Optimization Methods in Musculoskeletal Joints

by

Janine E. Pierce

ABSTRACT

Optimization methods are widely used to predict in-vivo muscle forces in musculoskeletal joints. Moment equilibrium at the joint center (usually defined as the origin of the joint coordinate system) has been used as a constraint condition for optimization procedures and the joint reaction moments were assumed to be zero. This research project, through the use of a three-dimensional elbow model, investigated the effect of joint center location on muscle forces predicted using a nonlinear static optimization method. The results demonstrated that moving the joint center medially and laterally along the flexion-extension axis caused dramatic variations in the predicted muscle forces. For example, moving the joint center from a position 5 mm medial to 5 mm lateral of the geometric elbow center caused the predicted biceps force to vary from 12% to 46% and the brachialis force to vary from 80% to 34% of the total muscle loading. The joint reaction force reduced by 24% with this medial to lateral variation of the joint center location. This data revealed that the muscle forces predicted using optimization methods are sensitive to the joint center location due to the zero joint reaction moment assumption in the moment constraint condition. For accurate prediction of muscle load distributions using optimization methods, it is necessary to determine the true joint center location where the condition of a zero joint reaction moment is satisfied. Furthermore, improvements to the current optimization methodology were suggested. Incorporation of the 3D joint center location, as three unknown variables, into the optimization program was proposed, and this procedure was investigated for a pilot case incorporating one of the joint center components (y-axis variable) into the optimization. This thesis work indicates that all previously published data on muscle and joint loads predicted via optimization methods should be revisited since the joint reaction moment was eliminated in those works.

Thesis Supervisor: Guoan Li
Title: Lecturer

Thesis Supervisor: Derek Rowell
Title: Professor of Mechanical Engineering

Acknowledgements

Table of Contents

9

List of Figures

11

12

List of Tables

13

Chapter 1: Introduction

Engineers are the innovators and designers of complex machines and those machines are designed with specific engineering principles and analytical tools in mind. However, the musculoskeletal system of the human body is a complicated apparatus more involved and complex than any man-made machine one could possibly fathom. Consequently, in order to study the mechanical behavior of the human body, the bones, muscles, tendons, ligaments, and other structures must be reduced to a less complex system comprised of rigid links, actuators, and constraint elements. The elements of the system need to be clearly defined in mechanical terms, the external constraints on the system must also be identified, and the laws of motion can then be applied. Thus, the methods of rigid body mechanics can be applied to study the function of the human body only after the system is simplified and the model elements and their complexities are clearly defined.

1.1 Human Joint Models

The measurement of in-vivo muscle and joint reaction forces poses a distinct challenge in biomedical engineering. To address this issue, numerous mathematical models have been broadly adapted to calculate the response of muscles and musculoskeletal joints to external loads [1-41]. Various biomechanical models of human joints have been developed which constrained joint motion to a single plane, usually the sagittal or "flexion" plane [30, 34, 42-44], without evaluating the appropriateness or estimating the associated error of such an assumption. Many three-dimensional studies partially reduced the force distribution problem to the quasi-planar case by defining many or all of the joints as hinge, or one degree of freedom, joints [10, 12, 17, 29]. This hinge assumption caused two of the moment constraints to be removed before the force computation was performed. Movement away from simple planar or quasi-planar models of human joints occurred in the early 90's with studies initiated by Kaufman et al. [21, 23] concerning the knee joint, followed by Glitsch and Baumann's [15] three-dimensional analysis of the lower extremity. In the paragraphs to follow, some of the major contributions to the field of joint modeling using inverse optimization methods are briefly summarized (Figure 1-1).
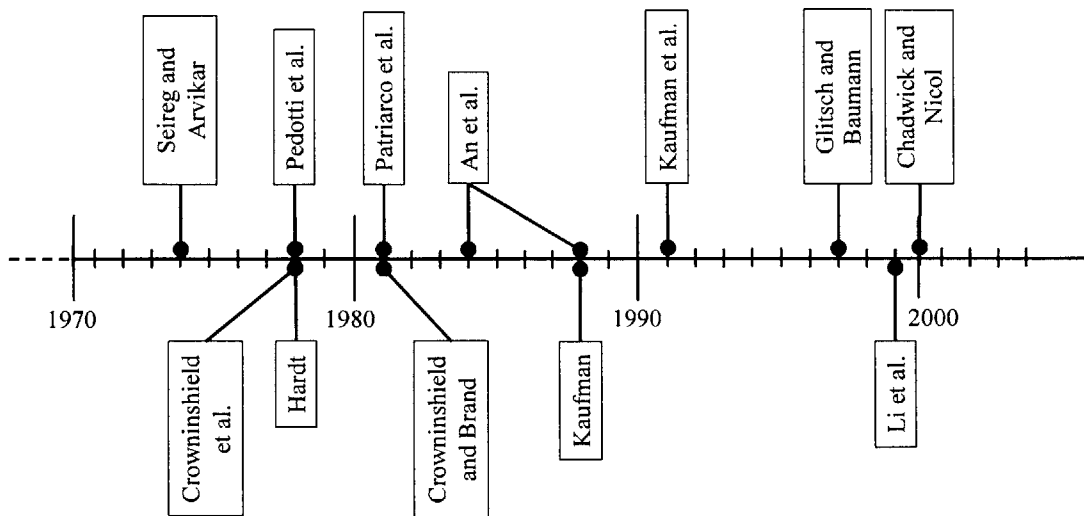
Figure 1-1. Timeline illustrating some of the major researcher papers published on joint optimization methods in the past three decades.

Seireg and Arvikar (1973, 1975) were quite possibly the first investigators to develop a mathematical model that simulated the muscular action of the lower extremity without previously defining the active muscles and the forces they produce (or their respective force ratios) for the modeled activity (i.e. the model "chose" which muscles to activate and the force ratios to assign, not the investigator). They established a model of the lower extremity to evaluate muscle and joint reaction forces during specific static postures, including standing, leaning, and stooping [35], as well as during dynamic movements such as walking [36]. The model segmented the lower extremity into five rigid bodies: the pelvis, femur, tibia, fibula, and foot. A total of 29 muscles were considered in the analysis of these various movements. Since all activities were assumed to occur symmetrical with respect to the sagittal plane, the equilibrium of the pelvis was two-dimensional, thus requiring only three equilibrium equations (two force and one moment equation). The other three segments, however, were not restricted to sagittal plane movement, and thus were described by six equilibrium equations each (3 force and 3 moment equations), respectively. A total of 21 equilibrium equations, 29 unknown muscle forces, as well as the unknown joint reaction forces and moments, made for an indeterminate problem. Using different linear optimization criteria, including minimization of muscular force and minimization of joint moment, and a simplex algorithm, the muscle and joint reaction forces for various activities were determined.

16

Pedotti et al. (1978) used a three link model of the lower extremity to investigate several different optimization criteria and the correlation of their force predictions with muscle EMG data [30]. Eleven muscles were used to simulate the gait motion, joint torques were computed from experimentally measured ground reaction forces and kinematic variables, and the model was restricted to an analysis of motion and forces in the sagittal plane. Analysis of four optimization criteria, all involving some form of total muscle force minimization, and comparison with recorded EGM data yielded the square of the (actual force)/(maximal force) for all muscles as the optimal performance criterion.

Hardt (1978) developed a model of the lower extremity, representing the hip and ankle as perfect ball joints and the knee as a simple hinge [17]. Thirty-one muscle forces were used in this 7 degree-of-freedom model. The linear minimization of muscle force criterion was used to solve for the unknown variables. The problem formulation involved 7 equality and no inequality constraints, leading to the prediction of only 7 active muscles for each time step analyzed. Hardt concluded that the linear penalty function employed was 'unnecessarily restrictive and leads to function definitions that are empirical in nature and may not have any physiological analog.' The proper solution to the optimization problem must therefore require more input regarding the physiology of the system and be viewed as an analogy to the physical system rather than purely a convenient mathematical methodology.

Crowninshield et al. (1978) developed an optimization model to investigate the mechanical environment of the human hip, i.e. the muscle and joint contact forces, during activities of daily living. The pelvis and lower extremity were modeled as four rigid segments: the pelvis, thigh, shank, and foot-shoe segment. These segments were assumed to be connected by smooth but loose ball-and-socket joints representing the hip, knee, and ankle, respectively. Twenty-seven muscles were identified as potential load-carrying structures at the hip during the daily activities simulated in the model. The knee and ankle were restricted to pure flexion-extensions motions, or sagittal plane motion, and modeled only for the sake of distributing the resultant forces at the hip. A linear objective function minimizing muscle stress was used to solve for the 27 muscles.

17

In 1981, Crowninshield and Brand defined what is currently the "gold standard" for objective functions used in joint optimization analyses, defining a new optimization criterion from the inversely-nonlinear relationship between muscle contraction force and endurance levels [12]. Crowninshield and Brand used this nonlinear optimization criterion to predict muscle forces in 1, the elbow during isometric contraction, and 2, the lower extremity (hip, knee, and ankle) during locomotion. For the elbow joint example, a simple planar model was employed requiring three of the elbow flexors (biceps, brachialis, and brachioradialis) to generate a fixed 10 N.m resultant moment. The lower extremity model was composed of 47 muscle elements, which were required to generate three orthogonal components of intersegmental moment at the hip and one component (flexion-extension) at the knee and ankle, respectively.

Hatze (1981) developed a mathematical model to simulate the motions of a 17-segment hominoid, or anthropomorphic mathematico-geometrical model of the segmented human body, under the influence of 46 muscles [18].

Based on a model of the lower extremity originally developed by Hardt [17], Patriarco et al. (1981) studied the reliability of data acquisition and optimization procedures used to predicted muscle forces during gait [29]. The lower extremity was modeled as a system of rigid links with the muscles regarded as torque generators. The seven measured joint torques, determined from kinematic studies, were used to loosely constrain the solution space when solving for the 31 muscles of the model. These torques corresponded to three degrees of freedom at the hip and ankle, and only one degree of freedom at the knee. Two optimization criteria were investigated, including total muscle force and the mechanico-chemical energy output of the muscles.

An et al. (1984) sought to establish a new optimization approach to study the indeterminate joint problem [3]. The elbow joint was studied in quasi-2D in order to illustrate this approach. This model was formulated with nine muscles, which included the biceps brachii, brachialis, brachioradialis, pronator teres, supinator, triceps brachii, flexor carpi radialis, extensor carpi ulnaris, and extensor carpi radialis longus. Only two equilibrium equations, balancing the flexion-extension moment and the pronation-supination moment, were used to solve for the nine unknown muscle forces. An et al. presented another model of the elbow in a 1989 publication,

18

and this time assumed that the exerted torque at the elbow was primarily due to three muscles: the biceps brachii, brachialis, and brachioradialis [45]. The contributions of other forearm muscles were assumed insignificant, based on cross-sectional area or moment arm data, and were ignored. The muscle forces were predicted using a linear optimization method which sought to minimize muscle activation. The 3D force and moment equilibrium equations, as well as a modified tension-length relationship equation, constrained the solution.

K. Kaufman completed a Ph.D. dissertation (1988) on the development of a mathematical model of muscle and joint forces in the knee during isokinetic exercise [20]. Subsequently, Kaufman published a number of articles with colleagues in 1991 on the topic of joint modeling [21-23]. These articles outlined the formulation of a physiological model for predicting muscle forces using optimization to resolve the indeterminacy, and reported the predictions of knee joint forces during isokinetic exercise. The lower extremity was modeled as four rigid body segments: the pelvis, thigh, shank, and foot, but the foot was assumed to move with the shank as one integrated body. Muscular activation was chosen as the optimal criteria for force prediction.

Glitsch and Baumann (1997) set out to tackle the problem of three-dimensional internal load determination in the lower extremity [15]. Inverse dynamic and static optimization techniques, using a squared muscle stress criterion, were applied to a 3D model of lower limb containing 47 muscles. The load bearing capabilities of various joint types (hinge, spherical, and intermediate joints) were tested for the knee and ankle, resulting in the conclusion that even during seemingly planar movements like walking, significant three-dimensional intersegmental moments were produced. This study claimed up to a 60% underestimation of loads predicted using 2D methods, and addressed the inappropriateness of modeling the knee and ankle as hinges.

Li et al. (1999) used an inverse dynamic optimization model to predict antagonistic muscle and joint reaction forces in the knee during isokinetic flexion and extension [26]. A total of ten muscles were used to simulate knee joint motion, which included flexion/extension, varus/valgus, and internal/external rotations. Four optimization criteria were implemented and all four predicted antagonistic muscle contraction. The results suggested that the kinematic

information involved in the inverse dynamic optimization was more crucial to the prediction of the antagonistic muscle forces than the selected optimization criterion.

Chadwick and Nicol (2000) developed a 3D model of the elbow and wrist joints comprised of 15 muscle, 3 ligament, and 4 joint forces [9]. External moments were experimentally determined with a newly developed strain gauge transducer, and these moments were assumed to be balanced by the internally generated joint moment, thereby yielding an indeterminate set of equations. A dual-stage linear programming approach was implemented to first minimize the sum of the muscle stresses and then minimize the sum of the joint and ligament forces. Four different grip positions were studied and the corresponding joint forces were determined.

1.2 Newton's Laws and Rigid Body Motion

Estimating the internal forces in the musculoskeletal system in response to any external loads requires the use of engineering mechanics, as governed by the laws of motion. The laws of motion for rigid bodies are derived from Newton's 1st, 2nd, and 3rd laws.

> Newton's 1st Law: When the sum of the forces acting on a particle is zero, its velocity is constant. In particular, if the particle is initially stationary, it will remain stationary.
>
> Newton's 2nd Law: When the sum of the forces acting on a particle is not zero, the sum of the forces is equal to the rate of change of the linear momentum of the particle. If the mass is constant, the sum of the forces is equal to the product of the mass of the particle and its acceleration.
>
> Newton's 3rd Law: The forces exerted by two particles on each other are equal in magnitude and opposite in direction [46].

The derivation of the rigid body motion equations can be found in Appendix A. The second law is probably most recognized in the form of the rigid body equilibrium equation,

$$\Sigma \vec{F} = m\vec{a}, \qquad (1\text{-}1)$$

where m is the mass of the body and a is its linear acceleration. This is probably the most utilized equation in the study of motion analysis, and is applicable when the mass is constant. Additionally, under any planar motion the total moment about the center of mass is denoted by

$$\Sigma M = I\alpha, \qquad (1\text{-}2)$$

20

where I is the mass moment of inertia about the center of mass and α is the angular acceleration. Additionally, if the rigid body rotates about a fixed axis O, the sum of the moments about O relates to the angular acceleration and moment of inertia about O by

$$\Sigma M_O = I_O \alpha \,. \tag{1-3}$$

However, in the absence of motion, the equations reduce to the simplified form:

$$\begin{aligned} \Sigma \vec{F} &= 0 \\ \Sigma \vec{M} &= 0 \end{aligned} \tag{1-4}$$

These two vector equations represent 4 scalar equations for the two-dimensional case and 6 scalar equations when considering the three-dimensional case. A simple example for the two-dimensional planar case can be seen in Appendix B.

1.3 Static Analysis of a Joint

At any flexion angle or position of the joint, the external force system (including applied moments and forces, and the weight of the limb) was balanced by the internal force system (including muscle forces, joint reaction forces and moments). The joint reaction force, illustrated in Figure 5-2b for the elbow joint, is comprised of the remaining internal forces (excluding muscle forces) which may include joint articular contact, ligamentous, capsular, and passive soft tissue deformation forces. Utilizing the simplified laws of motion for static analyses (Equation 1-4) and a free-body diagram of the joint (see Figure 5-1 for the elbow joint), the following force and moment equilibrium equations were obtained for the static joint analysis:

$$\begin{cases} (a) \quad \displaystyle\sum_{i=1}^{N} f_i^M \vec{e}_i + \vec{F}^{\text{Joint}} = \vec{F}^{\text{int}} \\[4mm] (b) \quad \displaystyle\sum_{i=1}^{N} f_i^M \left(\vec{r}_i \times \vec{e}_i \right) + \vec{M}^{\text{Joint}} = \vec{M}^{\text{int}} \end{cases} \,, \tag{1-5}$$

where f_i^M is the magnitude and $\vec{e}_i$ is the direction of the i-th muscle force; $\vec{r}_i$ is the vector pointing from the joint center to the insertion centroid of i-th muscle; $\vec{F}^{Joint}$ and $\vec{M}^{Joint}$ are the joint reaction forces and moments; and $\vec{F}^{\text{int}}$ and $\vec{M}^{\text{int}}$ are the intersegmental forces and moments due to the external force system. The 6 equilibrium equations shown above (i.e. a force and a

moment equation for each of the three dimensions) contain N muscle force magnitudes, 3 components of the joint reaction force, and 3 components of the joint reaction moment. This represents a statically indeterminate system. Thus, human joints are very complex indeterminate systems whose muscle and joint forces cannot be solved for directly and must instead be predicted using inverse optimization methods.

1.4 Inverse Optimization Methods

Optimization is a mathematical method by which an indeterminate system of equations is iteratively solved by maximizing or minimizing an objective function, often subjected to various constraints [3, 5, 9, 15, 23, 26, 30, 35, 36]. Thus, an optimization problem can be thought of as containing three major components:

1. An objective function which is either maximized or minimized.

2. A set of unknowns or variables which affect the value of the objective function.

3. A set of constraints that allow the unknowns to take on certain values but exclude others.

A human musculoskeletal joint (e.g., elbow, knee, etc.) is an indeterminate biomechanical system in nature. The number of unknown forces generated by each muscle, as well as the unknown joint reaction force and moment components, outnumber the equilibrium equations of the joint system [23]. A unique solution for these forces cannot be obtained directly and must instead be estimated through the use of optimization techniques.

1.4.1 Objective Functions

Optimization, as stated above, necessitates the definition of an objective or cost function for the purpose of mathematically finding its minima or maxima. This objective function is comprised of unknowns that are of interest to the problem at hand and, in the case of human joint function, this usually constitutes variables physiologic in nature.

1.4.1.1 Physiological Relevance

Studying energy expenditure and its minimization has long dominated research in the scientific and engineering disciplines. Muscular activity, not unlike a mechanical system, is also associated with energy expenditure in such forms as mechanical, chemical, and heat. For over a century, researchers have hypothesized that the body functions in such a way as to minimize the

22

amount of energy spent [47, 48]. Weber and Weber (1836) proposed that humans walk in a manner that requires the smallest amount of energy expenditure. Thus, the idea that the body moves in an efficient or optimal manner was popular long before optimization approaches were first utilized to estimate in-vivo muscle loads in the field of biomechanics. The introduction of optimization to study such physiologic parameters as muscle loads led to the investigation of potentially "physiologically relevant" objective functions which would ultimately minimize energy expenditure. Fittingly, MacConaill (1967) suggested that "no more total muscle force is used than is both necessary and sufficient for the task to be performed, whether this be one of supporting some weight or carrying out a movement, resistance to which may vary from zero upwards [49]."

Many of the objective functions used in the joint modeling literature were chosen because they made the most sense physiologically. The human body, just like any mechanical system, wants to maximize its performance while minimizing the forces or stresses on its components. Therefore, minimizing force, stress, and energy were deemed to be excellent objective functions for such an optimization since it would be tough on the body if it used more energy than it needed, given the number of cycles its joints are subjected to on a daily basis.

1.4.1.2 Common Examples

All optimization procedures operate under the assumption that the body selects muscles for a certain activity according to some criterion, usually seeking to minimize some "objective function" or "cost function", with muscle activity predictions often varying greatly depending on the choice of criteria. Some popular objective functions are discussed below and include the minimization of such parameters as the total muscular force, squared muscular force, muscle stress, squared or cubic muscle stress, ligament force, contact force, or instantaneous muscle power [43].

• Muscle Stress

Crowninshield and Brand [12] proposed the minimization of maximum stress in the active muscles as a physiological criterion to minimize muscle fatigue. More specifically, they recommended minimization of the total cubic muscle stress, and this particular objective function has been applied by many authors in the study of knee muscle forces during various in-

vivo functional activities, among other applications. Glitsch and Baumann used a squared muscle stress criterion for the determination of three-dimensional internal loads in the lower extremity [15]. The persistence of muscle stress as a popular cost function is illustrated by its recent appearance in a 2003 article by Oizumi et al. [28], in which the sum of the squared muscle force divided by the muscle cross-sectional area was used to perform a numerical analysis of cooperative abduction muscle forces in a human glenohumeral joint.

• Muscle Force

The minimization of the total muscle force criterion, implemented by MacConnaill (1967) in a study of knee joint equilibrium forces, assumed that the summation of the magnitude of individual muscle forces should be minimized in order to ensure dynamic equilibrium of the joint [49]. Seireg and Arvikar (1975) used a criterion which represented a weighted combination of two objectives: 1, minimizing the total sum of all muscle forces, and 2, minimizing the forces in the joint ligaments assumed to carry the unbalanced joint moments. The criterion consisted of the sum of the muscle forces plus four times the sum of the moments at all the joints [36].

Three decades after the introduction of the muscle force criterion my MacConnaill [49], Happee (1994) implemented a weighted sum of the squared muscle forces criterion, using inverse dynamic optimization to study goal directed movements [50].

Total muscle force and total squared muscle force [30, 49] both minimize the overall effort (muscular force) required for an activity. The squared force, however, has been shown to greatly penalize large individual muscle forces [30].

• Joint Reaction Force or Moment

In a 1973 study modeling the lower extremity, Seireg and Arvikar tested a number of possible optimization criteria, one being minimization of the sum of the three vertical reactions at the ankle, knee, and hip joints, respectively [35]. The joint moment criterion minimizes the total moment generated by all muscles with respect to the joint center, as used by Seireg and Arvikar [36] for the center of the knee joint.

• Muscular Activation

24

The muscular activation criterion minimizes the upper bound value of the overall activation of all muscles. Activation refers to both the number of active units (recruitment) and their degree of activity (firing frequency) [45]. Kaufman et al. (1991) put forth muscular activation as the optimal cost function for determining loads at the knee joint [21, 23]. This is similar to the criteria minimizing muscular stress (or maximizing endurance time) outlined by Crowninshield and Brand [12], which sought to minimize muscular fatigue.

• Mechanico-chemical energy output [29]

Hardt (1978) hypothesized that forces are distributed among muscles during activities, such as walking, by minimizing energy consumption [51]. Calculation of this muscle energy consumption was achieved through the development of a thermodynamic model relating input chemical energy to output mechanical power. This thermodynamic model took into account the chemico-mechanical dynamics of the energy transfers occurring in muscles. However, it was specified that this model, and thus this objective function, was only valid for low frequency activities in the same range as walking.

1.4.1.3 Linear verses Nonlinear

In order to predict co-activation between synergistic muscles, and achieve more accurate muscle force predictions in general, researchers have migrated away from linear cost functions. Linear optimization techniques have seemingly been used more out of mathematical convenience than to achieve physiologic accuracy in muscle load predictions. The primary characteristic of linear objective functions is to minimize the number of loaded structures whereas nonlinear objective functions tend to distribute the load among all the structures involved.

• Linear

One very attractive feature of the linear objective function, which may explain the persistence of linear objective functions in the joint modeling literature, is that it can be minimized, and the unknowns solved for, via a linear programming method. This is much easier to implement and code than a nonlinear scheme, giving rise to its popularity. An example of one such popular and easy to use linear objective function is the minimization of the total muscle forces [6, 11, 44]:

$$\text{Minimize} \quad J = \sum_{i=1}^{N} f_i \ . \tag{1-6}$$

As stated previously, linear objective functions often tend to minimize the number of loaded structures. This means that when using a linear objective function to solve for muscle forces, it will generally give the result that only one muscle force is active at a time (setting other muscle forces to zero) to achieve its minimum value. This is contrary to experimental results, such as electromyographic (EMG) analyses, which show generally more than one muscle active across a joint during a given activity. To try to combat this drawback of the linear objective function, additional constraints in the form of muscle force or stress limitations have been imposed to better define the solution space.

Barbenel (1972) challenged the principle of total muscle force while studying the temporomandibular joint [7]. Using linear programming to minimize the total muscular force, only the masseter muscle was predicted to be active during biting. EMG analysis and muscle palpation during biting showed, at minimum, the masseter, internal pterygoid, and temporal muscles were active. Likewise, Yeo et al. (1976) attempted to use the total muscle force objective function to predict muscle forces during elbow flexion [44]. The brachioradialis was predicted to be the primary flexor, with the biceps and brachialis only being activated if the brachioradialis was stimulated to saturation. EMG data, conducted by Basmajian and Latif (1957) contradicted such predictions [52], leading Yeo et al. to conclude that this objective function was insufficient for determining in-vivo muscle loads [44].

Seireg and Arvikar (1973, 1975) applied linear optimization criteria to a model of quasi-static locomotion and predicted very few simultaneously active muscles and unrealistically low joint contact forces during gait [35, 36]. This is an inherent problem in linear optimization and is related to the fact that the solution usually resides in the corner of the solution space, thereby predicting very few muscles to be active.

Hardt (1978) found that the number of predicted muscles for an activity simulated using linear optimization was limited to the total number of constraints placed on the optimization [17]. This inadequacy in force predictions clearly has no physiological significance and is purely a limitation of the optimization procedure itself.

26

An et al. (1984) experimented with different objective functions for calculating muscle forces across the elbow joint [3]. The summation of the muscle force and the summation of the muscle stress, both linear objective functions, predicted only one muscle to carry force in each solution. When minimizing the sum of the forces, the muscle with the largest moment arm was selected in the solution. Contrastingly, when minimizing the muscle stresses as the linear criterion, the muscle with the largest physiological cross-sectional area was selected in the solution. Practically speaking, this means that the optimization algorithm recruited the muscle with the largest PCSA until it reached its maximum force, and then, if necessary, it recruited the muscle with the next largest PCSA.

Advances in linear optimization have been made to try to address this problem. Efforts have been made to use weighted, linear combinations of muscle and joint forces as new criteria, but agreement of the force predictions with EMG experiments has not been desirable [3]. Bean et al. (1988) developed a double linear programming approach that simultaneously minimized two different objective functions, one being the minimization of muscle intensity (stress) and the other minimizing the sum of the muscle forces [53]. Through this method, it was demonstrated that co-activation predictions are possible with linear programming; however, results were not compared with EMG data. Kaufman et al. (1991) avoided the typical muscle and joint force criteria and used muscle activation as a cost function to predict muscle forces in the knee joint [23]. He concluded that properly constrained linear programming methods do not limit the number of active muscles and allow for uniform recruitment of the active muscles.

• Nonlinear

Unlike linear objective functions, nonlinear cost functions tend to distribute the load among all involved structures. In an effort to find a physiologically relevant objective function, Gracovetsky et al. (1977) minimized the sum of the squared shear forces in vertebral discs under the assumption that this parameter was related to human performance and injury prevention [54]. Likewise, Pedotti et al. (1978) used a number of objective functions, including the total squared muscle stress, to solve for muscle forces in walking under the hypothesis that such objective functions minimized energy during locomotive tasks. In 1981, Crowninshield and Brand [12] incorporated a physiological argument, supported by a quantitative force-endurance relationship

[55], into a nonlinear objective function by proposing the following objective function (Equation 1-7) to minimize the sum of the muscle stresses, raised to nth power:

$$\text{Minimize } J = \sum_{i=1}^{N} \left(\frac{f_i}{A_i} \right)^n .$$

(1-7)

This objective function was based on the idea that muscle fatigue must be related to the physiologic stress in the muscle. It can be solved by linear, quadratic, or nonlinear programming depending on choice of n. Crowninshield and Brand [12] recommended the choice of $n = 3$ since the amount of time a muscle can sustain activity is inversely proportional to the muscle stress raised to the power of three [55]. This seems to make physiological sense due to the fact that relatively high muscle stress can only be sustained for short periods of time whereas lower muscle stresses can be sustained for much longer time periods. Thus, in an objective or cost function sense, high muscle stresses are costly and should be avoided.

1.4.2 Constraints

Optimization is a mathematical method of minimizing an objective function subjected to various constraints. The typical constraints used to limit the solutions obtained from a joint optimization problem can be seen below:

$$
\begin{cases}
(a) & \sum_{i=1}^{N} f_i^M \vec{e}_i + \vec{F}^{Jo\,int} = \vec{F}^{int} \\
(b) & \sum_{i=1}^{N} f_i^M \left(\vec{r}_i \times \vec{e}_i \right) = \vec{M}^{int} \\
(c) & 0 \le f_i^M \le \sigma \cdot A_i
\end{cases}
$$

(1-8)

The first constraint (a) is easily recognized as the force equilibrium equation, requiring that the muscle forces, joint reaction forces, and intersegmental forces must balance each other in all three directions. The moment equilibrium about the selected joint center (b) must also be satisfied [21, 23, 25, 26]. This constraint requires that the moments about the joint center, induced internally by muscle forces and externally by applied loads, sum to zero in all three directions, with the assumption of no joint reaction moment [15, 25, 26, 32]. The third constraint (c) requires that the muscle forces be positive, or non-compressive, since physiologically-

28

speaking muscles can only exert a tensile force. Additionally, the force values were further constrained with a condition limiting the upper bound on muscle force to a maximum isometric force value, obtained by multiplying the individual muscle physiological cross-sectional area (A_i) by a constant maximum physiological muscle stress value (σ) [9, 10, 23, 30, 45, 56].

Historically, additional constraints to try to redistribute the loads between functionally similar muscles have also been imposed. Similar to the constraint described above, Patriarco et al. (1981) tried to encourage simultaneous muscle activations in a lower extremity model by imposing stress limits on muscles which forced synergistic action if a muscle exceeded its stress limit [29]. These bounds, however, were defined by the velocity and length dependence of stress limits, as determined from Hill's (1953) muscle model [57]. A second technique employed by Patriarco et al. (1981) to encourage synergistic action during gait constrained similar muscles to share load in proportion to their cross-sectional areas [29]. This was based on the physiological assumption that anatomically distinct muscles with very similar moment arms are functionally interchangeable during gait and, although unproven, this assumption was suggested after observing the close correlation of their EMG data.

1.5 Other Methods for Muscle Load Determination

There are many methods that have been developed to solve for in-vivo muscle loads without the use of a mathematical system of equations, or by reducing an initially indeterminate system to one that is determinate through simplification.

1.5.1 Force Reduction Method

If optimization methods are not employed to solve the indeterminate system which describes a complex joint, researchers tend to simplify the system to include only as many unknowns as they have equations [58-60]. Muscles are either grouped together, deemed insignificant, or altogether ignored. When considering a single joint, if the joint reaction force is considered an unknown variable (with 3 components for the 3D case), then only 3 additional unknown variables can be determined from the equilibrium equations (Equation 1-5). This corresponds to 3 muscle force magnitudes if the muscle lines of action are known. The simplest means of reducing the number of muscles is to set enough individual forces to zero until the number of unknowns matches the number of equations. This can include identifying and using only the most dominant muscles for

29

that activity, or grouping multiple muscles which insert at a single point (e.g. the quadriceps insertion on the patella) together as one resultant force. Muscles are often combined into groups on the basis of synchronous EMG activity for a certain action [61]. Also, muscles become good contenders for being set to zero if they lack significant EMG activity for the specified action. This force reduction method of eliminating/combining variables to reduce the number of unknown muscle forces around a joint in a distribution problem results in the loss of information about the function of individual muscles [37, 60], thereby making it a highly undesirable approach.

1.5.2 Muscle Scaling Approach

Another alternative method for solving the indeterminate system is to eliminate the indeterminacy by introducing additional equations based on the equal stress hypothesis for groups of co-operating muscles. This hypothesis states that, in a strenuous situation, muscles which are co-operating in a group (such as the flexors of the forearm) are likely to have their fibers similarly stressed as their maximum strength is approached [2]. Thus, the forces, F_i, of the different muscles contributing to the activity being modeled can be estimated by assuming each muscle acts at the same stress level, denoted by σ, where $\sigma = F_i / A_i$ for each individual muscle i with physiological cross-sectional area A_i. Using this method, without the use of optimization, Amis et al.[2] predicted the loading of individual flexor muscles at equilibrium from a known external force.

1.5.3 Cross-Sectional Area and EMG Estimations

It is also common to apportion muscle loading in accordance with muscular size and activity. Muscle force ratios have been defined directly from EMG data in combination with physiological cross-sectional areas [31, 62, 63], estimated solely from a ratio of physiological cross-sectional areas [39], or arbitrarily assigned specific ratios or magnitudes [64-66]. Poppen and Walker (1978) performed an analysis to determine the forces in the glenohumeral joint during isometric abduction. The main assumption in their analysis was that the force in a muscle was proportional to its area times the integrated electromyographic signal [31]. Likewise, Johnson et al. (2000), in an attempt to simulate elbow joint motion with a load controlled testing apparatus, used a muscle loading ratio criterion determined directly from the product of the relative muscle EMG activity and the muscle physiological cross-sectional area data [62].

30

Wuelker et al. (1995) used a constant force ratio, determined from the ratio of muscle cross-sectional areas, to define forces in the shoulder musculature [39]. In an effort to study unconstrained glenohumeral joint motion, Debski et al. (1995) applied the same force to each tendon of the rotator cuff [66] during experiments performed in a dynamic shoulder testing apparatus.

Chapter 2: Forearm Anatomy and Relevant Terminology

2.1 Forearm Bones

The human arm is composed of three bones: the humerus, radius, and ulna. The distal end of the humerus articulates with the proximal ends of the forearm bones, the radius and ulna, constituting the elbow joint. Two epicondyles project from the lateral and medial sides of the distal humerus. The articulating surface of the humerus extends slightly lower than the epicondyles and includes the capitulum, a knob-like structure on the lateral aspect that articulates with the radial head, and the trochlea, a spool or pulley-shaped boney structure on the medial aspect that articulates with the semiulnar notch of the ulna.

2.2 Major Forearm Muscles

Six major flexors and extensors of the forearm [5, 32, 67] were identified prior to the formulation of the elbow joint model. The **triceps brachii** (TRI) is a large spindle-shaped muscle which lies on the posterior side of the arm, with an insertion on the olecranon process of the ulna. It is composed of three components: the long head, medial head, and lateral head, which have three separate origin sites on the inferior portion of the glenoid (on the scapula), the entire posterior surface of the humerus below the radial groove, and the posterior surface of the upper humerus (above the radial groove), respectively. The main functions of the triceps brachii include extension of the forearm and adduction of the arm (shoulder compression). The **biceps brachii** (BIC) is a powerful muscle which lies anteriorly in the arm. It consists of two heads: the long head, which wraps around the head of the humerus, and the short head. The biceps brachii scapula and coracoid process of the scapula, respectively. Its main functions include flexion and supination of the forearm. The **brachialis** (BRA) is a flattened, spindle-shaped muscle which lies posterior to the biceps brachii. It inserts on the front of the coronoid process of the ulna, and originated on the lower frontal portion of the humerus. The primary function of the brachialis is to flex the forearm. The **brachioradialis** (BRD) is an elongated, spindle-shaped muscle which runs along the outer side of the radius. It inserts on the lateral port of the radius above the styloid process, and originates on the lateral supracondylar ridge of the humerus. The brachioradialis functions mainly as a flexor of the forearm, and is also utilized for supination during forearm extension. The **anconeus** (ANC) is a triangular-shaped muscle which wraps across the posterior

portion of the radial head. It inserts on the outer margin of the olecranon process of the ulna and originates on the posterior surface of the external condyle of the humerus. The anconeus is actively involved in extension of the forearm. The **pronator teres** (PRT) is a small rounded muscle lying on the frontal side of the forearm. The insertion is near the middle of the radius on the outer side of the shaft, and its origin lies on the medial epicondyle of the humerus. The primary function of the pronator teres is to pronate the forearm [68, 69].

2.3 Terminology

Flexion angle refers to the angle made by the long axis of the humerus and the axis of the forearm, as measured in the sagittal or flexion plane (Figure 2-1). Supination refers to the rotation of the radius about the ulna, such that the palm faces forward or upward and the radius lies parallel to the ulna. Pronation refers to the opposite direction of rotation of the radius about the ulna such that the palm faces backwards or downwards. The neutral forearm position, often termed the neutral wrist position, refers to a position of the radius with respect to the ulna that is halfway between fully pronated and fully supinated rotation, or a mid-pronation/supination position (Figure 2-2).

The physiological cross-sectional area (PCSA) of a muscle is obtained by dividing the muscle volume by its true fiber length, and is defined in units of length squared. "The rationale of this definition is simply that the cross-sectional area of a muscle is proportional to the number of its fibers and the individual muscle fiber is the basic element which generates the active tension [23]." PCSA values of the primary forearm muscle flexors and extensors are defined in Table 2-1 and were obtained from data complied by An et al. [5].

Table 2-1. Muscle physiological cross-sectional areas (An et al., 1981 [5])

Muscle Group	Muscle	Abbreviation	PCSA (cm^2)	Total PCSA (cm^2)
Triceps Brachii	Long Head	TRI	6.7	18.8
	Medial Head		6.1	
	Lateral Head		6.0	
Biceps Brachii	Long Head	BIC	2.5	4.6
	Short Head		2.1	
Brachialis		BRA	7.0	7.0
Brachioradialis		BRD	1.5	1.5
Anconeus		ANC	2.5	2.5
Pronator Teres		PRT	3.4	3.4
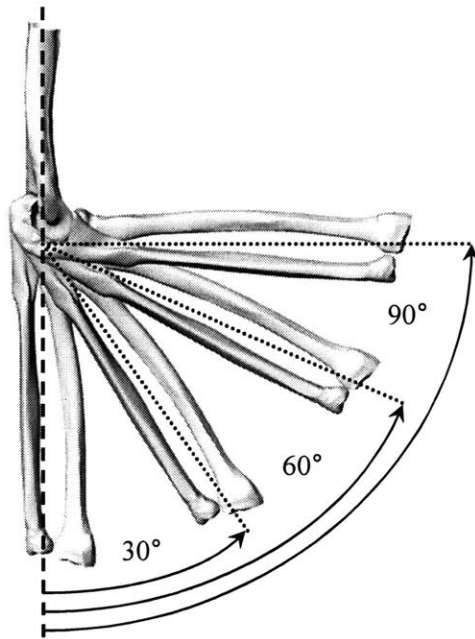
Figure 2-1. Neutral forearm flexion, as viewed from the sagittal (flexion) plane.
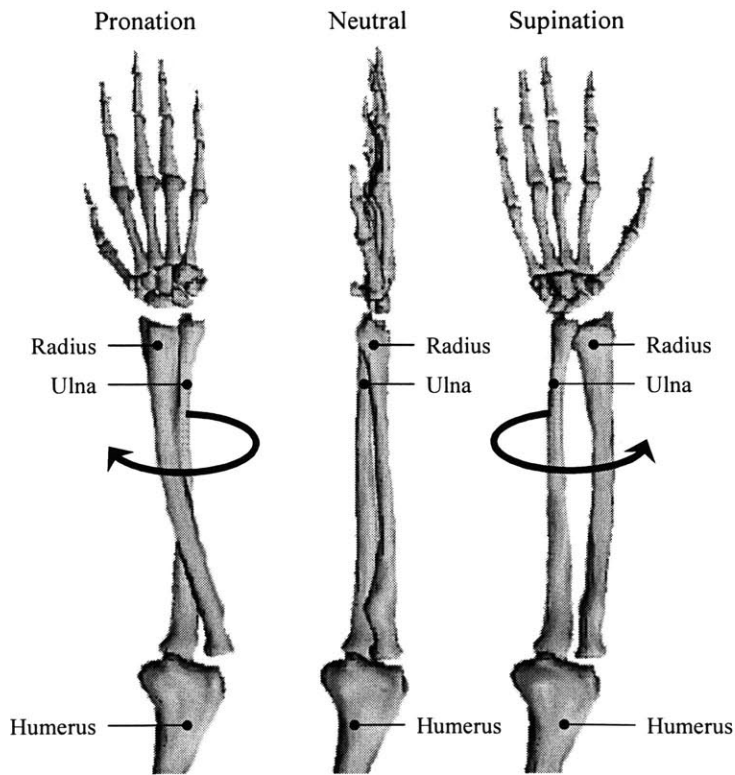
Figure 2-2. Illustration of pronated, neutral, and supinated forearm positions for a right forearm.

Chapter 3: Motivation and Objective

3.1 Motivation

Knowledge of in-vivo muscle forces and joint reaction forces produced during various functional activities is of great importance to the engineering and medical communities from a biomedical, biomechanical, and motor control point of view.

In regards to the biomedical viewpoint, knowledge of forces acting on the musculoskeletal system is essential for understanding the function of passive and active components of the human body and their mechanical-physiological capabilities [37]. The most commonly recognized medical application lies within the area of orthopaedic biomechanics and is especially relevant to the development of joint prostheses. To aid in the design of joint replacements, it is essential to determine the magnitudes of the forces which act on the components and contribute to the functionality of the joint during assorted daily activities. The magnitude of such forces will influence the choice of materials, manufacturing methods, sterilization mechanisms, implantation techniques, and other design and development considerations. Another important reason for acquiring accurate muscle load distributions lies in the development of post-operative rehabilitation regimens for musculoskeletal systems. For instance, one might want to know what weight can be safely used to exercise a reconstructed quadriceps tendon. Post surgery exercise routines need to be designed with physiological muscle loads and joint reaction forces in mind to minimize the chance of re-injury and to optimize physical therapy techniques and patient recovery.

Biomechanically, knowledge of in-vivo muscle and joint reaction forces provides information on the demands of a sport or daily activity relative to the actual limitations of the human body. Specifically, in the context of sport or working environment activities, this muscle loading information can assist in the prevention of injuries and in the understanding of the mechanism that affect performance. For instance, axial forces applied to the radius can be simulated to study carpal tunnel syndrome, as induced by repetitive work tasks, if the correct muscle force loading distributions are known.

From the motor control point of view, the knowledge of forces exerted by synergistic muscles provides information on strategies utilized by the neural system during motor tasks [37]. Knowledge of muscular strategies implemented during specific motor tasks allows for exploration of central nervous system function relative to environmental-structural constraints and the physiological capabilities of the body.

3.2 Objective

The original goal of this research was to quantify the 3D muscle forces, including the out-of-plane contributions, during quasi-static forearm flexion using human anatomic forearm models and a 3D inverse dynamic optimization method. In the course of developing the optimization model, some serious questions were raised regarding the validity of the moment constraint condition used to obtain the muscle forces, thereby redirecting the goal of this research.

The moment equilibrium constraint (Equation 1-8b) requires that the moments about the joint center sum to zero in all three directions, under the assumption that there is no joint reaction moment [15, 25, 26, 32]. The selection of the joint center in space will alter the moment arms of the forces applied to the musculoskeletal segments and alter the value of the joint reaction moment. Thus, an arbitrarily selected joint center may not satisfy the zero joint reaction moment assumption, and the predicted muscle forces may vary depending on the selected location of the joint center. The true joint center location, corresponding to the site where the joint reaction moment is zero, may also change with joint position and applied loading conditions. Therefore, accurate knowledge of the joint center location that satisfies the moment equilibrium condition is necessary for an appropriate prediction of muscle load distributions using static optimization methods. There is no data in the literature illustrating the variation in predicted muscle forces due to the selection of joint center location.

Thus, the objective of this research was to determine the effects of the joint center location on muscle loads predicted via an optimization procedure using a human elbow joint model. A three-dimensional static optimization procedure was used to provide a non-invasive estimation of six forearm muscle forces and three joint reaction forces in the elbow joint during an isometric flexion activity when the joint center was varied along the flexion-extension axis.

38

Chapter 4: Experimental Setup

This chapter seeks to explain the processes (outlined in Figure 4-1) by which the anatomic data was obtained from cadaver specimens for use as input to the elbow joint optimization model (Chapter 5). First, the cadaver specimens were prepared for installation on the robotic testing system (Section 4.1); the muscle tendons and insertions of interest were exposed (Section 4.1); and the specimen was installed on the testing system (Section 4.2.1). Next, the "neutral" path or flexion path was determined (Section 4.2.1) and the important features were digitized at various flexion angles and forearm positions of interest (Section 4.2.2). Next, the same specimen was subjected to a CT scan and a 3D model was subsequently produced (Section 4.2.3). The digitized data was superimposed on top of the 3D model, and the joint coordinate system was established (Section 4.3). The anatomic data was imported into the optimization model (Chapter 5), the muscle and joint reaction forces were predicted (Chapter 7), and the forces were validated with EMG data (Chapter 6).
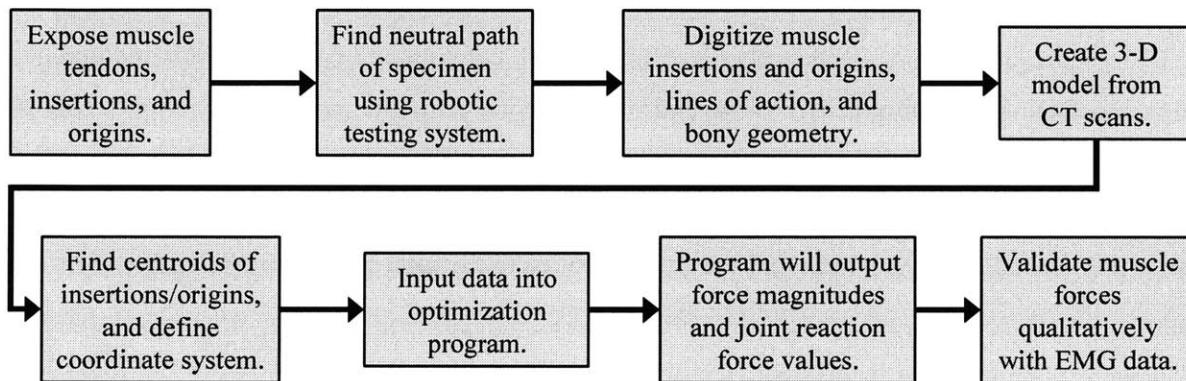
Figure 4-1. Protocol for experimental setup and model development.

4.1 Cadaveric Specimen Preparation

One fresh frozen cadaveric human forearm specimen, severed mid-humerus, was used in this study (left arm, female, 62 years old). Prior to testing, the specimen was thawed overnight at room temperature. The integrity of the specimen was then assessed via visual examination and palpation to ensure no gross deformities.

The hand and the scaphoid were removed to expose the distal radius. A threaded rod was then inserted into the intramedullary canal of the radius and secured in place using bone cement. The distal and proximal radioulnar joints remained intact. The distal portion of the humeral shaft was cleared of soft tissue and another rod was inserted into this canal and secured using bone cement. Two cylinders, made of bone cement, were constructed around the exposed ends of the rods for ease of specimen installation on the robotic testing system (see Section 4.2.1).

The remaining soft tissue was removed from the specimen to expose the muscle tendons and insertions of the primary muscle flexors and extensors of the forearm (Section 2.2), which consisted of the BIC, BRA, BRD, PRT, ANC, and TRI, taking care to leave the elbow capsule intact.

4.2 Cadaveric Experimental Testing

4.2.1 Robotic Testing System

The 6 degree-of-freedom (DOF) robotic testing system consists of a 6 DOF robotic manipulator arm, a 6 DOF load cell attached to the end of the robotic arm, and an external computer set-up running Visual Basic (Microsoft, Seattle, WA) programs. The UZ150 robot (Kawasaki, Japan) was able to move its end effector to a given position with a repeatability of 0.3 mm. The load cell (JR3, Woodland, CA) measured the forces applied to the joint by the robotic arm.

The cadaveric specimen is installed upside-down on the robotic testing system. In the case of the knee joint, seen in Figure 4-2, the femur is rigidly fixed to the pedestal at the base of the robot and the tibia is attached to the load cell. The same set-up can be seen for the forearm in Figure 4-3a, with the humerus fixed to the pedestal and the radius attached to the load cell. The forearm was installed at full extension in the neutral rotation position, and the 6 DOF pedestal allowed the specimen to be properly aligned with the robot manipulator arm.

The robot can operate in both force-control (with force measurement input from the load cell) and position-control (with positional measurements made by the robotic arm) modes. In force-control mode,

40

Robot

Load Cell

Knee Specimen
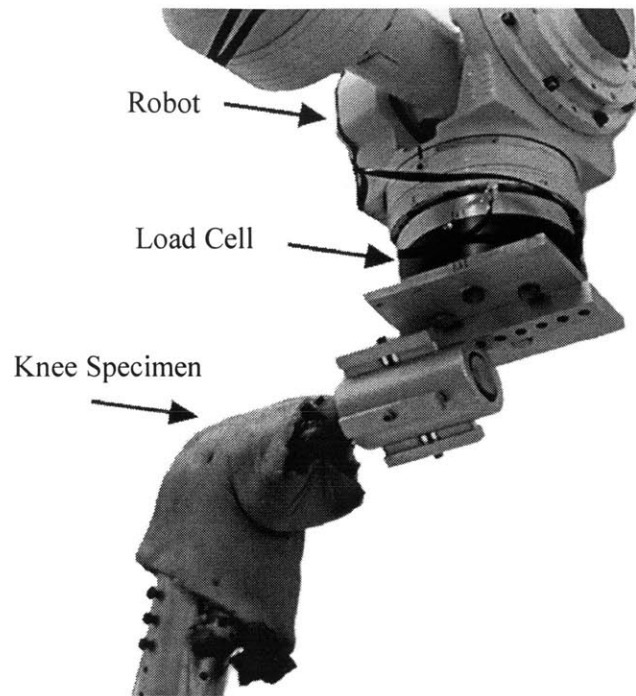
Figure 4-2. Robotic testing system

(a)

(b)
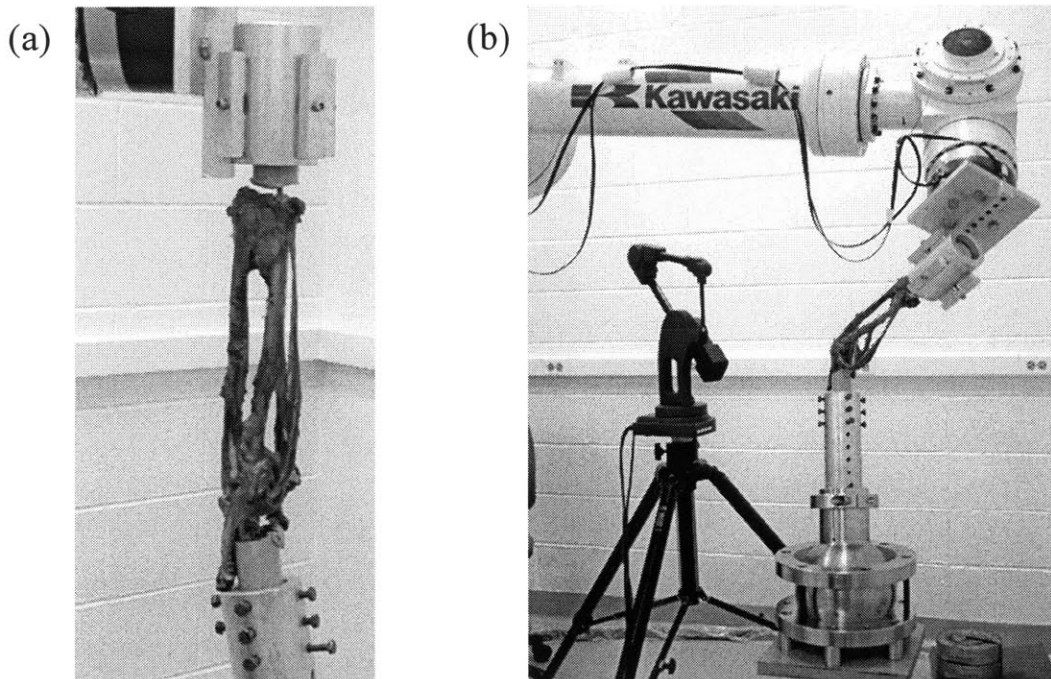
Figure 4-3. A forearm specimen, with skin removed and muscles exposed, is rigidly fixed to the robotic system (a). The humerus is fixed to the pedestal on the base of the system, and the radius is attached to the load cell. The neutral path of the forearm is obtained (b) by incrementally flexing the radius with the robot operating in force-control mode.

the position of the specimen is recorded as the robot incrementally moves the specimen (i.e. moves the tibia or radius) while simultaneously minimizing the forces and moments about the specimen's joint center. In position-control mode, however, the resulting forces are measured as the specimen is moved along a specific path.

A common experimental starting point is to find the "neutral path" of the specimen, which involves operating the robot in force-control mode and flexing the joint through its entire range of movement (Figure 4-3b). This positional data or "neutral path" is recorded and can be replayed at any time using the position-control mode feature.

4.2.2 Microscribe 3DX® Digitizer

This three-dimensional digitizing system (Microscribe 3DX, Immersion Corporation, San Jose, CA), illustrated in Figure 4-4a, was used to define the relative position and orientation of the load cell, robotic arm, and cadaveric joint, and subsequently construct individual coordinate reference systems for these structures (Figure 4-4b).

Anatomic data was obtained from the cadaveric forearm including, but not limited to, information on the insertion, origin, and direction (line of action) of each of the primary flexors and extensors. The muscles were constrained to follow their anatomical paths using strings to route the tendons from the insertions to the origin sites. Then, the muscle origins, insertions, and lines of action were digitized using the 3D digitization platform (Figure 4-4a) with the forearm held in the neutral (mid pronation/supination) position. The bony surfaces of the humerus, ulna, and radius were also digitized to provide anatomic landmarks for establishment of a coordinate system for the elbow joint model. This data was imported into a solid modeling program to create a 3D representation of the elbow joint system, and to obtain the centroids of the digitized origin and insertion sites of the muscles.

4.2.3 Cross-Sectional Computerized Tomography (CT)

The cadaveric forearm was placed in the neutral, full-extension position and scanned from the mid-humerus through to the wrist in increments of 1.25 mm using a CT scanner under the supervision of a radiologist at Massachusetts General Hospital.

The 1.25 mm-spaced CT slices (Figure 4-5a) were imported into the 3DSlicer® software, which outlined the contours of the bones on each slice to create a three-dimensional image (Figure 4-5b).

4.3 Three-Dimensional Modeling Software

The contour curves obtained from the CT scan were lofted using the Rhinoceros® (Robert McNeel & Associates, Seattle, WA) modeling software to create a 3D surface representation of the bone. Next, the 3D bone surface was overlaid and matched to the digitized bony geometry outlines obtained using the Microscribe® digitizer, thereby incorporating the 3D model into the same reference system as the digitized muscle lines of actions and other landmarks.

A joint coordinate system, similar to that defined by Morrey and Chao [70], was set up to describe the position and orientation of the muscles in the forearm system (Figure 5-2a). The y-axis, defined as the elbow flexion-extension axis, was found by passing a line through the center of the three concentric circles formed by the bottom of the trochlear sulcus, the periphery of the capitulum, and the medial facet of the trochlea [42, 71, 72] (Figure 4-6). The z-axis was defined perpendicular to the y-axis, passing proximally along the longitudinal axis of the humerus. The geometric elbow joint center, defined as the midpoint of the flexion-extension axis (center of the trochlea) [5, 70], was used as the origin of the coordinate system. Rotation about the y-axis was defined as flexion-extension.
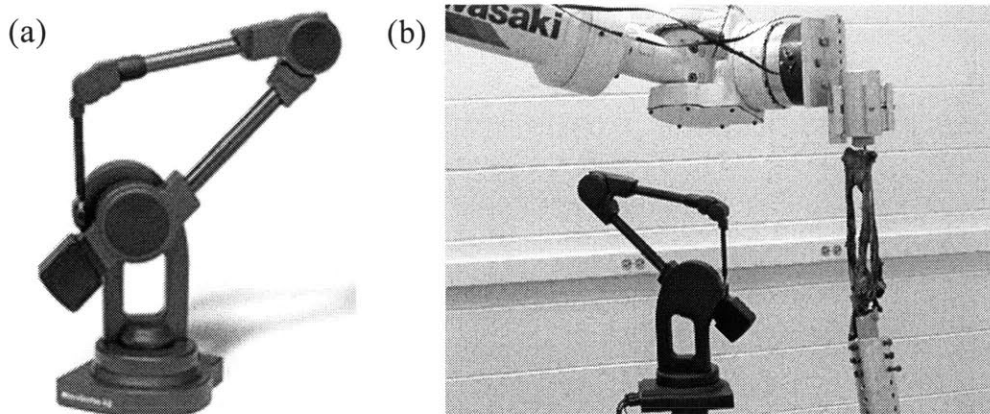
Figure 4-4 (a) The Microscribe 3DX digitizer, made by Immersion Corporation (San Jose, CA), was used to trace the muscle insertions, origins, and lines of action, and bony geometry of the specimen. (b) It was also used to set up a coordinate system for the robot/load cell with respect to the joint center.
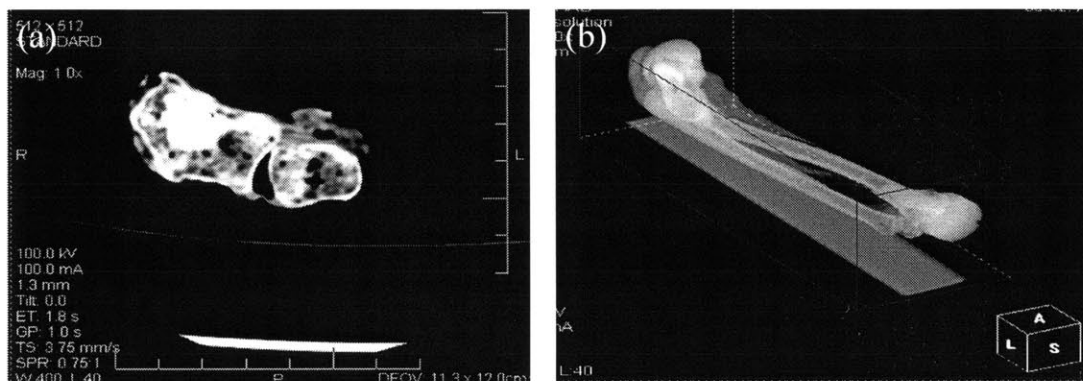
Figure 4-5. (a) Single CT slice of forearm bones were reconstructed into a 3D solid image (b).
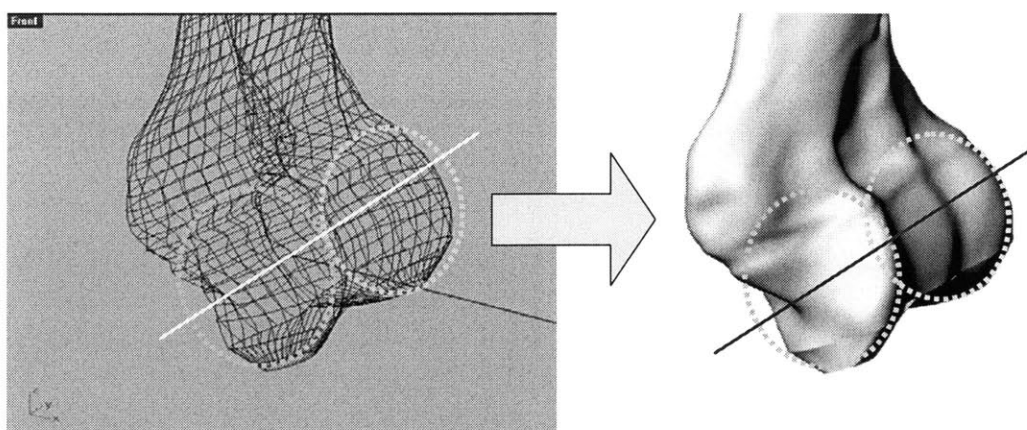
Figure 4-6. Calculated flexion-extension axis by fitting circles to the bottom of the trochlear sulcus, the periphery of the capitulum, and the medial facet of the trochlea.

Chapter 5: Model Development

A three-dimensional elbow joint model was formulated using six forearm muscles (Section 2.2). An optimization algorithm was employed to solve the nonlinear objective function, subjected to a set of constraints, and muscle loads and joint reaction forces were obtained.

5.1 Muscle Lines of Actions

The incorporation of muscle forces into a joint model requires knowledge of the muscle lines of action. The simplest approach is to assume that the muscles act along straight lines pointing from the origins to insertions [35]. However, most muscles do not truly act along straight lines since their movement is constrained by adjacent muscles and tissue. Muscles often lie over deeper structures which restrict their tendency to straighten under tension. The fact that many muscles have broad attachment sites or multiple heads is also a concern when using the straight line approximation. Additionally, in order to more accurately represent muscle actions, it is sometimes necessary to divide the muscle into several subunits and model each unit's action individually [10, 35].

Keeping these limitations in mind, the lines of action of the six muscles used in the formulation of this elbow joint model (Section 2.2) were obtained as anatomically correct as possible. This is important because the muscle forces were applied to the bones at their respective points of insertion and along the lines of action of the muscles. The lines of action of the brachioradialis, pronator teres, and anconeus muscles were represented as vectors along the straight line connecting their respective origin and insertion points. The remaining muscles were represented by digitized lines of action, which consisted of a line digitized along the muscle tendon in the direction of the muscle orientation and measuring about 5 cm in length.

5.2 Equilibrium Equations

The static joint equilibrium equations were formulated based on the free body diagram of the elbow joint system seen in Figure 5-1. The generalized joint equilibrium equations, seen in Equation 1-5, were adapted for use in this model using $N=6$, representing the six forearm flexors and extensors chosen to describe the elbow joint system (Section 2.2). In addition to muscle forces, ligament and contact forces also affect the load distribution at the joint. To account for

these forces without solving for them directly, a joint reaction force, $\vec{F}^{Joint}$, was introduced into the equations which represents the summation of these ancillary internal forces (Figure 5-2b).
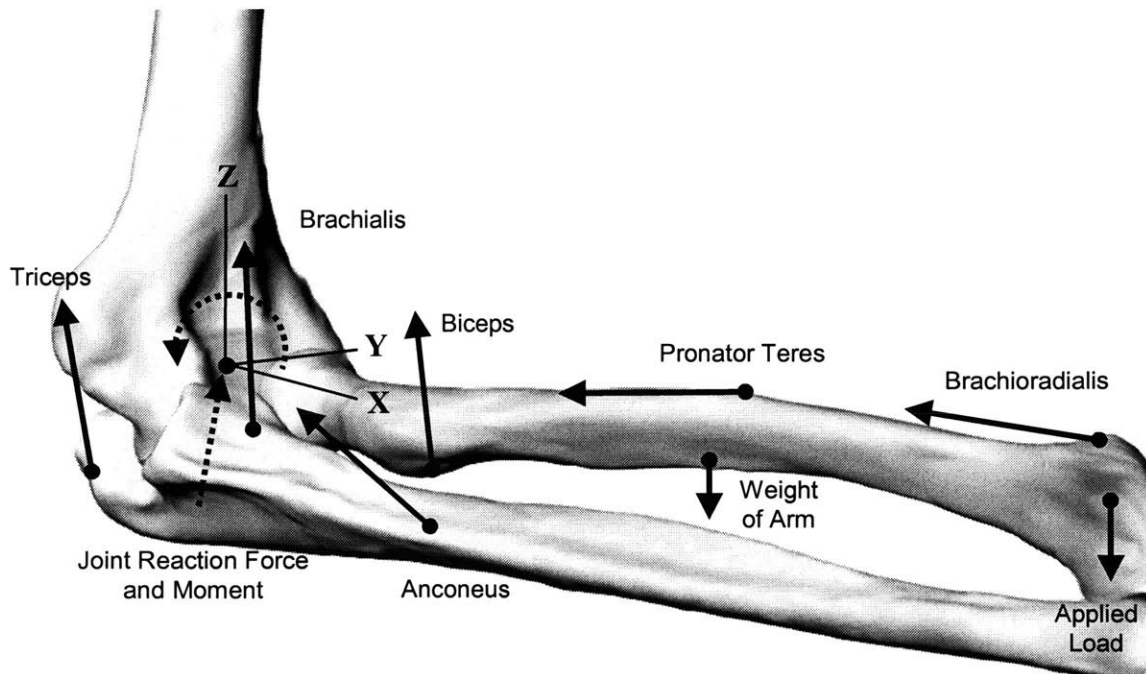
Figure 5-1. Free-body diagram of forearm system, including muscle forces, external loads, and joint reaction force and moment.
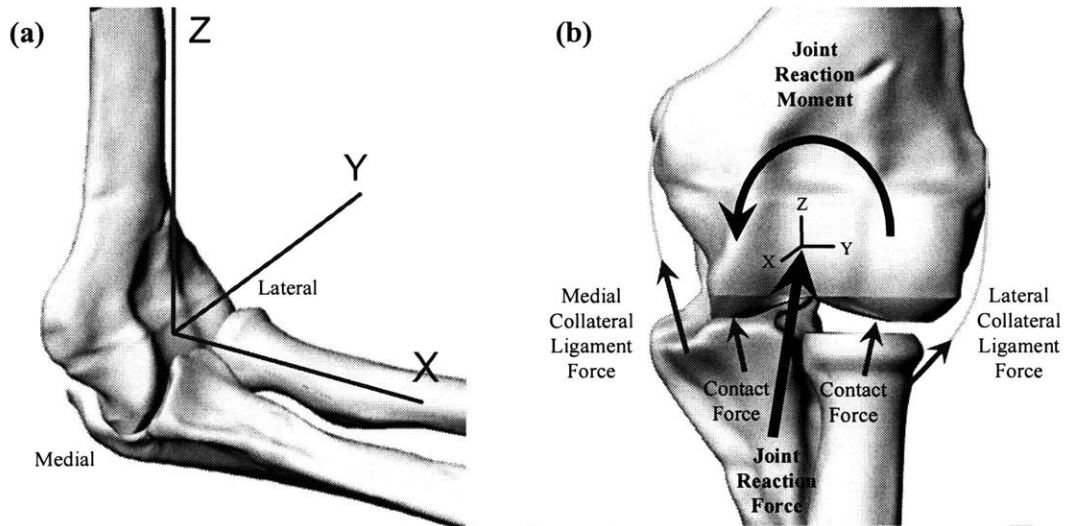
Figure 5-2. (a) Computer-generated 3D model of the elbow joint at 90° of flexion and (b) Free-body diagram of elbow joint where the joint reaction force includes the ligament tensions and articular joint contact forces.

5.3 Optimization

5.3.1 Objective Function and Constraints

The cubic muscle stress objective function (use an exponent value of $n=3$ in Equation 1-7), proposed by Crowninshield and Brand [12], was used to predict the muscle and joint forces in this elbow joint model. The constraints used in this model were described previously in Section 1.4.2, and imposed upper and lower limits on the muscle force values (Equation 1-8c). The absolute strength or maximum stress value, denoted by σ in Equation 1-8c, of human skeletal muscle has been of interest for nearly a century. In 1910, Fick [73] described the absolute stress that skeletal muscles exert as a constant 100 N/cm². Maximum muscle stress values have since been reported in literature ranging from a mere 10 N/cm² to 100 N/cm² [11, 23, 45, 56, 73-81]. For this study, a value of 100 N/cm² [23, 45, 73] was used for the maximum muscle stress value and it was assumed constant for each muscle [23, 82]. The force and moment equilibrium equations were also employed as constraints (Equations 1-8a, 1-8b), and were adjusted using $N=6$ for the six forearm muscles involved in this study.

5.3.2 Optimization Algorithm

The optimization code for this model was written in the Mathematica© (Wolfram Research, Inc., Champaign, IL) programming software (see code in Appendix D). The global minimization function in Mathematica©, NMinimize®, was used to solve the indeterminate system of equations describing the joint system. NMinimize® utilized a simplex algorithm [83, 84] developed by Nelder and Mead [85], and if that method did poorly or failed, the differential evolution method of Price and Storn [86] was implemented. Below is a brief description of each method, although the source material should be referenced for a more complete explanation.

The nonrandom numerical technique devised by Nelder and Mead is sometimes referred to as the downhill simplex method. The function moves slowly downhill in a straightforward manner, requiring no derivatives, and relies solely on function evaluations [83, 84]. The method minimizes a function of N variables by comparing the function values at the (N+1) vertices of a general simplex (Figure 5-3), and replacing the highest valued vertex by another point.

Three operations are used when replacing this point: reflection, contraction, and expansion, all of which involve deforming the simplex to the local landscape of the function which ultimately allows the simplex to contract onto the final minimum. Reflection refers to the movement of the highest vertex (point with the largest function value) through the opposite face of the simplex to a lower point, conserving the volume of the simplex. Expansion refers to the growing of the simplex in one direction, thereby taking larger steps than prescribed by the reflection method. And lastly, contraction occurs when the simplex nears the minimum of the function and the method contracts itself in the transverse direction to move nearer to the function minimum. Further description of this algorithm can be found in the Mathematica© software documentation [83], as well as in the literature published by Nelder and Mead [85].

If the deterministic search algorithm of Nelder and Mead [85] failed, the genetic algorithm of Price and Storn [86] was employed. "Genetic algorithms attempt to transform an initial population of randomly generated vectors into a solution vector through repeated cycles of mutation, recombination, and selection [86]." Mutation, an important operation for maintaining diversity in a population, makes small random alterations to one or more parameters of an existing population vector. Recombination economically reorders information about successful combinations to narrow the focus on the most promising areas of the solution space by building new parameter combinations from the components of existing vectors. Differential evolution's recombination method is non-uniform in that child vector parameters can be taken from one parent more often than the other parent (i.e. does not need to be taken from each parent with equal probability). Lastly, selection determines which trial solution will survive into the next generation. Differential evolution's acceptance strategy pits each child against one of its parents, only allowing one of the two to advance to the next generation. Differential evolution is a very robust method, but can be relatively slow due to the reasonably large set of points it maintains.

52
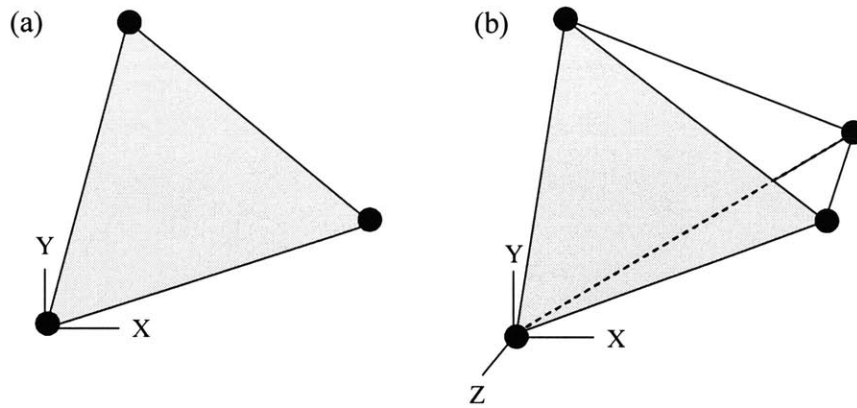
Figure 5-3. A simplex is the geometric figure composed of N+1 vertices interconnected by line segments, with N denoting the number of variables used in the optimization. A simplex is (a) triangular in two dimensions (i.e. two variables in the objective function) and (b) tetrahedral in three dimensions (i.e. three variables), and so forth.

Chapter 6: Model Validation

6.1 Moment Arms

The moment arm values calculated within the model (Figure 6-1) were compared with moment arms values published in literature for validation [72, 87, 88]. The moment arms calculated in the model were dependent on the experimentally obtained muscle origin, insertion, and line-of-action data. Murray et al. (2002) published a range of moment arm magnitudes for 10 upper extremity specimens maintained in the neutral forearm position, and the range of values for muscle moment arms at 90° of flexion (visually obtained from a published figure, see [72]) were: 6-9 cm for brachioradialis, 4-5.5 cm for biceps, 2-3 cm for brachialis, 1.5-2 cm for triceps, and 1-2 cm for pronator teres.
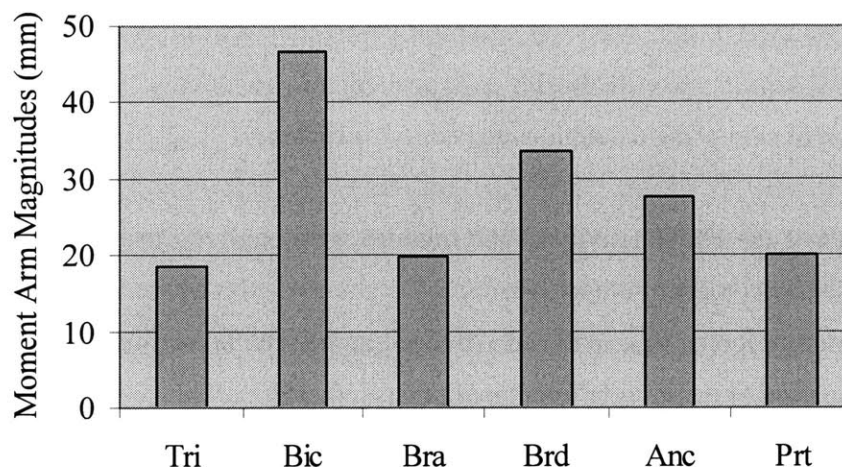
Figure 6-1. Moment arm magnitudes (given in mm) calculated for the three-dimensional case.

All calculated three-dimensional moment arms agreed well with Murray's data, with the exception of the brachioradialis. This discrepancy is perhaps due to a slight variation in the definitions of the brachioradialis line of action (Murray connected the insertion centroid to a point more distal than the centroid of the origin, instead of to the origin centroid itself), or perhaps the small anatomic size of the single specimen used in this study was the reason for disagreement. Data from Pigeon et al. (1996) and Winters and Kleweno (1993) depicted moment arm values similar to Murray for this forearm position and flexion angle [87, 88].

6.2 Electromyography (EMG)

Electromyography (EMG) describes the process by which signals are recorded using electrodes to measure the voltage or potential difference between two points, such as the electric potential across a muscle fiber membrane. There are two main groups of electrodes: the invasive sub-surface or needle electrodes placed inside the muscle, and the noninvasive surface electrodes placed on top of the skin (overlying the muscle).

6.2.1 EMG Setup

Silver-silver chloride surface electrodes were used to collect EMG signal data for the TRI, BIC, BRA, BRD, ANC, and PRT muscles at various flexion angles and positions using a 16-channel active electrode system (Motion Lab Systems, Inc., Baton Rouge, LA) pictured in Figure 6-2. The subjects volunteered to participate in this study and, since surface EMGs are universally recognized as safe, non-invasive measurement devices, this study did not require review board approval. The subject's skin was first cleansed with rubbing alcohol and allowed to air-dry. Then, the EMG sensor was filled with a hypoallergenic conductive gel and secured to the cleansed portion of skin using a double-sided adhesive sticker.

The magnitudes of the EMG activity of the muscles were analyzed using appropriately placed surface EMG sensors on each subject (Figure 6-2). A correlation between the EMG activity and the predicted muscle forces was analyzed [26] and can be seen in Section 6.2.5. This provided a qualitative validation of the muscle force predictions [30, 35].

6.2.2 Maximum Voluntary Contraction

Maximum voluntary contraction (MVC) tests were performed to establish a maximum muscle activation value for each muscle to be used as a normalization value when processing the flexion test data (see Appendix C.1). This test involved performing a series of resisted flexion tests, in the neutral, pronated, and supinated forearm positions, and a resisted extension test in the neutral forearm position, all at the maximum limit of the muscles. These MVC flexion tests produced the maximum values for the BIC, BRA, and BRD, and the MVC extension test was used to define a maximum for the TRI. In the analysis of the BIC and BRA muscles, there is a large

56

Figure 6-2. Subject 2 performs passive contraction test in the supinated forearm position, with the elbow held at 90° of static flexion.

(a) Passive Flexion   **(b)** Resisted Flexion

90°

90°
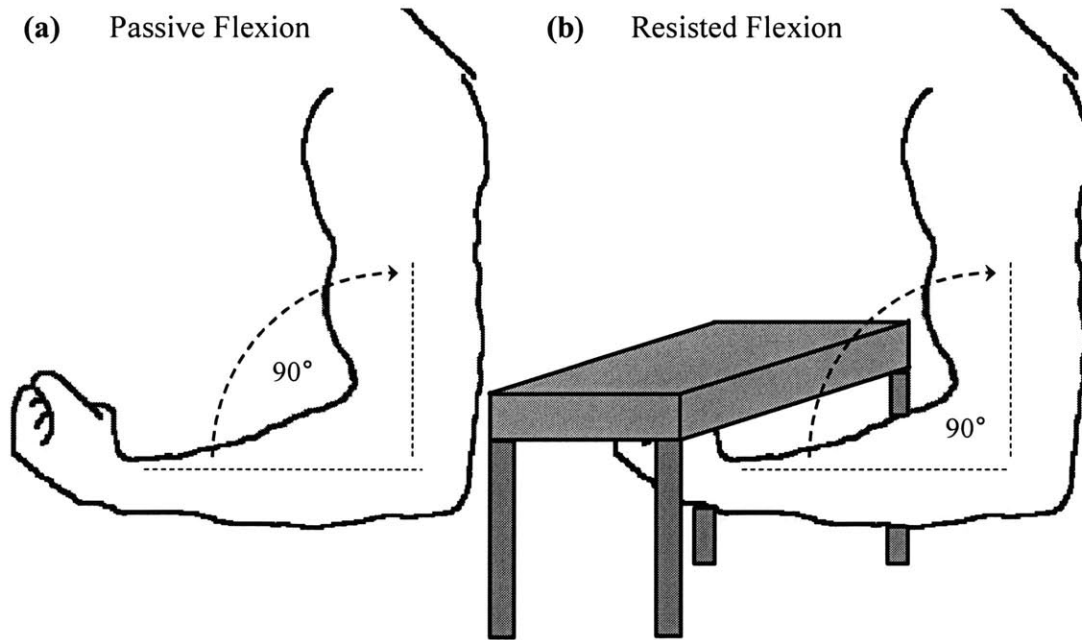
Figure 6-3. Schematic of subject positioning for passive and resisted contraction EMG studies.

amount of crosstalk between the two signals as the BIC muscle lies on top of the BRA and it is hard to get a pure signal without using invasive (needle) EMG sensors. Nonetheless, the maximum value recorded for each muscle out of all four tests was the value used for normalization.

6.2.3 Passive and Resisted Contraction Tests

The volunteer subjects were instructed to hold their arms in the position illustrated in Figure 6-2 and Figure 6-3, with the humerus held vertical and parallel to their side and the elbow flexed to 90 degrees. The passive contraction test required the subjects, starting in the neutral forearm position, to perform a static exercise for 2-3 seconds. The subjects were asked to flex their forearm muscles, as if performing a dumbbell curl, without changing the flexion angle of the elbow, and then relax (Figure 6-3a). This static passive contraction test was repeated in the pronated and supinated forearm positions (Figure 6-2). The static resisted contraction tests were then performed with resistance to flexion imposed by a stationary object (Figure 6-3b). Instead of passively flexing ones muscles, the subjects were asked to attempt a dumbbell curl with flexion being resisted by a fixed horizontal surface (Figure 6-3b). See Appendix C.2 for results of the flexion tests. The resisted flexion test more closely simulated the activity represented by the elbow joint model than the passive flexion test, and thus only the resisted flexion data was used to validate the model.

6.2.4 Data Processing

The EMG signal data for the resisted flexion tests (Appendix C.2.2) was RMS-averaged and then normalized with respect to the MVC data, also RMS-averaged (Appendix C.1.2), and can be seen in Appendix C.3. The MATLAB© codes used to RMS-average and normalize the resisted flexion test data can be found in Appendix C.4.

The raw EMG signal looks very much like a noise signal distributed about the zero point (see Appendix C.2). Thus, before any correlations can be drawn between the EMG signal data and the force predictions of the optimization model, the raw data must be processed in either the time or the frequency domain. There are a number of ways to process EMG signal data and, in this study, the root mean square (RMS) value of the EMG signal was chosen as a means of quantifying the magnitude of the signal. The RMS values were calculated by summing the

squared values of the raw EMG signal, determining the mean of the sum, and taking the square root of the mean [89]. In mathematical form, the root mean square formulation can be written as:

$$RMS = \sqrt{\frac{1}{T} \int_{t}^{t+T} EMG^2(t)dt}, \tag{6-1}$$

where T represents the period over which the signal is evaluated. The Matlab© routine to perform this calculation can be found in Appendix C.4. The RMS-value is an easy way to quantify the magnitude of a signal and has frequently been used to study muscle fatigue [89]. Once the RMS values for both the MVC and flexion test data were obtained, the flexion test data was normalized using the MVC data. The entire process is outlined in the flow chart in Figure 6-4. For example, the RMS value of the BRD for subject 1's left arm resisted flexion test was normalized using the maximum RMS value obtained for the BRD recorded during subject 1's left arm MVC test (which was the maximum value out of the four tests, including a neutral flexion, pronated flexion, supinated flexion, and extension MVC test).

6.2.5 Force Validation

The muscle forces predicted using the optimization code, with the joint center located at the geometric center (y=0), were qualitatively compared with EMG data (see Appendix C.3) for validation. In Figure 6-5a, the ratio of the predicted muscle force (F_i) to the maximum isometric muscle force ($F_{max,i}$) was plotted for the TRI, BIC, BRA, and BRD. The maximum isometric muscle force, $F_{max,i}$, was calculated by multiplying the individual muscle $PCSA_i$ (Table 2-1) by a constant maximum physiological muscle stress (σ) value of $100N/cm^2$. The EMG activation data for the TRI, BIC, BRA, and BRD, averaged over data from four neutral resisted flexion tests (more values can be found in Appendix C.3), can be seen in Figure 6-5b. EMG data was not collected for the ANC or PRT. Qualitative comparison with the EMG data shows that the BIC, BRA, and BRD are all activated at 90° flexion, as predicted in the optimization. It is important to note that EMG is related to the force, but the force may not be proportional to the EMG. Thus, a direct comparison of the predicted muscle forces and the EMG signals could lead to wrong conclusions, hence our simple qualitative analysis to merely see if the same muscles are activated.
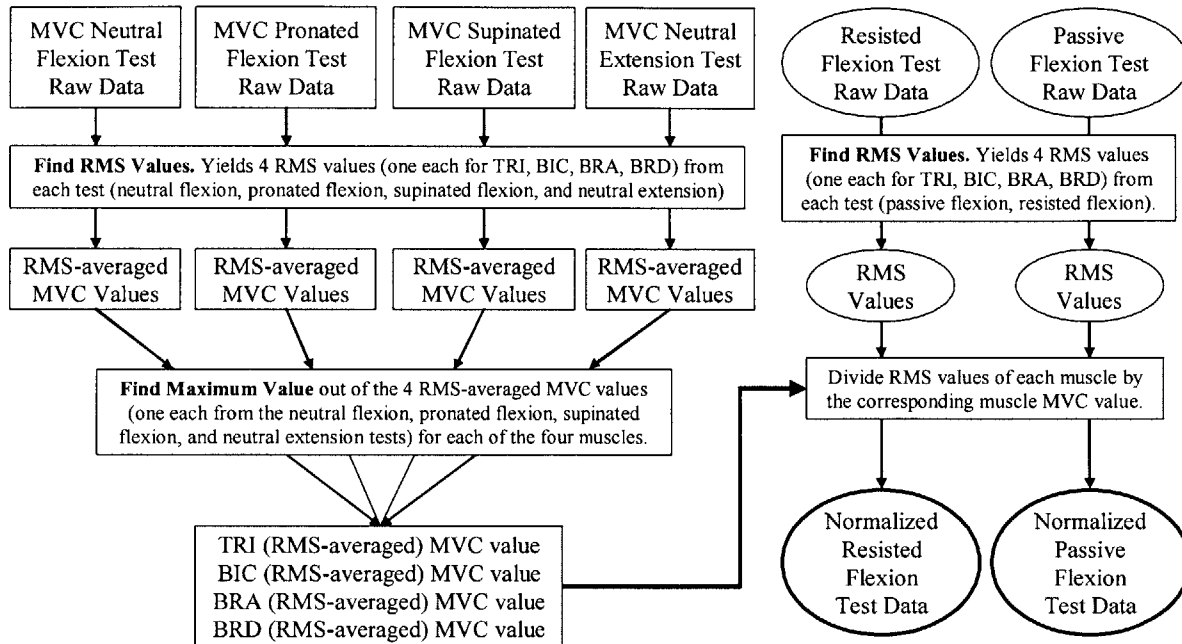
Figure 6-4. This flow chart depicts the process by which the raw EMG data was processed and normalized.

(a)

(b)
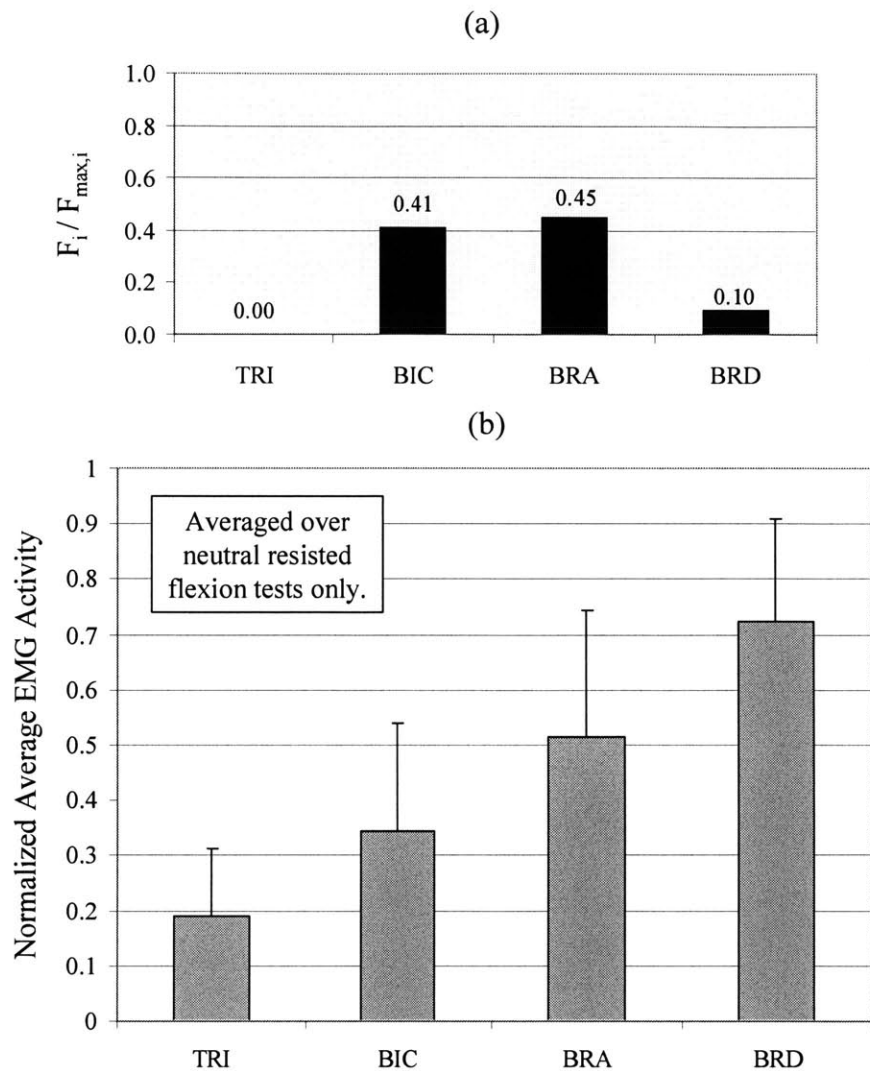
Figure 6-5. (a) Ratio of predicted muscle force magnitudes (F_i) to maximum isometric muscle force ($F_{max,i}$) values (calculated from σ*$PCSA_i$) for the triceps (TRI), biceps (BIC), brachialis (BRA), brachioradialis (BRD), anconeus (ANC), and pronator teres (PRT) at 90° of flexion, calculated at the geometric elbow joint center (y=0). (b) The EMG activation data, averaged over data from four neutral resisted flexion tests, is shown for the TRI, BIC, BRA, and BRD. EMG data was not collected for the ANC or PRT. The EMG data shows that the BIC, BRA, and BRD are all activated at 90° flexion, as predicted in the optimization (a).

Chapter 7: Results

Various sensitivity studies were performed to determine the effect of joint center location on muscle loads predicted using the inverse optimization method described previously.

7.1 Joint Center Variation along Flexion-Extension Axis

The joint center was varied in one-dimension, along the flexion-extension (y) axis of the elbow (Figure 7-1), and the muscle and joint forces were calculated for each new position of the joint center. These forces were plotted with respect to the joint center location along the flexion-extension axis, as seen in the following sections. The objective function value was also recorded at each joint center position so that a global minimum of the objective function with respect to joint center movement could be determined.

7.1.1 Muscle Loading Ratios

The predicted muscle loading was sensitive to the change of the elbow joint center location under a 50 N load applied at the distal radius, the weight of the forearm acting at the center of mass, and no additional applied moments (Figure 7-2). Each muscle force magnitude was expressed as a "muscle loading ratio", or percentage of the total muscle loading value (i.e. the sum of all the muscle force values at that position), as the joint center moved medially and laterally from the geometric center (defined by the "0 mm" position in Figure 7-2). Negative values indicate joint center translation towards the medial edge of the elbow joint and positive values indicate movement towards the lateral edge.

When the joint center was located at the geometric center ("0 mm") of the elbow, the BRA muscle exerted the largest force, accounting for 55% of the total muscle force, with the BIC and PRT contributing 33% and 10%, respectively (Figure 7-2). The TRI, ANC, and BRD made little contribution to the total muscle loading at this position.

Movement of the joint center location medially along the flexion-extension axis, toward the ulnotrochlear joint, resulted in a decrease in the BIC loading ratio and an almost linear increase in the BRA loading ratio (Figure 7-2). A 5 mm medial movement of the joint center location along the flexion-extension axis resulted in a BRA loading ratio of 80%, much larger than that

calculated at the geometric center location. Contrastingly, the BIC loading ratio at this position was found to be only 12%.

Lateral translation of the joint center location along the flexion-extension axis, toward the radiocapitellar joint, yielded an increase in the BIC loading ratio and a seemingly linear decrease in the BRA loading ratio. A 5 mm lateral movement of the joint center resulted in a BRA loading ratio of only 34% and a BIC loading ratio of 46%, an expected switch in the BIC verses BRA trend found during medial joint center translation.
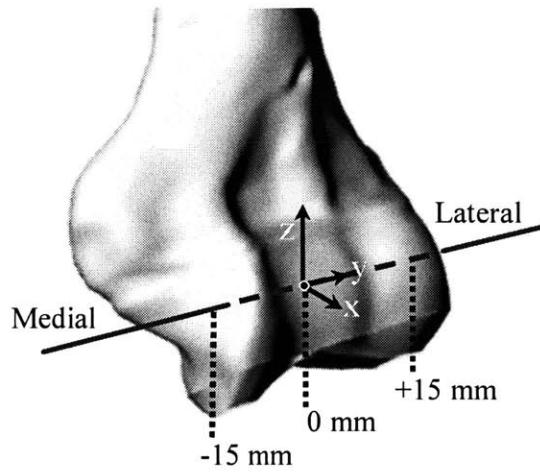
Figure 7-1. The joint center was varied ± 15 mm along the flexion-extension, or y, axis of the elbow.
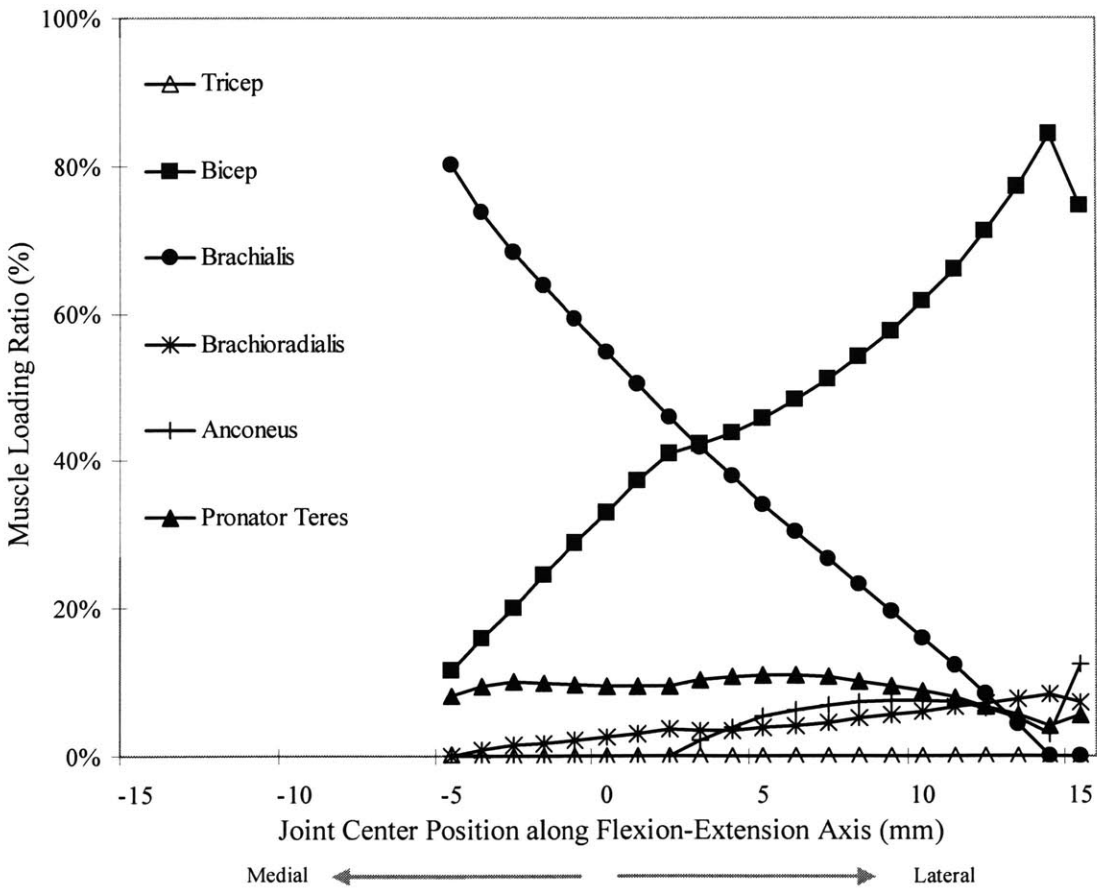
Figure 7-2. The predicted muscle loading ratios are plotted against their corresponding joint center location along the flexion-extension axis (with a 50 N load applied at the distal radius and no applied axial moment). The predicted muscle forces were highly sensitive to the position of the elbow joint center.

7.1.2 Joint Reaction Force

The sensitivity of the joint reaction force to the joint center location (under the 50 N load applied at the distal radius and no applied moments) was also investigated (Figure 7-3).
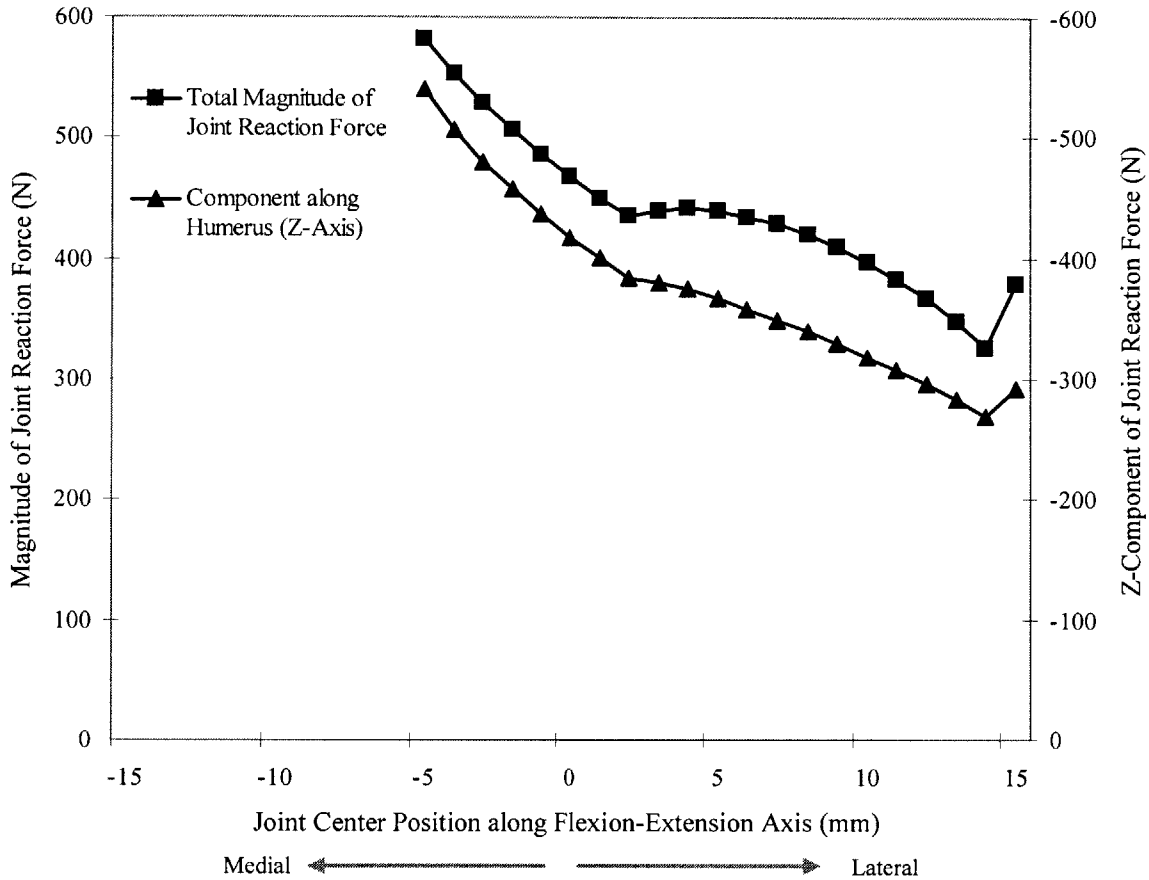
Figure 7-3. The change in the joint reaction force (total magnitude and humeral, or z-axis, component) is plotted against the corresponding joint center location along the flexion-extension axis (with a 50 N load applied at the distal radius and no applied axial moment).

Movement of the joint center from 5 mm of medial (negative) translation along the flexion-extension axis to 5 mm of lateral (positive) translation resulted in a 24% decrease in the magnitude of the joint reaction force. This was accompanied by a similar change in the humeral, or z-axis, component of the joint reaction force, which also exhibited a 32% decreased in value over this 10 mm of translation, suggesting that this particular component is directly responsible for the change in the joint reaction force. The x- and y- components were also analyzed and exhibited very little change in value over the course of the joint center movement.

7.1.3 Objective Function Minimum

The value of the objective function was recorded, after calculation of the muscle and joint forces, for each position of the joint center along the flexion-extension axis. Then, the values were compared over the range of joint center movement to determine a global minimum point. This study of the objective function minimization was performed not only for the original '50 N load at the distal radius and zero applied moment' loading condition, but also for various other loading conditions.

Not surprisingly, in addition to the muscle and joint reaction forces the objective function value was also sensitive to the location of the joint center along the flexion-extension axis (Figure 7-4). The objective function reached a global minimum with the joint center translated 1 mm lateral of the geometric center. Moving the joint center medially caused a sharp increase in the values of the objective function and beyond 5 mm of medial translation, the optimization was unable to converge on a solution which satisfied all of the constraints, probably because most of the muscles were located lateral of the joint center. As the joint center location was translated laterally, the value of the objective function again increased, again most likely due to the fact that most of the muscles were now located medial to the joint center (Figure 7-4).

When an applied moment about the x-axis was varied from -5 to +5 N.m (Figure 7-5), the joint center location coinciding with the objective function global minima moved along the flexion-extension axis from 7 mm medial to 12 mm lateral of the geometric center, respectively (Figure 7-6). A negative moment of -5 N.m resulted in an objective function minimum at a joint center location 7 mm medial of the geometric elbow center. As the moment was decreased (-5 N.m to 0 N.m), the location of the minimal value of the objective function moved laterally in an almost linear fashion. This linear trend continued as the positive moment was applied (0 N.m to +5 N.m). With a 5 N.m applied moment, the minimum point of the objective function did not occur until the joint center reached a location 12 mm lateral of the geometric center.
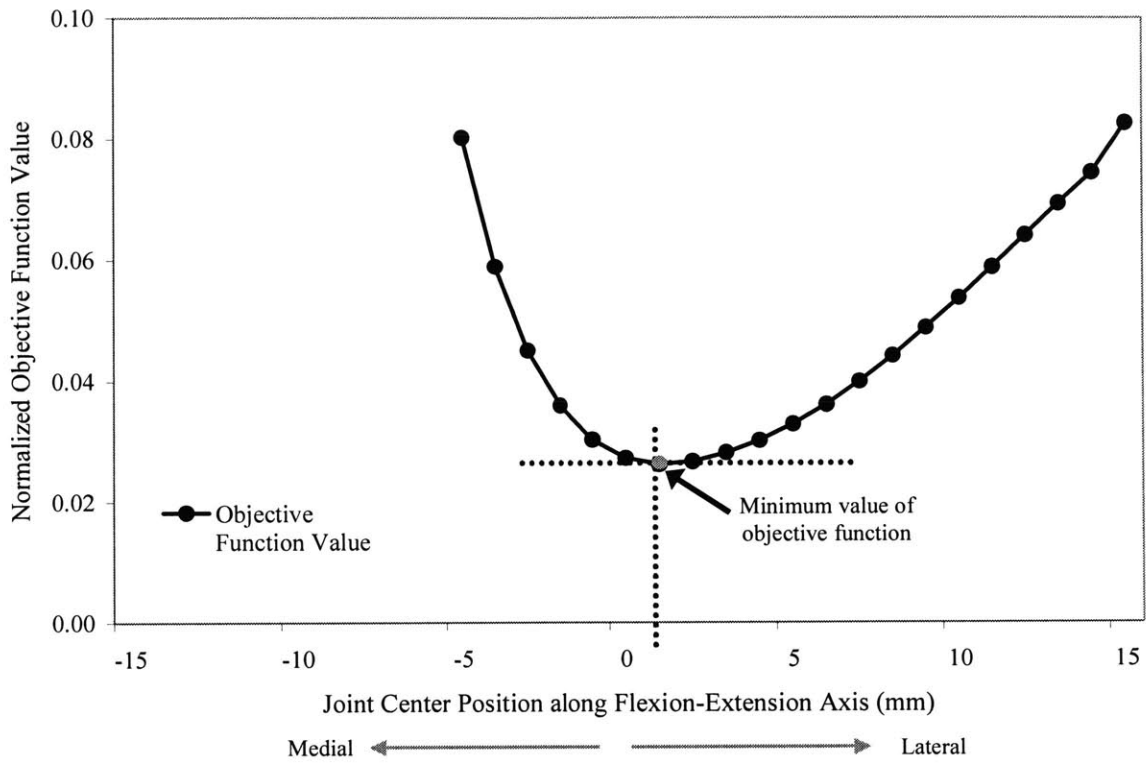
Figure 7-4. The value of the objective function (normalized to the maximum possible sum of the cubic muscle stresses, $6\sigma^3$) was recorded as the joint center location was translated. This objective function reached a minimum value at 1 mm of lateral translation.

$$F = (5 \text{ kg}) \cdot \left(9.81 \frac{\text{m}}{\text{s}^2}\right) \cong 50 \text{ N}$$
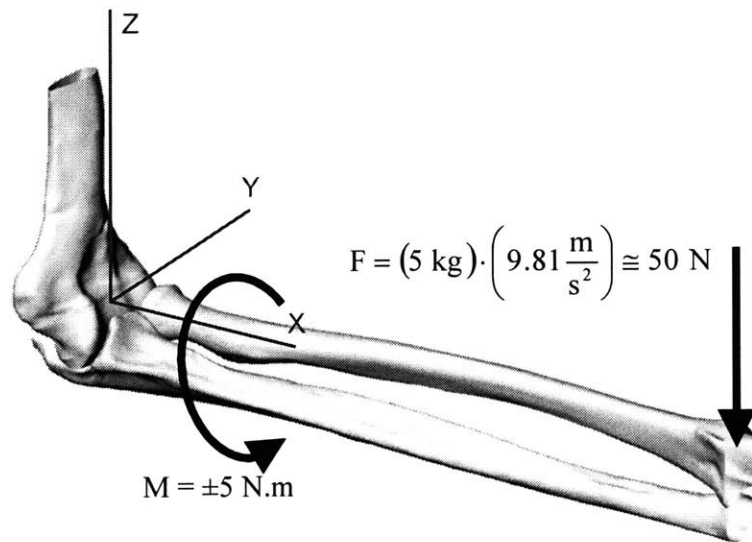
$$M = \pm 5 \text{ N.m}$$

Figure 7-5. Variable loading conditions including an applied moment ±5 N.m about the x-axis and an applied load of ~50N at the distal radius.
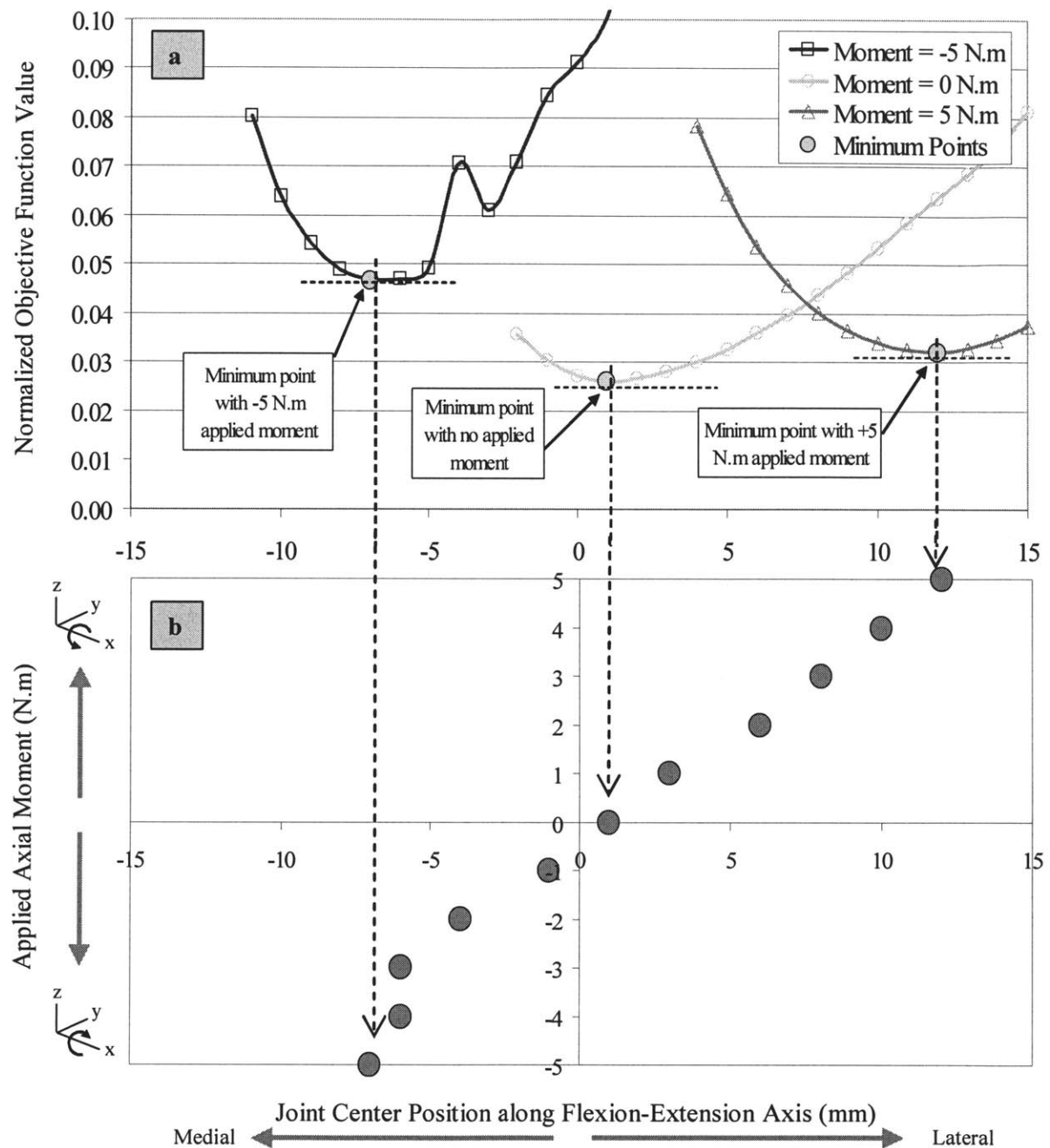
Figure 7-6. External moments ranging from ± 5 N.m were applied to the x-axis of the forearm system. These external loading conditions affected the joint center location at which the objective function reached a minimum value, as depicted for selected loading conditions in (a). The minima locations for the entire range of applied moments (-5 to 5 N.m) can be seen in (b), where negative axial moments were shown to cause a medial shift and positive axial moments a lateral shift in the objective function minima location.

7.2 Joint Center Variation along Humeral Axis

Sensitivity of the joint center location along the humeral, or z, axis was also briefly addressed. The same study was performed, but this time the joint center position along the flexion-extension axis was held constant at the geometric, or trochlea, center, and the z-coordinate of the joint center was varied ±15 mm proximally and distally along the humeral (z) axis. The x-component of the joint center also remained constant.

7.2.1 Muscle Loading Ratios

The change in the values of the muscle loading ratios was recorded as the joint center was varied along the humeral (z) axis (Figure 7-7) under the original loading condition used in the previous sensitivity analysis (50 N load applied at the distal radius and no applied moment). There was no substantial change in any muscle loading ratio value over the entire course of translation (30 mm of overall joint center movement).

7.2.2 Joint Reaction Force

Sensitivity of the joint reaction force to movement of the joint center along the humeral (z) axis, under the same loading conditions (50 N load applied at the distal radius and no applied moment) was also investigated (Figure 7-8). The total magnitude and humeral component of the joint reaction force exhibited similar trends during the joint center movement, showing increased magnitudes as the joint center moved proximally. The magnitude of the joint reaction force increased by 20% over 10 mm of variation as the joint center was translated from 5 mm distal (negative) to 5 mm proximal (positive) of the geometric joint center. The x- and y- components (not shown) exhibited negligible fluctuation during this joint center movement.

77
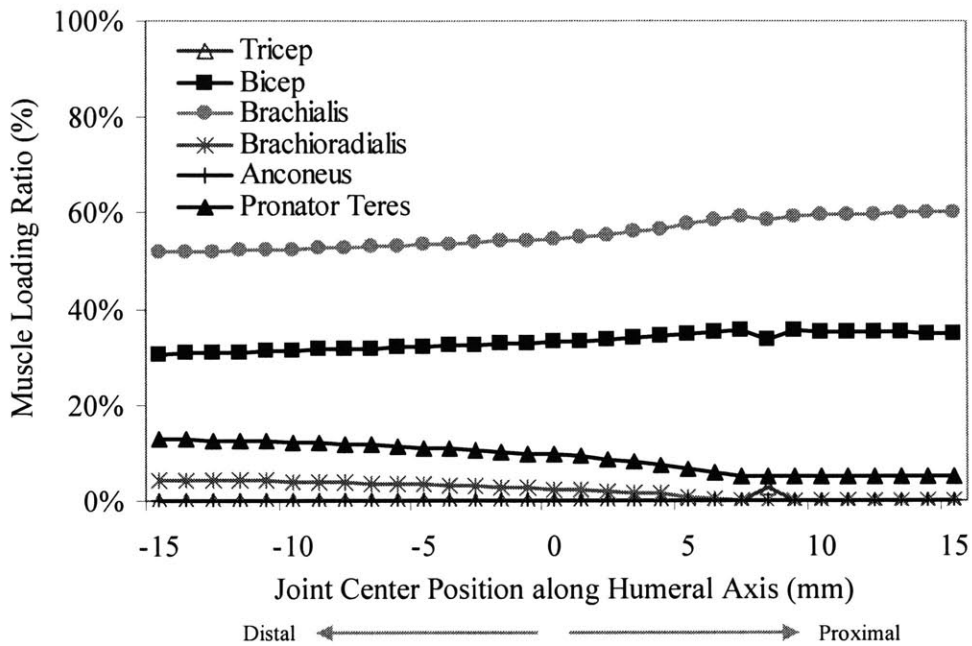
Figure 7-7. Movement of the joint center proximally and distally along the humeral (z) axis resulted in very little change in the predicted muscle loading ratios.
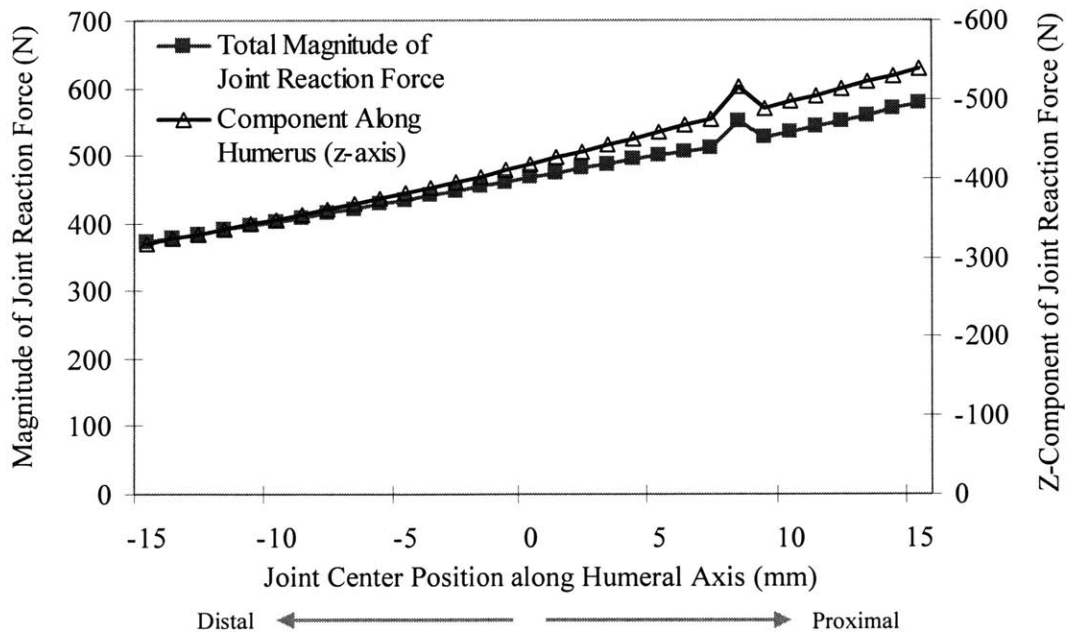
Figure 7-8. This figure depicts the change in the joint reaction force (total magnitude and humeral, or z-axis, component) with proximal and distal variation of the joint center location along the humeral (z) axis (under the condition of a 50 N load applied at the distal radius and no applied moment).

7.3 Automated Joint Center Optimization

The y-coordinate of the joint center was added into the optimization program as an undefined variable, and the optimization determined the muscle forces and then the "y" value that subsequently minimized the objective function. This ability of the optimization program to find a joint center location corresponding to the global minimum of the objective function was tested for various loading conditions. These automatically-calculated y-coordinate locations were compared with global minimum locations found by manually moving the joint center location (as seen in Figure 7-6a). As previously noted, changing the external loading conditions affected the joint center location at which the objective function reached a minimum value (Figure 7-6b). In order to validate this automated joint center optimization process, two sets of data will be plotted in the graphs to follow: the "manual" and the "auto" datasets. The "manual" dataset represents the objective function minimum point as found by manually moving the joint center along the flexion-extension axis. The "auto" dataset represents the joint center location, as calculated by the optimization program. As depicted in the following sections, incorporating the y-variable of the joint center into the optimization yielded almost identical results compared to manually finding the y-variable corresponding to the global minimum.

7.3.1 Constant Force

A constant force was applied at the distal radius either in the direction of gravity (negative z-direction, see Figure 7-9a) or along the axis of the radius (pointing from the distal radius to the geometric joint center, see Figure 7-9b). The corresponding optimized joint center locations, calculated both automatically and manually as the point corresponding to the minimum of the objective function, are summarized in Table 7-1.

Under the external loading condition comprised by a force acting at the distal radius in the direction of gravity (Figure 7-9a) and the weight of the forearm acting at the center of mass, the objective function reached a global minimum at a joint center position of 1.158 and 1.155 mm of lateral translation for the 50 N and 100 N applied forces, respectively.

Likewise, under the loading conditions illustrated in Figure 7-9b, which included an applied load along the radius and no additional loads or moments other than the weight of the limb, the

objective function reached a global minimum at a joint center position of 1.176 and 1.131 mm of lateral translation for the 5 N and 10 N applied forces, respectively.

These automatically calculated or "optimized" joint center locations are plotted along the flexion extension axis, along with the 0 N condition which corresponds to no additional applied loading (other than the weight of the limb), in Figure 7-10.
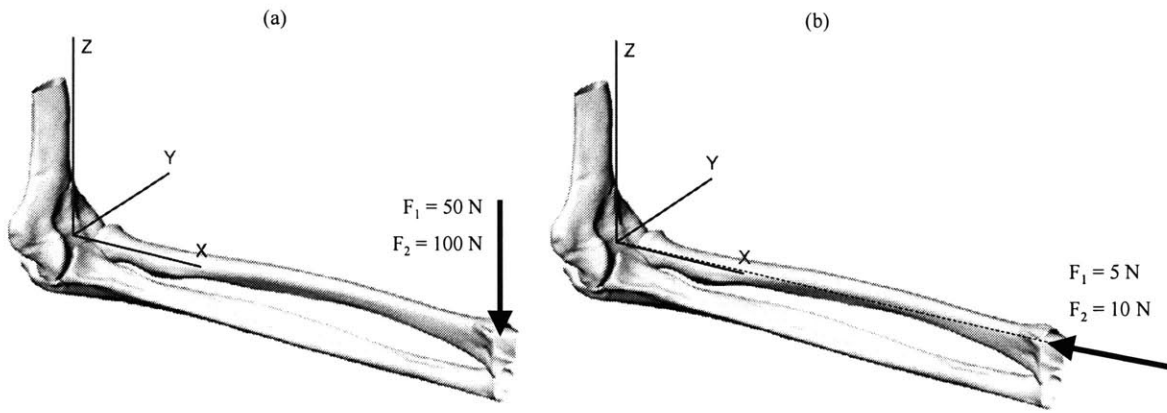
Figure 7-9. A constant load was applied at the distal radius (a) in the direction of gravity with a magnitude of 50 N or 100 N, and (b) acting along the axis of the radius with a magnitude of 5 N or 10 N.

Table 7-1. The joint center location, estimated manually and from the automated program, is shown for various loading conditions.

Symbol	Loading Condition		Joint Center Location (along y-axis)	
	Applied Force [↓]	Applied Force [←]	Automatic	Manual
◊	0	0	1.218	1
□	50 N	0	1.158	1
Δ	100 N	0	1.155	1
○	0	5 N	1.176	1
*	0	10 N	1.131	1

◊ 0 N (No additional loading)
□ 50 N (Applied ↓)
△ 100 N (Applied ↓)
○ 5 N (Applied ←)
✗ 10 N (Applied ←)

1.05   1.10   1.15   1.20   1.25

Joint Center Position along Flexion-Extension Axis (mm)

- - - - - - → Lateral Translation
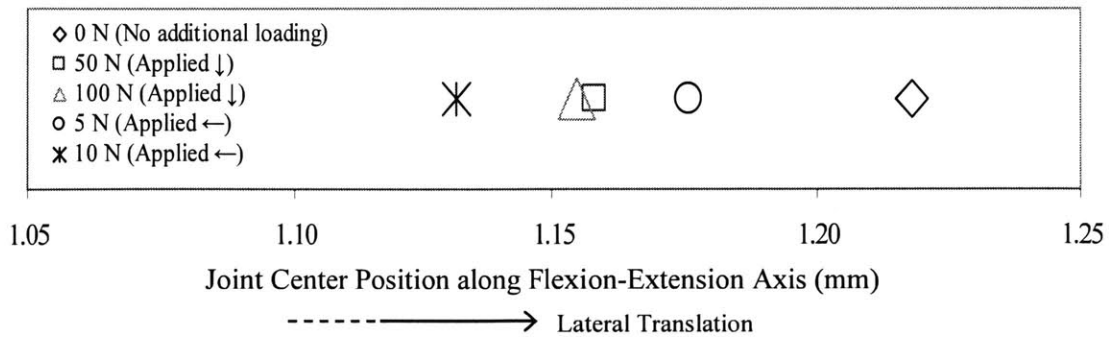
Figure 7-10. Position of optimized joint center, as calculated automatically from the modified optimization program, under various loads applied at the distal radius.

7.3.2 Variable Axial Moment

With an applied axial moment and no externally applied load (other than the weight of the limb), as seen in Figure 7-11, the objective function reached a global minimum at a joint center position ranging from 7 mm of medial translation to 15 mm of lateral translation from the geometric center (Figure 7-12).
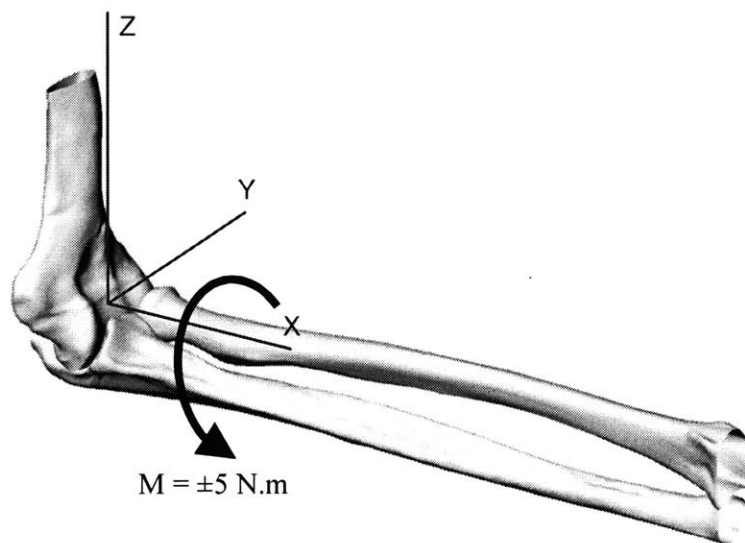
Figure 7-11. A moment was applied about the x-axis of the joint system for values ranging between ± 5 N.m in overall magnitude.

The "manual" dataset in Figure 7-12 corresponds to the objective function minimum points found by manually moving the joint center along the flexion-extension axis, as depicted in Figure 7-6 for a slightly different loading condition. The "auto" dataset represents the joint center location calculated by the optimization program directly, which yielded almost identical results compared to manually finding the y-variable corresponding to the global minimum (Figure 7-12).
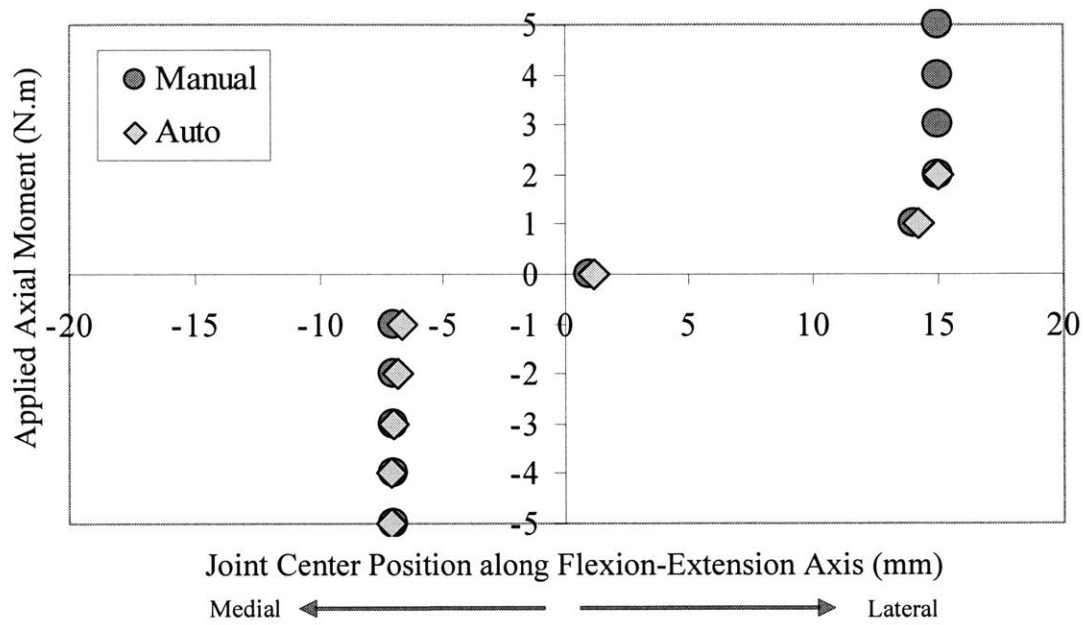
Figure 7-12. External moments ranging from ± 5 N.m were applied to the x-axis of the forearm system, with no additional applied loads other than the weight of the forearm. The "manual" dataset represents objective function minima found by manually moving the joint center along the flexion-extension axis. The "auto" dataset represents objective function minima determined automatically from the optimization.

7.3.3 Combined Loading

A combination of external moments about the x-axis as well as various external loads at the distal radius was applied to the forearm system, and the resulting joint center locations were compared.
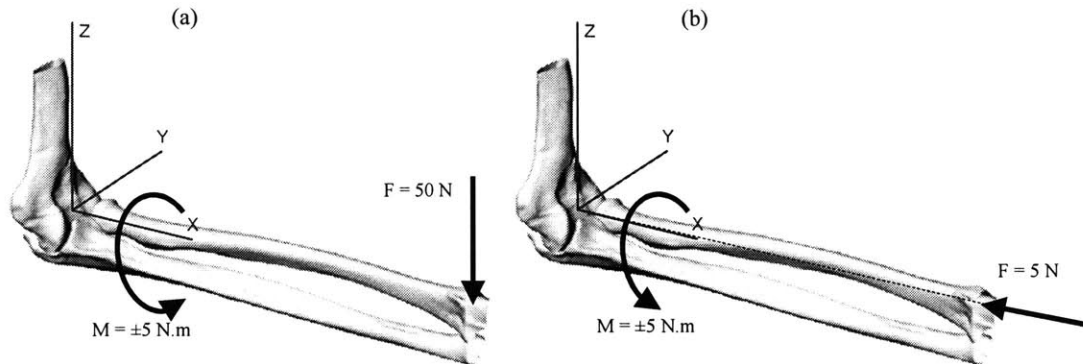
Figure 7-13. The combined loading conditions include an applied axial moment (± 5 N.m) about the x-axis of the joint system and either (a) an applied load (50 N) at the distal radius acting in the direction of gravity or (b) an applied load (5 N) at the distal radius acting along the radial axis.

In the first case, depicted in Figure 7-13a, external moments ranging from ± 5 N.m were applied to the x-axis of the forearm system, in addition to the 50 N force applied in the direction of gravity at the distal radius (Figure 7-13a) and the weight of the limb. The joint center location corresponding to the objective function minimum translated from 7 mm medial to 12 mm lateral over the course of these loading conditions (Figure 7-14).

In the second case, depicted in Figure 7-13b, the variable axial moment was combined with a 5 N applied load acting along the radius. Under these loading conditions, the objective function reached a global minimum at a joint center position ranging from 7 mm of medial translation to 15 mm of lateral translation, as seen in Figure 7-15.
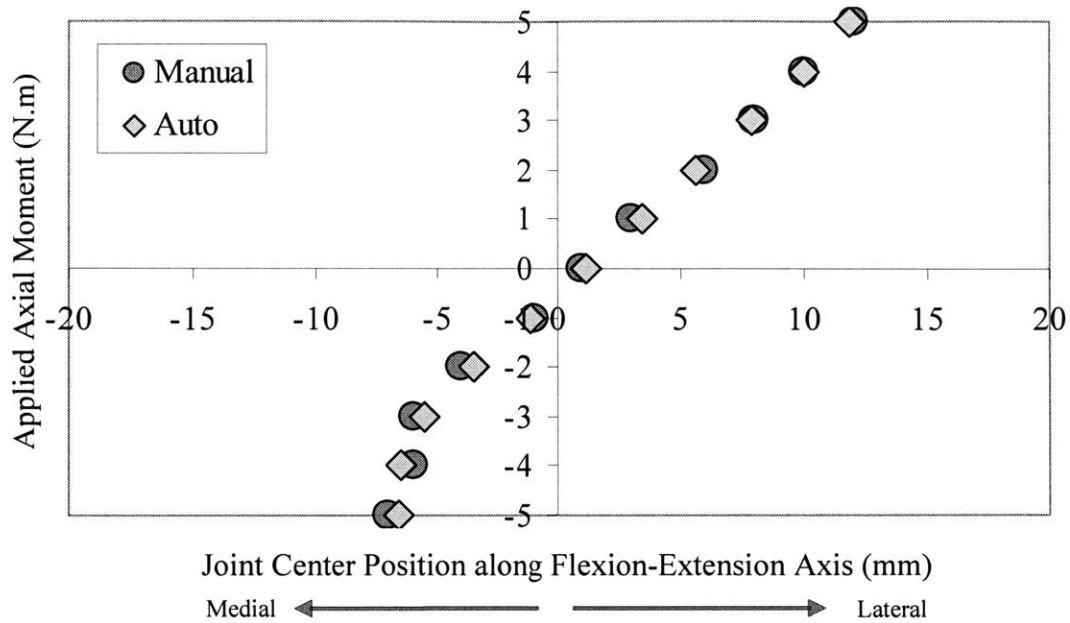
Figure 7-14. External moments ranging from ± 5 N.m were applied to the x-axis of the forearm system, with a 50 N load applied at the distal radius in the direction of gravity. The "manual" dataset represents objective function minima found by manually moving the joint center along the flexion-extension axis. The "auto" dataset represents objective function minima determined automatically from the optimization.
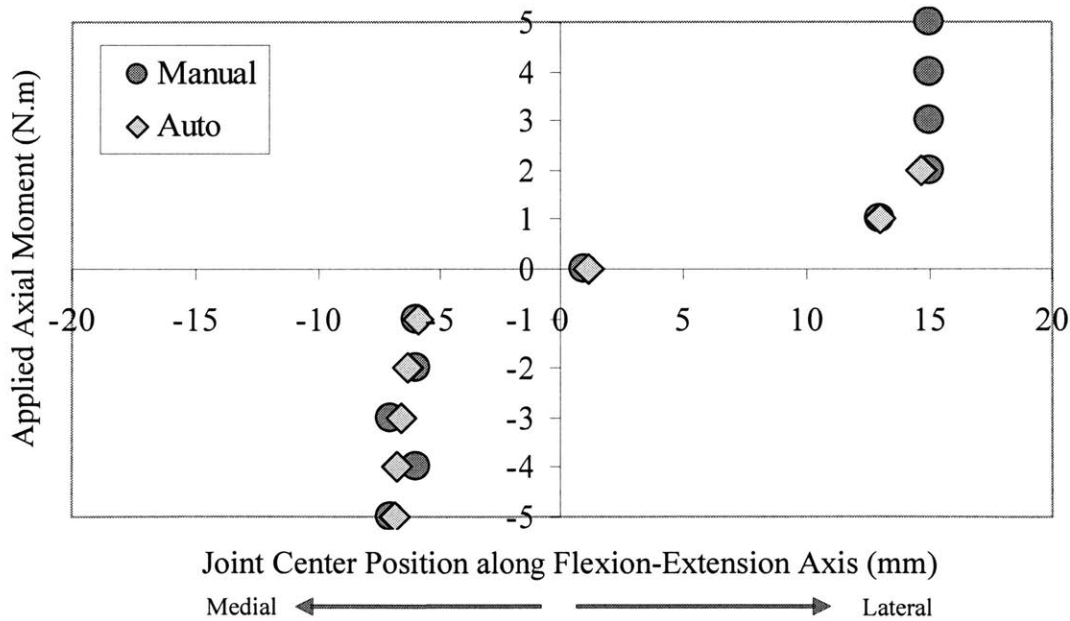
Figure 7-15. External moments ranging from ± 5 N.m were applied to the x-axis of the forearm system, with a 5 N load applied at the distal radius along the axis of the radius. The "manual" dataset represents objective function minima found by manually moving the joint center along the flexion-extension axis. The "auto" dataset represents objective function minima determined automatically from the optimization.

Chapter 8: Discussion

This study utilized an elbow joint model to perform a parametric analysis of the effect of joint center location on predicted muscle and joint force distributions. The experimental results described previously demonstrate that the prediction of muscle and joint force distributions varied with the selection of the joint center location (origin of the coordinate system) using the current optimization methodology. Neglecting the joint reaction moment in the moment constraint condition of Equation 1-8b violates the moment equilibrium equations of Equation 1-5b unless a true joint rotation center is found at which the joint reaction moment is, in reality, equal to zero.

Section 8.1 addresses the assumptions behind the historical elimination of the joint reaction moment, and the subsequent consequences of that assumption. Then, Section 8.2 gives a brief background on the approach used to define the joint center or coordinate system origin in the past, as well as the current research which supports the theory that the joint center should not be represented as a fixed point over the course of joint flexion. The results discussed in Section 8.3 address the muscle and joint forces predicted during one-dimensional movement of the coordinate system origin (joint center) either along the flexion-extension axis (Section 8.3.1) or humeral axis (Section 8.3.2) of the elbow joint. The potential for variation between results obtained using different objective functions was addressed in Section 8.4. Additionally, the joint center location should vary in 3D space, not only one-dimensionally as simulated in Section 8.3.1 and Section 8.3.2. Thus, three more variables will need to be introduced into the optimization procedure if the optimized joint center location is to be defined by the minimization of the objective function (see Section 8.5). Lastly, the clinical relevance of this thesis research is briefly addressed in Section 8.6.

8.1 Zero Joint Reaction Moment Assumption

It is noted that the joint reaction moment, $\bar{M}^{Joint}$, was set to zero in the moment constraint condition of Equation 1-8b, as is customary in joint optimization methods [9, 15, 25, 26, 32]. Such an assumption is similar to modeling the joint as a frictionless pure rotation joint with its center located at the origin of the coordinate system [26], thus representing an additional constraint to the optimization procedure, i.e. $\bar{M}^{Joint} = 0$.

The selection of the joint center may therefore directly affect the moment constraint conditions since the muscle force moment arms and the intersegmental moment both vary with changing joint center location. An inaccurate selection of the joint center, where the joint reaction moment is actually not zero, may lead to unrealistic muscle force predictions using the stated optimization procedure (Equations 1-5 and 1-8).

Thus, if the joint reaction moment is included in the moment constraint equation, the optimization program will yield the trivial solution and set all muscle forces to zero in order to satisfy the moment constraint condition. However, if the joint reaction moment is set to zero, the predicted muscle forces may not reflect true physiological loading conditions.

8.2 The Case for a Moving Joint Center Location

The location of the joint center corresponding to zero joint reaction moment is unknown for a given musculoskeletal joint. Establishment of the coordinate system of the joint has historically relied on the anatomy of the specimen. In elbow joint models, the general consensus was that the joint center, or origin of the coordinate system, was defined within the trochlea. Deland et al. [90] defined the axis of elbow rotation as the axis bisecting the humeral and forearm axes with the arm in extension. This axis was found to approximate the center of the trochlea and capitulum. An et al. [5], Bottlang et al. [71], and Fischer [91] all defined the origin of the forearm system at the center of the trochlea. Morrey and Chao [70] established that a single point approximating the instantaneous center of rotation of the elbow lies on a line passing through the center of the trochlea.

However, in the 1970's Ewald [92] and Ishizuki [93] noted that the axis of rotation changes with flexion, concluding that the elbow is not a simple fixed hinge joint [67]. This concept that the joint center location varies during flexion was further supported in a recent study by Bottlang et al. [71], which showed that the rotation center of the elbow joint may be located over 20 mm medial to the lateral border of capitulum (medial border of the trochlear facet) during passive flexion. Furthermore, Li et al. illustrated in a recent study of high flexion knee kinematics that

94

the knee joint center also varies location during flexion, experiencing over 30 mm of anterior tibial translation over the course of the flexion activity [94].

Thus, the joint position and flexion angle will play a major role in defining the location of the coordinated system origin (joint center), as will the particular loading condition for the modeled activity (as addressed in Section 8.3.1).

8.3 Variable Joint Center Location

The results discussed in this section (Section 8.3) are limited to the case in which the joint center location was moved in one-dimension either along the flexion-extension axis of the elbow joint (Section 8.3.1), or along the humeral axis (Section 8.3.2).

8.3.1 Joint Center Variation along Flexion-Extension Axis

The muscle loading ratios and joint reaction forces, as well as the objective function minima, were shown to be sensitive to the coordinate system origin location as it was translated medially and laterally along the flexion-extension axis of the forearm.

8.3.1.1 Effect of Location on Muscle and Joint Forces

The predicted muscle loads were highly sensitive to the coordinate system origin (joint center) location (Figure 7-2), as reported in Section 7.1.1. The movement of the joint center laterally resulted in an increase in the moment arm of the BRA muscle since it has an insertion point on the ulna. Likewise, movement of the joint center medially resulted in an increase in the moment arms of the BIC and BRD muscles, both of which have radial insertions. As the moment arms of the muscles decrease, the amount of load needed to sustain the moment equilibrium will increase, provided that there is no joint reaction moment contributing to (or restoring) this equilibrium state. Therefore, a movement of the joint center away from the insertion point of a muscle will result in a decrease in the loading level of that muscle. This can be seen in Figure 7-2 where, for example, the BRA decreased from an 80% loading ratio when the joint center was located at 5 mm medial to the geometric center, to exerting only 34% of the total muscle load when the joint center was 5 mm lateral to the geometric center, due to the increase in BRA moment arm with medial-to-lateral joint center location movement.

Joint center movement along the flexion-extension axis (Section 7.1.2) produced a substantial change in the overall magnitude and humeral (z-axis) component of the joint reaction force (Figure 7-3). For instance, translation of the joint center location from a position 5mm medial to 5mm lateral of the geometric center (a total of 10 mm of translation) resulted in a 25% decrease in the magnitude of the joint reaction force. Joint force values are often used, for instance, in the design and testing of total joint replacements (e.g. joint implants). A significant under- or over-estimation of the joint loads, as predicted if the joint center is not properly defined at the true rotation center, may produce completely erroneous results and could possibly lead to the development of unsound devices incapable of withstanding actual physiological loading conditions.

8.3.1.2 Effect of Location on Objective Function Minima

• Fixed loading condition

It is interesting to note that while displacing the joint center location altered the magnitude of the predicted muscle loads (Section 7.1.1), it also altered the value of the objective function even though the loading condition remained unchanged (Section 7.1.3). There is a point corresponding to a minimum of the objective function values along the flexion-extension axis of the elbow joint as shown in Figure 7-4. If the joint center location is used as an additional variable in the optimization procedure, a convergent solution can be obtained that represents the minimum of the objective function (see Section 8.5).

• Variable loading conditions

When an additional negative moment was applied about the x-axis, the minimum of the objective function shifted medially (Figure 7-6). As an increasingly positive moment was applied about the x-axis, the minimum of the objective function shifted laterally. This data implied that the joint center location may also depend on the loading conditions and indicated that it is necessary to determine the true rotation center location in order to accurately calculate the muscle loads in response to various external loading conditions using a static optimization method.

8.3.2 Joint Center Variation along Humeral Axis

The coordinate system origin location was translated proximally and distally along the humeral (z) axis of the elbow joint system, and the response of the muscle loading ratios and joint reaction force values were studied. This movement resulted in insignificant variations in the muscle loading values (Figure 7-7). This suggests that the position of the joint center along the flexion-extension axis is much more critical for load predictions. However, as the joint center was varied along the humeral (z) axis, the joint reaction force exhibited a considerable change in its overall magnitude and humeral (z-axis) component (Figure 7-8), which will require further investigation.

8.4 Different Objective Functions

This study used one objective function for the calculation of muscle loads. Li et al. [26] tested different objective functions in a 3D inverse dynamic optimization model and found that they all predicted nearly identical muscle forces in the optimization procedure when the knee was simulated as a three-dimensional ball-and-socket joint. It was concluded that the objective functions can be used interchangeably [26]. Glitsch and Baumann [15] also noted that muscle recruitment in a lower extremity model was more dependent on the three-dimensional external loading condition and anatomy than on the choice of any nonlinear cost function. Similarly, Patriarco et al. [29] concluded that improvements on existing optimization approaches were more crucially dependent on the accurate measurement of joint angles and torques than on the particular optimization criteria employed. Raikova and Prilutsky [33] reported that muscle force magnitudes calculated by several different nonlinear cost functions were similar in value. Additional investigations should examine if various objective functions will show a similar response to the variation of the joint center locations.

8.5 Improvements to Current Inverse Optimization Methods

The current optimization method used to predict muscle and joint forces in the human body must be reformulated in order to predict accurate and physiologically relevant forces. It is proposed that this can be accomplished in one of two ways:

(1) The joint reaction moment can be added back into the moment constraint equation, thereby making the equation valid, once again, for any joint center location. This would

be a wonderful option; however, unless a new objective function is formulated that includes the components of the joint reaction moment, only the trivial solution will be obtained for this problem (i.e. all the muscle forces will be set to zero to satisfy the moment equilibrium). Additionally, if a new objective function is formulated, it needs to minimize some physiologically relevant parameter, such as the energy of the system. This will open up a heated debate regarding the validity and reasonableness of this newly formulated objective function.

(2) The second option is that the joint reaction moment can be left out of the moment constraint equations, as before, except that the optimization program will now be required to find the "true rotation center" where setting the joint reaction moment to zero is a valid assumption. The joint center location will vary in 3D space as the flexion angle, joint position, and external loading conditions change. In order to identify an optimum joint center location, defined by the minimum point of the objective function, three more variables will need to be introduced into the optimization procedure. The three coordinates of the joint center location will be determined in the process of solving for the muscle and joint reaction forces. The question that naturally arises out of this formulation is: "Does the objective function minimum point correspond to the 'true rotation center' of the joint, where the joint reaction moment is zero?" This will need to be addressed in a future study utilizing motion tracking devices or some other means of capturing the rotation center movement.

After analyzing these two options, the second option appeared to be the easiest to implement in this model. Rather than adding all three variables into the optimization all at once, a sensitivity study incorporating only the y-component of the joint reaction moment into the optimization was performed.

There is a point corresponding to a minimum of the objective function values along the flexion-extension axis of the elbow joint, as shown in Figure 7-4 and Figure 7-6. If the joint center (coordinate system origin) location is used as an additional variable in the optimization procedure, a solution for the new origin location can be obtained that represents the location of the minimum of the objective function. The y-component of the joint center was added as a variable into the optimization program. The optimization program then output not only the

98

predicted muscle and joint reaction forces, but also the y-component of the coordinate system origin. The ability of the program to find a joint center location corresponding to the global minimum of the objective function was tested for various loading conditions (Section 7.3). These results were compared with global minimum locations found by manually moving the joint center location. As seen in Figure 7-14, for instance, the automatically calculated joint center locations corresponded very well with those manually determined. In fact, for all loading schemes depicted in Section 7.3, the automatic and manual datasets coincided almost exactly, suggesting that the optimization program can accurately find the joint center location corresponding to the objective function minimum. If the joint center had been manually moved in increments smaller than 1 mm, the "manual" and "auto" results would have coincided with increased accuracy. Thus, this method of incorporating the joint center as three variables into the optimization program is very promising for reformulating the inverse optimization methods of the past and bodes well for the future of in vivo muscle load predictions.

8.6 Clinical Relevance

The current elbow joint prostheses were designed under the assumption that the elbow joint can be approximated as a simple hinge. Thus, when studying the elbow under a hinge assumption, a two-dimensional analysis is sufficient. To study the effects of joint center location in a 2D study, the equilibrium equations reduce to one moment and two force equations. Using these three equilibrium equations as constraints, along with the lower and upper bounds on muscle force (Equation 1-8c), a 2D sensitivity analysis was performed. As seen in Figure 8-1a, the joint center location was varied along the humeral or z-axis of the forearm system. Likewise, in Figure 8-1b, the joint center location was varied along the x-axis of the forearm system.

Movement of the joint center along the x-axis of the system resulted in a greater change in the muscle loading and joint reaction force magnitudes than joint center movement along the z-axis. For instance, 10 mm of movement along the z-axis (from 5 mm distal to 5 mm proximal of the geometric center) resulted in a 17% increase in the BIC loading ration, 14% increase in the BRA loading ratio, and 15% increase in the joint reaction force magnitude (Figure 8-1a). The same amount of movement of the joint center along the x-axis (10 mm) from 5 mm posterior to 5 mm anterior of the geometric joint center resulted in increases that were almost double in value

compared to those found during z-axis joint center translation. The BIC and BRA exhibited a 38% and 21% increase, respectively, and the joint reaction force magnitude increased by 33% over the 10 mm of translation (Figure 8-1b). Based on these observations, the joint center location is much more sensitive to positioning along the x-axis of the system, and thus extra care should be given to ensure correct x-axis placement of the hinge center when installing hinged elbow joint replacements and other such devices.
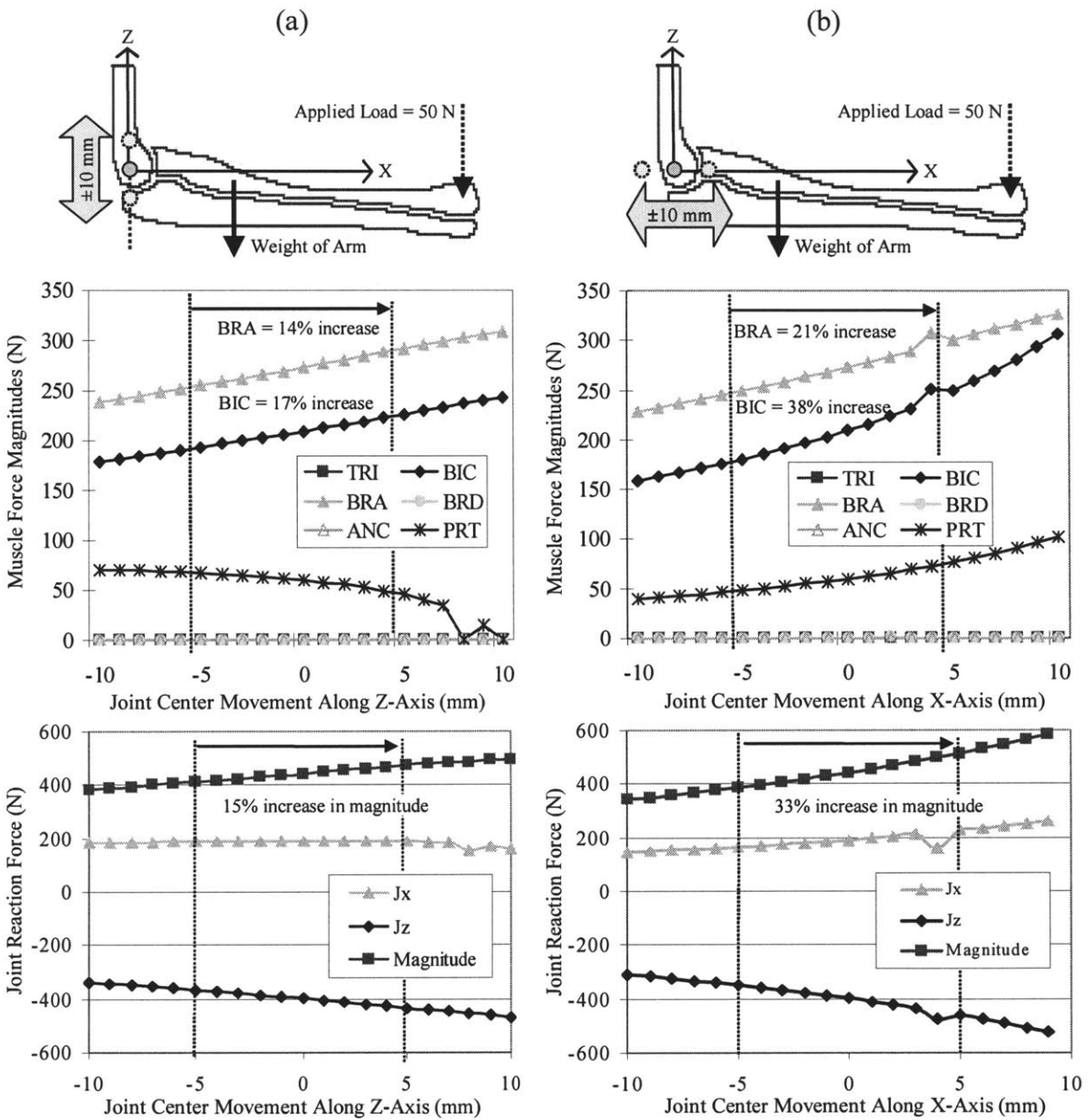
Figure 8-1. Two-dimensional sensitivity analysis. The joint center was varied along the z-axis (a) and along the x-axis (b) to determine how sensitive the predicted muscle and joint force were to the joint center location.

Chapter 9: Conclusions and Future Work

9.1 Conclusion

The results presented in this thesis have suggested that the rotation center of the joint may vary its position with both the kinematics and kinetic conditions, and further implied that previous optimization procedures in literature, as outlined in Equation 1-5 and 1-8, are coordinate system dependent and may not provide an accurate prediction of muscle and joint reaction forces if the selected joint center does not satisfy the zero joint reaction moment condition. Forcing the joint reaction moment to be zero in the optimization procedure violates the equilibrium conditions of the joint. It is unknown if the joint center location corresponding to the minimum of the objective function value is representative of the true rotation center. A further study is required to investigate the relationship between the optimized origin location and the true rotation center (where the zero joint reaction moment condition is satisfied) before the coordinate system origin can be included as a variable in the optimization procedure. If this relationship is verified and the joint center location can be incorporated into the optimization and solved by means of minimizing the objective function, then the age-old problem of joint optimization will finally be coordinate system independent. It is also important to note that only several simple loading conditions were considered for these parametric analyses. Future studies should include loading at physiological levels to better understand the movement of the joint center location. This entire thesis work has been conducted purely from a mechanical point of view in order to analyze the theory behind inverse optimization of a joint system. In no way were conclusions made regarding the correctness of the muscle force magnitudes or joint reaction forces as of yet.

9.2 Future Work

9.2.1 Advanced EMG Studies

In order to obtain a more comprehensive picture concerning the number of muscles activated during specific flexion activities, it is proposed that fine wire EMG studies be carried out on a larger number of subjects (i.e. N>2, since that was the number of subjects in this validation study). These sub-surface EMG studies will enhance the accuracy of the signal results by reducing crosstalk between muscles and noise in the signal.

9.2.2 Rotation Center Validation

Validation of the new methodology of incorporating the joint center location as three variables into the optimization itself must be performed to ensure that the objective function global minimum corresponds to the location of the rotation center. Using a dual-imaging technique, as formulated by Li et al. [95], the helical axis can be calculated at different flexion angles and positions to study joint center movement during various functional activities.

9.2.3 Experimental Studies

Once the model predictions are validated using the improved EMG data, and the new optimization methodology is validated by the dual-imaging technique, the muscle loading ratios can be determined for various flexion angles, joint positions, and loading scenarios. Knowledge of these physiological loading ratios can then be used to perform experimental tests on cadaveric specimens using the robotic testing system described in Chapter 4.2.1. Some areas of interest include studying the interosseous ligament function in regards to load transfer between the radius and the ulna, and the ability of current radial head replacements and total elbow replacements to restore normal joint kinematics.

104

Appendices

Appendix A: Rigid Body Mechanics

This appendix briefly covers the derivation of the rigid body motion equations [46, 96], set forth by Newton's laws of motion (Section 1.2). The term "rigid body" refers to an object that is not deformable, requiring that the distance between every pair of points in the body remains constant (i.e. the body does not change shape). The humerus and forearm were both modeled as rigid bodies in the course of this work. The equilibrium conditions utilized in this thesis work applied the same equations derived below, except all acceleration terms were set to zero to accommodate the static conditions of the model.

The second law is generalized here for a rigid body system, composed of N particles, bounded by a closed surface (Figure A-1).
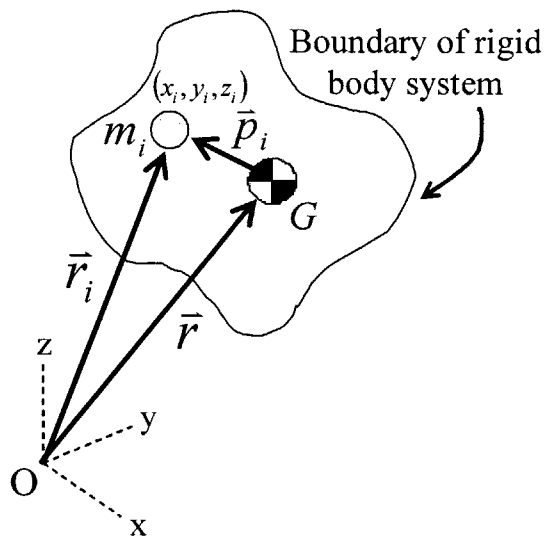
Figure A-1. Description of the rigid body system of n particles, each having a unique mass m_i, with the origin of the coordinate system centered at point O.

Let m_i be the mass of the i th particle of a rigid body, and thus the summation of these particles, $\sum_{i=1}^{n} m_i$, represents the total mass, m, of the system. The position particle i relative to a fixed reference point O is denoted by $\vec{r}_i$, the force of particle j on particle i is $\vec{f}_{ij}$, the external force on

107

particle i from something other than another particle is $\bar{f}_i^E$, the velocity of particle i is denoted by $\bar{v}_i$ and its acceleration by $\bar{a}_i$. The center of mass of the system is denoted by G with position vector $\bar{r}$, and the position of particle i with respect to G is given by the vector $\bar{p}_i$.

A.1 Force Equilibrium

Newton's Second Law states that the sum of the forces acting on a particle is equal to the rate of change of the linear momentum, or product of mass and velocity, of that particle. So, summing over the N particles in the rigid body system, the second law can be written as

$$\sum_i \sum_j \bar{f}_{ij} + \sum_i \bar{f}_i^E = \frac{d}{dt} \sum_i m_i \bar{v}_i = \left(\sum_i m_i \right) \left(\sum_i \frac{d\bar{v}_i}{dt} \right) = m \left(\sum_i \bar{a}_i \right) = m\bar{a}, \qquad (A\text{-}1)$$

where, assuming mass remains constant, $\bar{a} = \sum_{i=1}^{N} \bar{a}_i$ denotes the linear acceleration of the system

of particles, or the rigid body. By Newton's third law, which states that $\bar{f}_{ij} = -\bar{f}_{ji}$, the sum of the internal forces on the system is zero:

$$\sum_i \sum_j \bar{f}_{ij} = \bar{f}_{12} + \bar{f}_{21} + \bar{f}_{13} + \bar{f}_{31} + \cdots = 0. \qquad (A\text{-}2)$$

Thus, rewriting the sum of the external forces as $\sum_{i=1}^{N} \bar{f}_i^E = \sum \bar{F}$, we obtain the general equation

of motion ,

$$\sum \bar{F} = m\bar{a}, \qquad (A\text{-}3)$$

relating the external forces to the acceleration of the center of mass for a system of particles or any collection of objects, including a rigid body:

A.2 Moment Equilibrium

The relationship between the total moment exerted on the system and its angular momentum is now derived. The position vector of particle i relative to O can be written in an alternative form, $\bar{r}_i = \bar{r} + \bar{p}_i$, using simple vector addition properties. The angular momentum about the system's

108

center of mass is denoted by H, where $\vec{H} = \sum_{i=1}^{N} \vec{p}_i \times m_i \vec{v}_i$. Now, by definition of the center of

mass, we know that $\sum_{i=1}^{N} m_i \vec{p}_i = 0$, thus giving rise to the following expression

$$\vec{H}_O = \sum_{i=1}^{N} \vec{r}_i \times m_i \vec{v}_i = \sum_{i=1}^{N} (\vec{r} + \vec{p}_i) \times m_i \vec{v}_i$$

$$= \sum_{i=1}^{N} \vec{r} \times m_i \vec{v}_i + \sum_{i=1}^{N} \vec{p}_i \times m_i \vec{v}_i = \vec{r} \times m\vec{v} + \vec{H}$$

(A-4)

describing the total angular momentum of the entire system of particles about point O.

Now to relate the total angular momentum to the total moment exerted on the system, recall that the moment is equal to the cross product of the position vector and force vector (i.e. $\vec{M} = \vec{r} \times \vec{f}$). Thus, using the position vector $\vec{r}_i$ and the force-linear momentum description of the second law, defined earlier (Equation A-1), the following equation is obtained:

$$(\vec{r}_i) \times \left(\sum_i \sum_j \vec{f}_{ij} + \sum_i \vec{f}_i^E = \frac{d}{dt} \sum_i m_i \vec{v}_i \right) \qquad \text{(a)}$$

$$\Rightarrow \sum_i \vec{r}_i \times \frac{d}{dt}(m_i \vec{v}_i) = \sum_i \left[\frac{d}{dt}(\vec{r}_i \times m_i \vec{v}_i) - \vec{v}_i \times m_i \vec{v}_i \right] \qquad \text{(b)}$$

(A-5)

$$\Rightarrow \sum_i \vec{r}_i \times \frac{d}{dt}(m_i \vec{v}_i) = \frac{d\vec{H}_O}{dt} \qquad \text{(c)}$$

$$\Rightarrow \sum M_O = \frac{d\vec{H}_O}{dt} \qquad \text{(d)}$$

Assuming that the rigid body rotates about the fixed point O, we can generalize Equation A-5d to the following:

$$\sum \vec{M}_O = I_O \vec{\alpha} \qquad \text{(A-6)}$$

where the total moment about O is equal to the product of the mass moment of inertial about O, I_O, and the angular acceleration of the rigid body, $\vec{\alpha}$.

Thus, the equations that govern rigid body motion can be summed up by Equation A-3 and Equation A-6, and for a static system, the linear ($\bar{a}$) and angular ($\bar{\alpha}$) accelerations of the body can be set to zero, yielding Equation 1-4 (also summarized below):

$$\left.\begin{array}{l} \sum \bar{F} = m\bar{a} \\ \sum \bar{M} = I\bar{\alpha} \end{array}\right\} \text{ for static systems yields} \Rightarrow \left\{\begin{array}{l} \sum \bar{F} = 0 \\ \sum \bar{M} = 0 \end{array}\right. . \tag{A-7}$$

Appendix B: Two-Dimensional Static Equilibrium Examples

Below are several versions of a two-dimensional planar static flexion problem which demonstrate how to solve a determinate static equilibrium problem (Example 1) and the troubles encountered when there are too many muscles forces (Example 2).

Example 1:

The brachialis muscle force, denoted by F_{BRA}, has a moment arm, d_a, equal to 3 cm. The angle of the muscle line of action with respect to the x-axis, θ_a, is 70°. The weight of the arm, acting purely in the negative y-direction, is 10 N, and the applied load at the distal radius, also acting in the negative y-direction, is 25 N. The distances between the joint center and the location of these two external loads are 12 cm and 30 cm, respectively. See Figure B-1 for a schematic of this system.
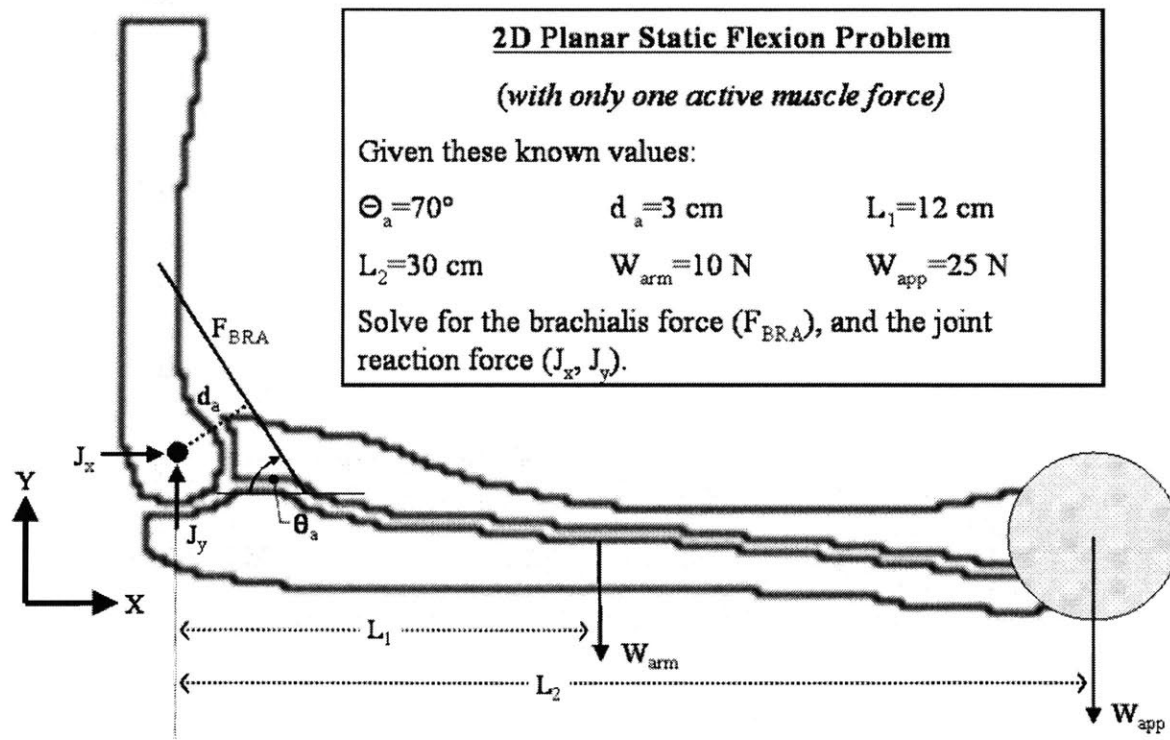
Figure B-1. Two-dimensional static flexion example involving only one muscle force, the brachialis, and two known external loads, the weight of the arm and an applied load at the distal radius. The two components of the joint reaction force are also unknown values.

First, one must establish the static equilibrium conditions of the system (Equations 1-4 and 1-5). Since this is a two-dimensional problem, equilibrium analysis will yield three equations: two force and one moment equations. The force equilibrium equations ($\Sigma F = 0$) for this static two-dimensional system can be seen, in scalar form, in Equations B-1 and B-2. The moment equilibrium equation about the joint center ($\Sigma M_{JointCenter} = 0$), also in scalar form, can be seen in Equation B-3.

Force equilibrium in the x-direction: $J_x - F_{BRA} \cdot \cos(\theta_a) = 0$ (B-1)

Force equilibrium in the y-direction: $J_y + F_{BRA} \cdot \sin(\theta_a) - W_{arm} - W_{app} = 0$ (B-2)

Moment equilibrium about the joint center: $d_a \cdot F_{BRA} - L_1 \cdot W_{arm} - L_2 \cdot W_{app} = 0$ (B-3)

Solving Equation B-3 for F_{BRA}:

$$F_{BRA} = \left(L_1 \cdot W_{arm} + L_2 \cdot W_{app}\right)/d_a$$
$$= \left(12\,cm \cdot 10\,N + 30\,cm \cdot 25\,N\right)/3cm$$
$$= 290\,N$$

Solving Equation B-1 for J_x:

$$J_x = F_{BRA} \cdot \cos(\theta_a)$$
$$= 290\,N \cdot \cos(70)$$
$$= 99.2\,N$$

Solving Equation B-2 for J_y:

$$J_y = -F_{BRA} \cdot \sin(\theta_a) + W_{arm} + W_{app} =$$
$$= -290\,N \cdot \sin(70) + 10\,N + 25\,N$$
$$= -237.5\,N$$
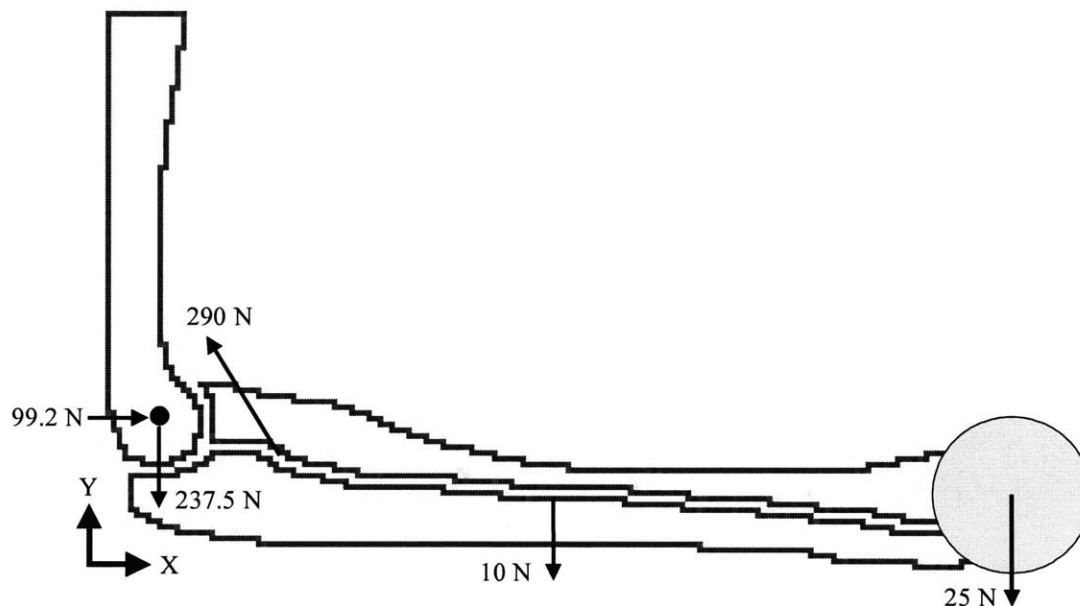
Thus, the magnitude of the joint reaction force, J, can be calculated as follows:

$$J = \sqrt{(J_x)^2 + (J_y)^2}$$
$$= \sqrt{(99.2\ N)^2 + (-237.5\ N)^2}$$
$$= 257.4\ N$$

Example 2:

The brachialis (F_{BRA}), biceps (F_{BIC}), and brachioradialis (F_{BRD}) muscle forces have moment arms d_a=3 cm, d_b=4 cm, and d_c=7 cm, respectively. The angle of the muscle lines of action with respect to the x-axis are θ_a=70°, θ_b=70°, θ_c=70°, for the brachialis, biceps, and brachioradialis, respectively. The weight of the arm, acting purely in the negative y-direction, is 10 N, and the applied load at the distal radius, also acting in the negative y-direction, is 25 N. The distances between the joint center and the location of these two external loads are 12 cm and 30 cm, respectively. See Figure B-2 for a schematic of this system.
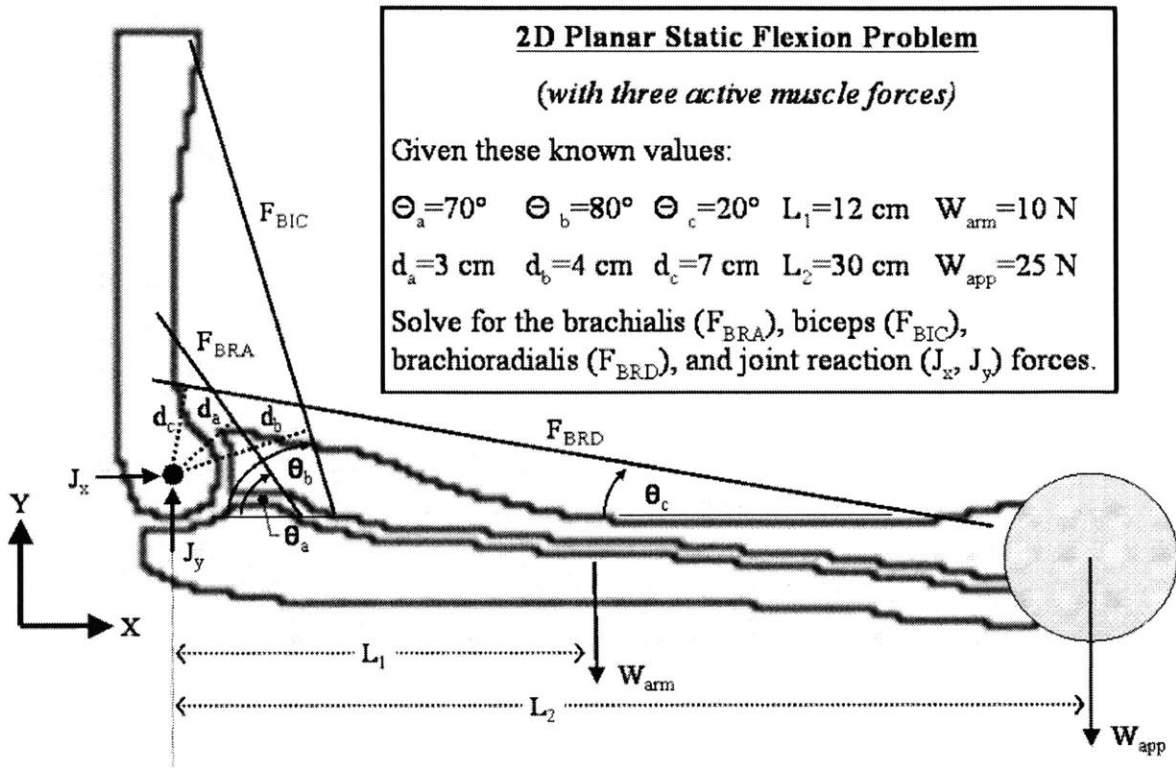
Figure B-2. This two-dimensional static flexion problem involves three muscle forces (brachialis, biceps, and brachioradialis) and two known external loads, the weight of the arm and an applied load at the distal radius. The two components of the joint reaction force are also unknown values.

First, one must again establish the static equilibrium conditions of the system (Equations 1-4 and 1-5). The equilibrium analysis will again yield three equations (two force and one moment equations). The force equilibrium equations ($\Sigma F = 0$) for this static two-dimensional system can be seen, in scalar form, in Equations B-4 and B-5. The moment equilibrium equation about the joint center ($\Sigma M_{JointCenter} = 0$), also in scalar form, can be seen in Equation B-6.

Force equilibrium in the x-direction:

$$J_x - F_{BRA} \cdot \cos(\theta_a) - F_{BIC} \cdot \cos(\theta_b) - F_{BRD} \cdot \cos(\theta_c) = 0 \qquad \text{(B-4)}$$

Force equilibrium in the y-direction:

$$J_y + F_{BRA} \cdot \sin(\theta_a) + F_{BIC} \cdot \sin(\theta_b) + F_{BRD} \cdot \sin(\theta_c) - W_{arm} - W_{app} = 0 \qquad \text{(B-5)}$$

Moment equilibrium about the joint center:

$$d_a \cdot F_{BRA} + d_b \cdot F_{BIC} + d_c \cdot F_{BRD} - L_1 \cdot W_{arm} - L_2 \cdot W_{app} = 0 \qquad \text{(B-6)}$$

Now there are only 3 equations available to solve for 5 unknown variables: the three muscle force magnitudes and two components of the joint reaction force. Thus, in order to solve this indeterminate system of equations, one must employ the methods of optimization (described in Section 1.4), reduce the number of unknowns to only three (Section 1.5.1), or include additional equations relating the unknown variables (Section 1.5.2).

Appendix C: EMG Data

C.1 Maximum Voluntary Contraction (MVC) Tests

C.1.1 Raw MVC Data

Below is the raw MVC data, which was processed by finding the root mean square (RMS) average over the active time period of the signal (using the Matlab® code in Appendix C.4.1).
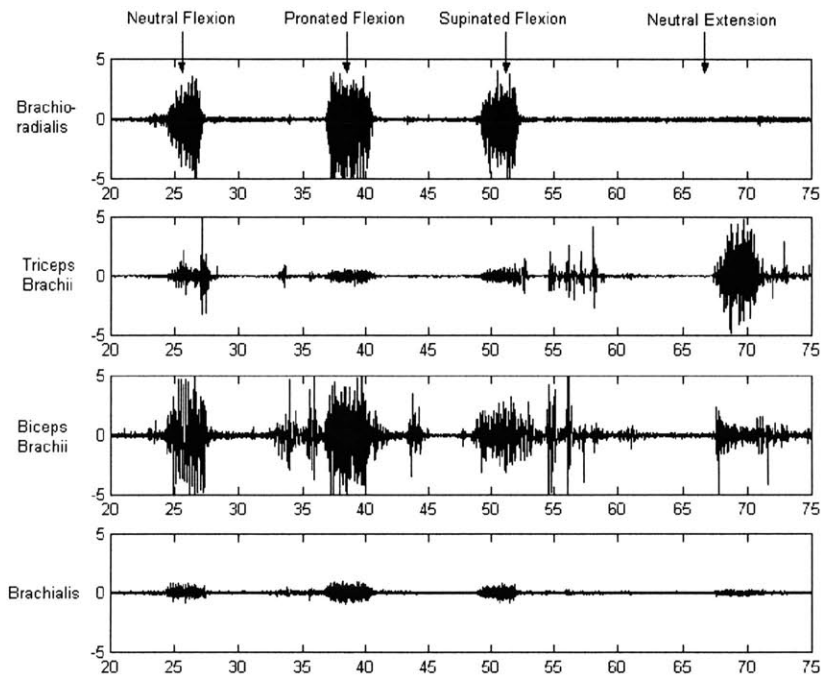
Figure C-1. Subject 1, Maximum Voluntary Muscle Contraction Test, Left Arm

116
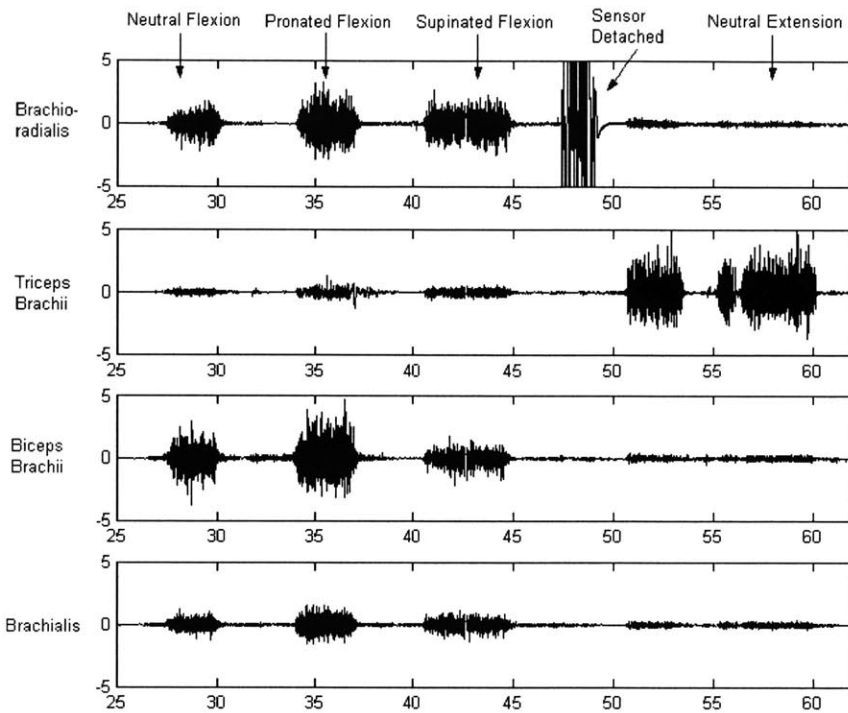
Figure C-2. Subject 1, Maximum Voluntary Muscle Contraction Test, Right Arm
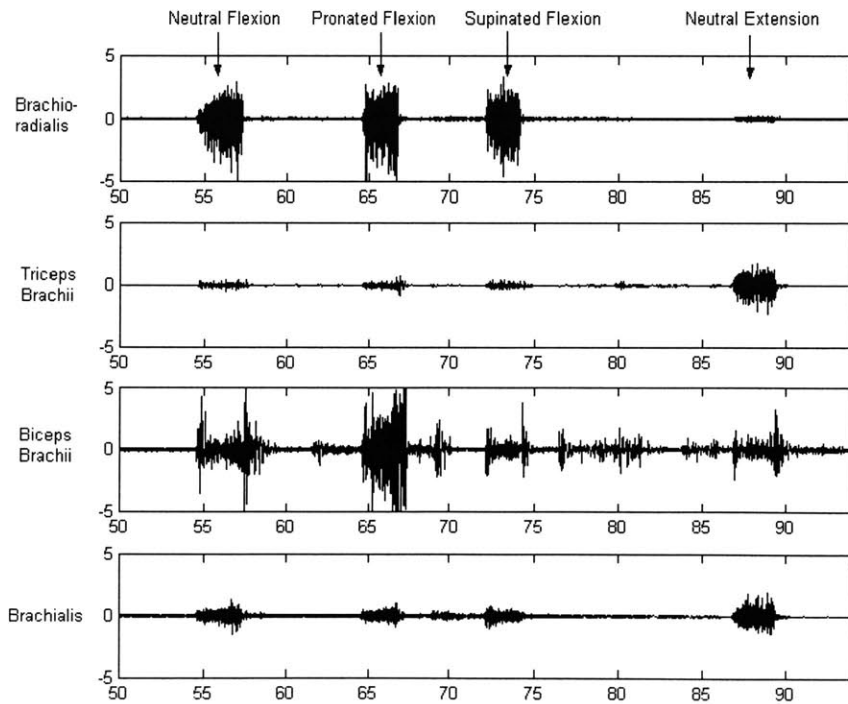
Figure C-3. Subject 2, Maximum Voluntary Muscle Contraction Test, Left Arm

117
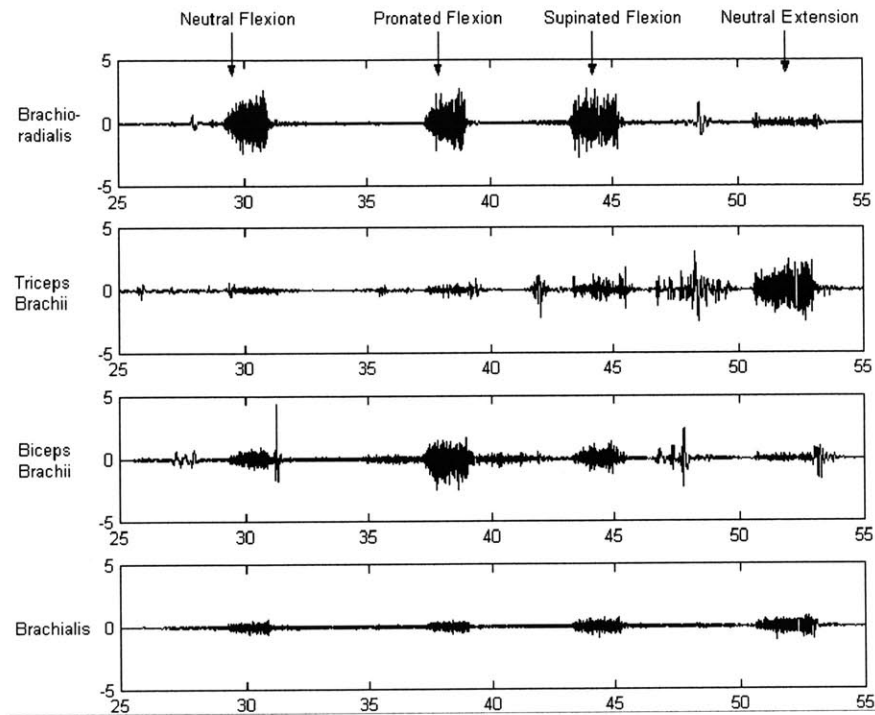
Figure C-4. Subject 2, Maximum Voluntary Muscle Contraction Test, Right Arm

C.1.2 RMS-Averaged MVC Data

The maximum RMS value for each muscle (BRD, TRI, BIC, BRA) was defined as the largest of the four RMS values calculated from the (1) neutral flexion, (2) pronated flexion, (3) supinated flexion, and (4) neutral extension MVC tests. These maximum RMS values (Figure C-5) were assumed to be the maximum voluntary contraction (MVC) value for each muscle, and thus were used to normalize the test results from the passive and resisted flexion tests (see Appendix C.4.3).

118
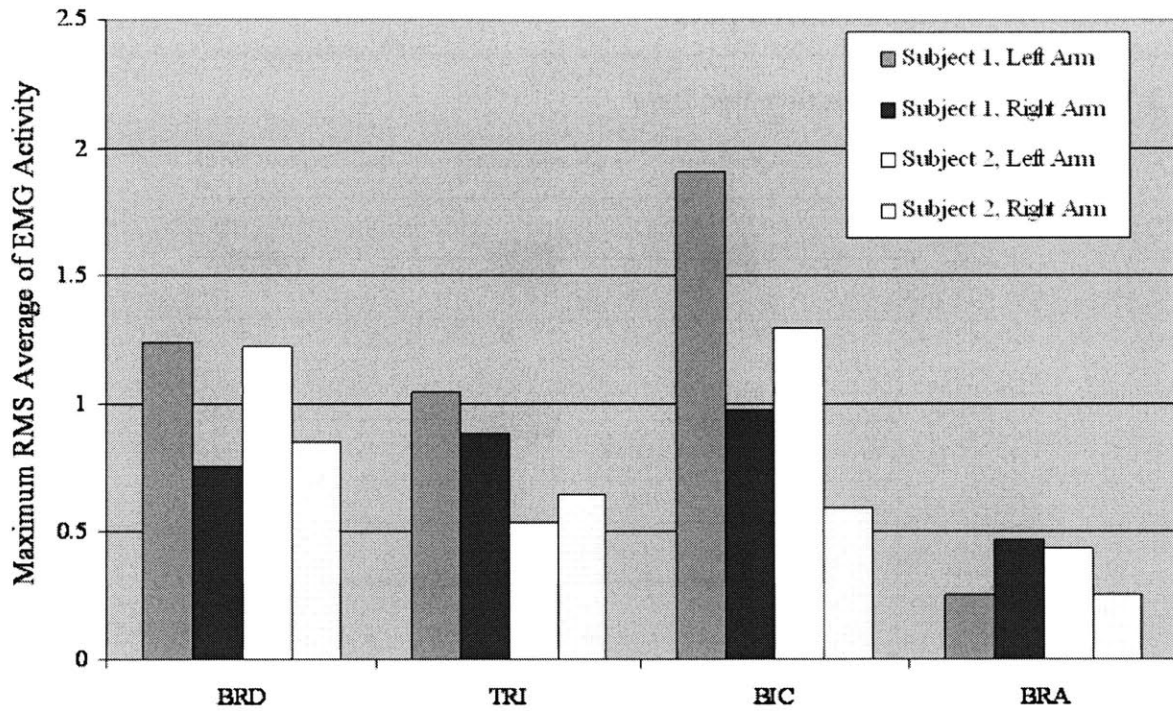
Figure C-5. Maximum of the RMS-averaged values (calculated from four flexion/extension tests) for the BRD, TRI, BIC, and BRA muscles. These maximum RMS values, assumed to be the maximum voluntary contraction (MVC) value for each muscle, were used to normalize the test results (for the corresponding subject/arm combination) from the passive and resisted flexion tests.

C.2 Electromyographic (EMG) Data

C.2.1 Raw EMG Passive Flexion Test Data
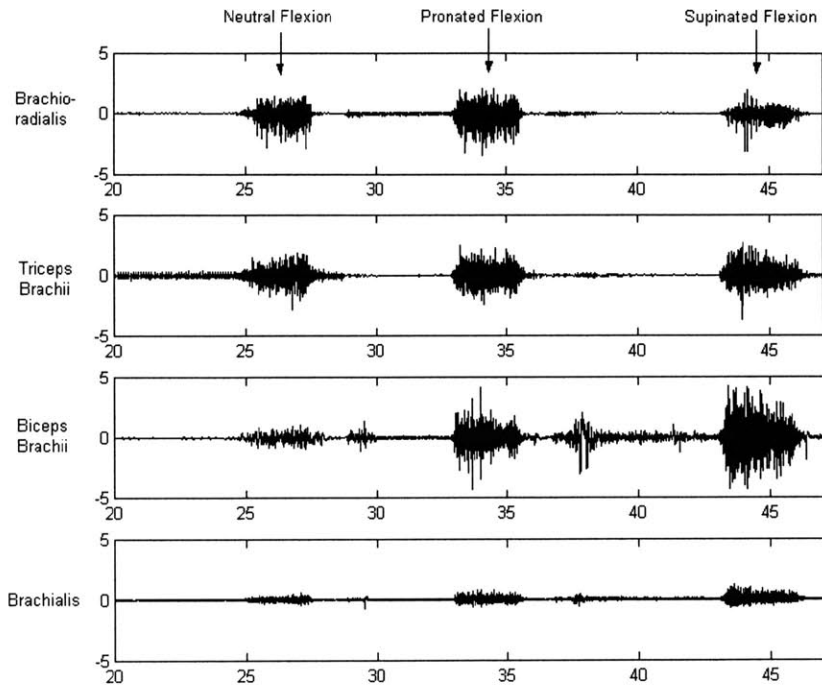
Figure C-6. Subject 1, Passive Flexion, Left Arm
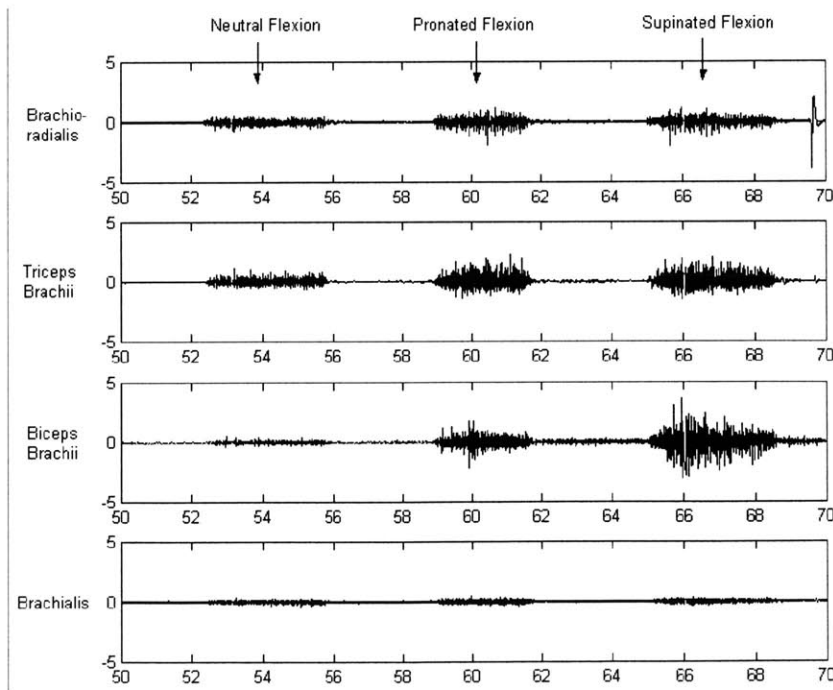
Figure C-7. Subject 1, Passive Flexion, Right Arm
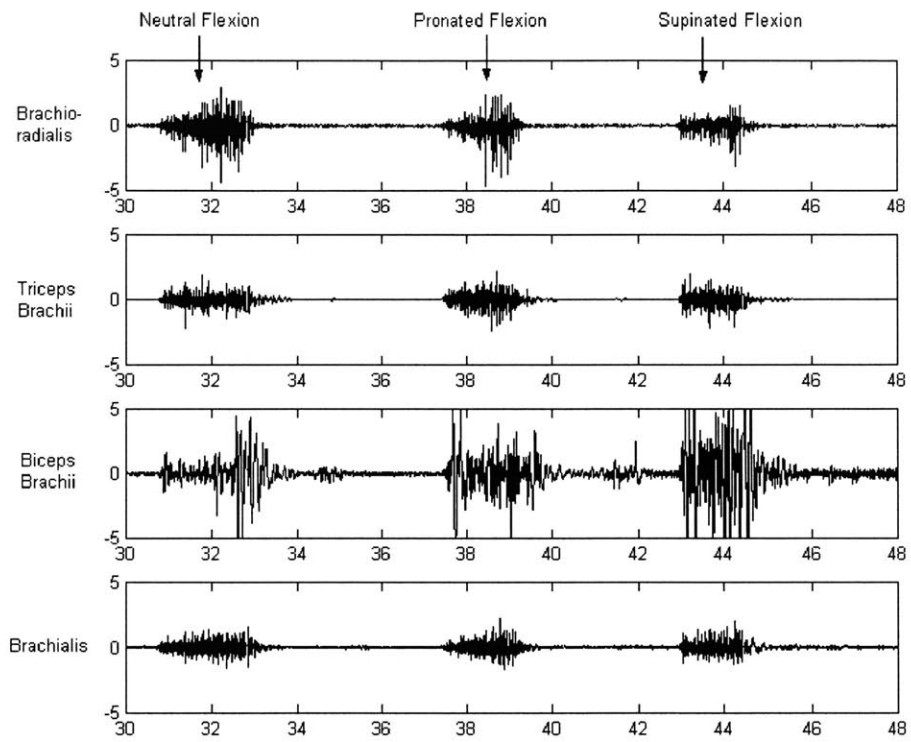
Figure C-8. Subject 2, Passive Flexion, Left Arm
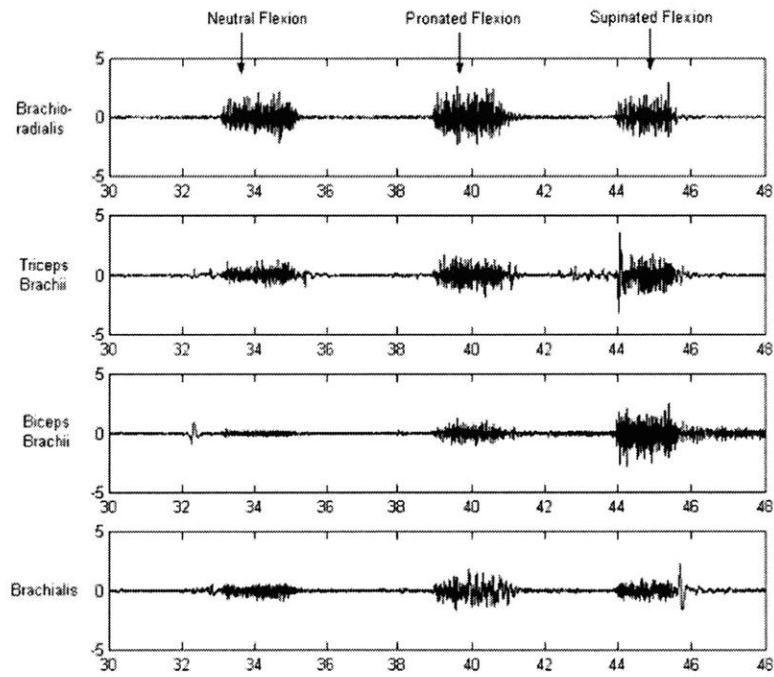
Figure C-9. Subject 2, Passive Flexion, Right Arm

C.2.2 Raw EMG Resisted Flexion Test Data
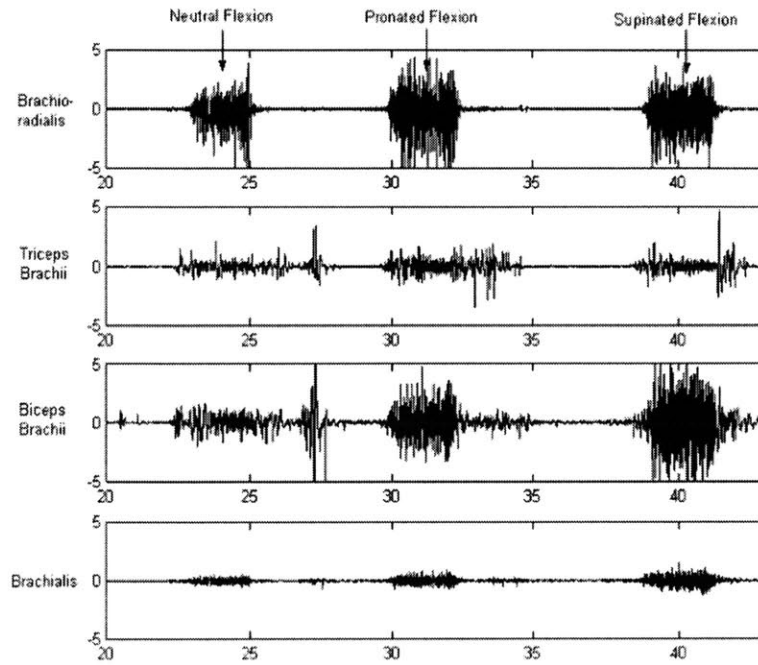
Figure C-10. Subject 1, Resisted Flexion, Left Arm
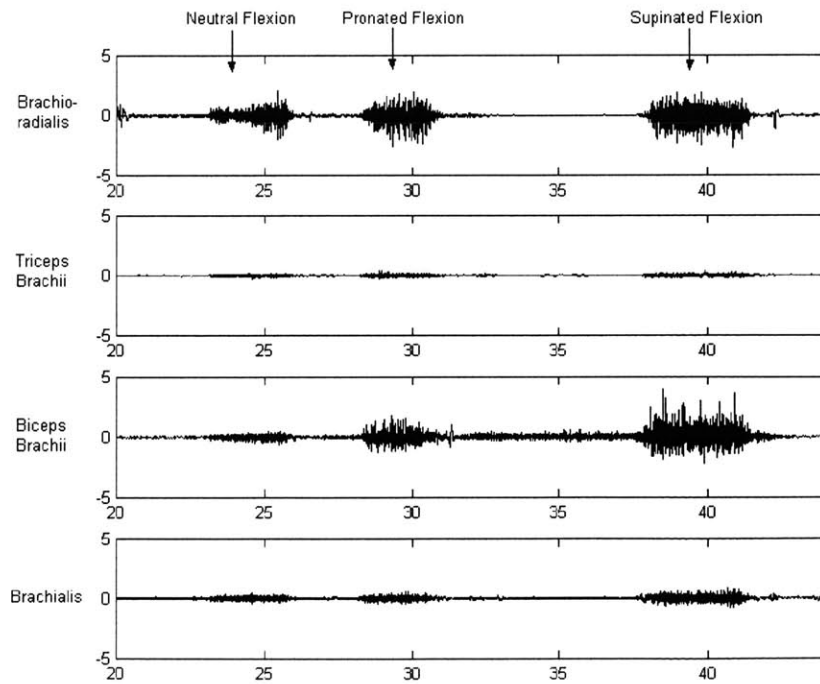
Figure C-11. Subject 1, Resisted Flexion, Right Arm

122
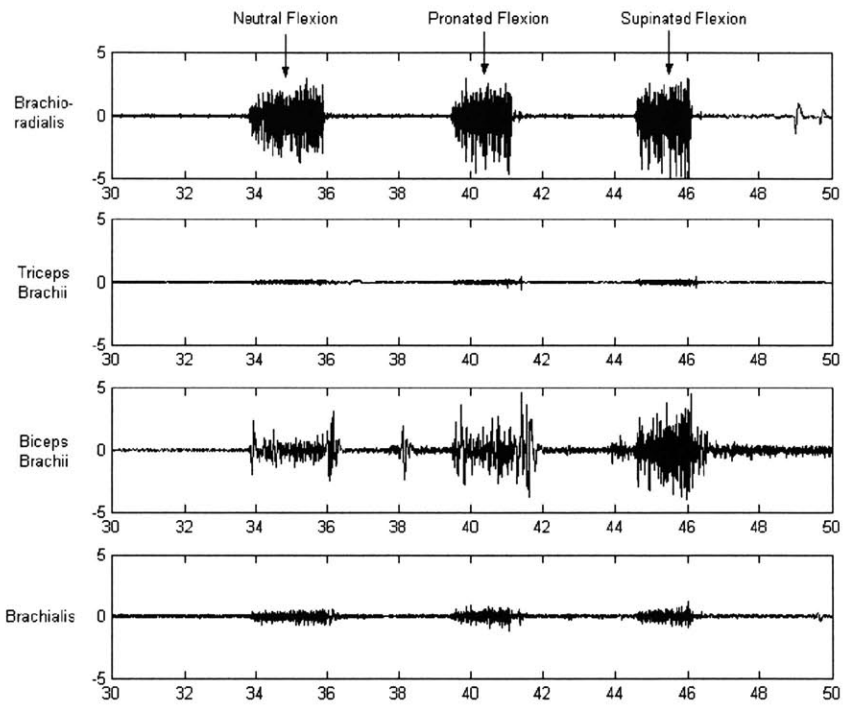
Figure C-12. Subject 2, Resisted Flexion, Left Arm
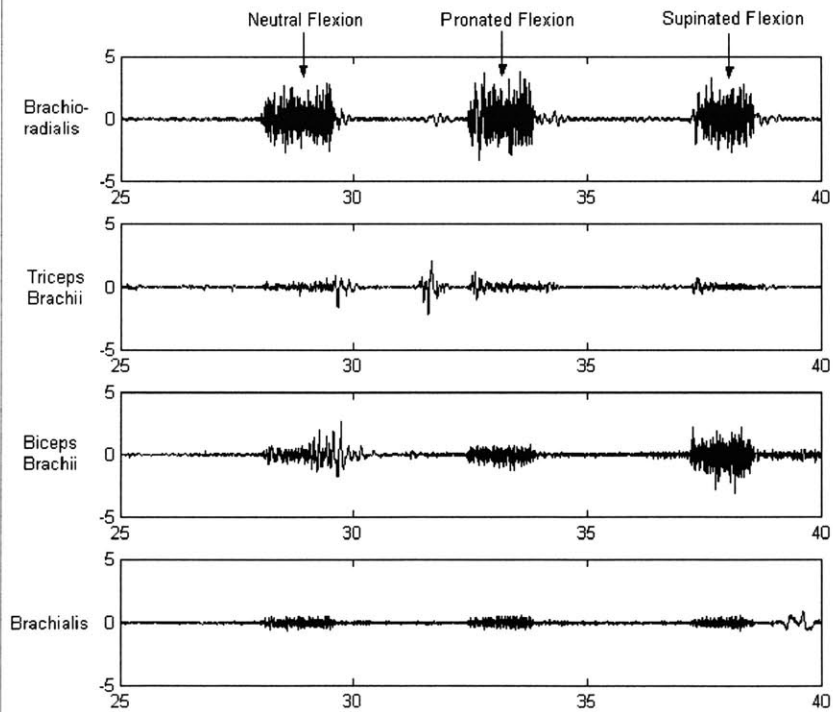
Figure C-13. Subject 2, Resisted Flexion, Right Arm

C.3 Normalized EMG Data

All data presented in this section has been normalized with respect to the maximum muscle EMG data, as outlined in Section 6.2.4.
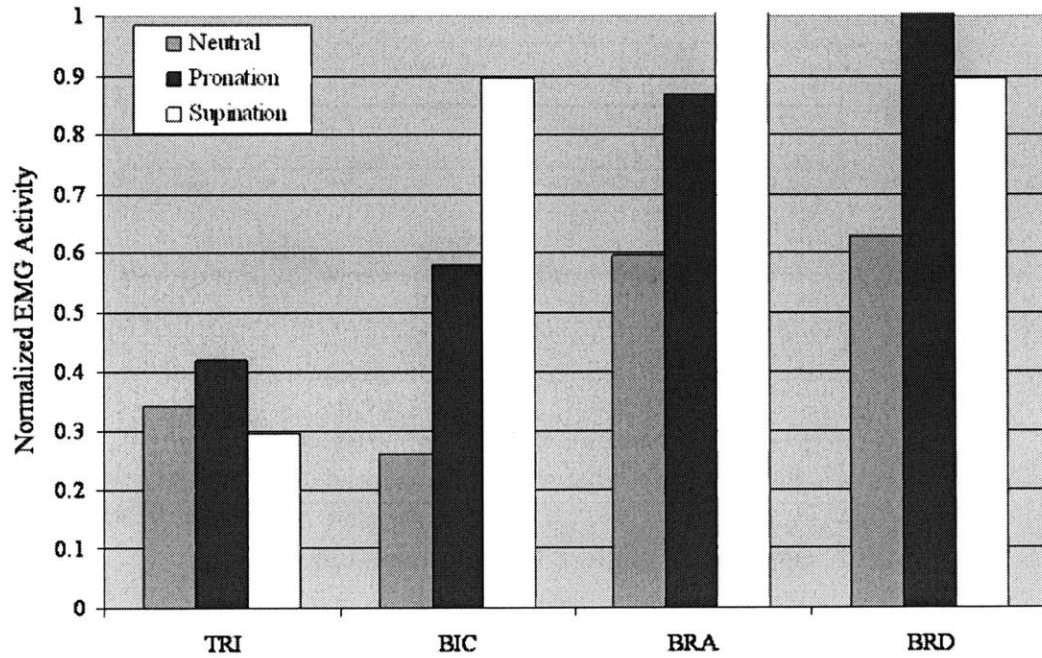
Figure C-14. Normalized Data, Subject 1, Resisted Flexion, Left Arm
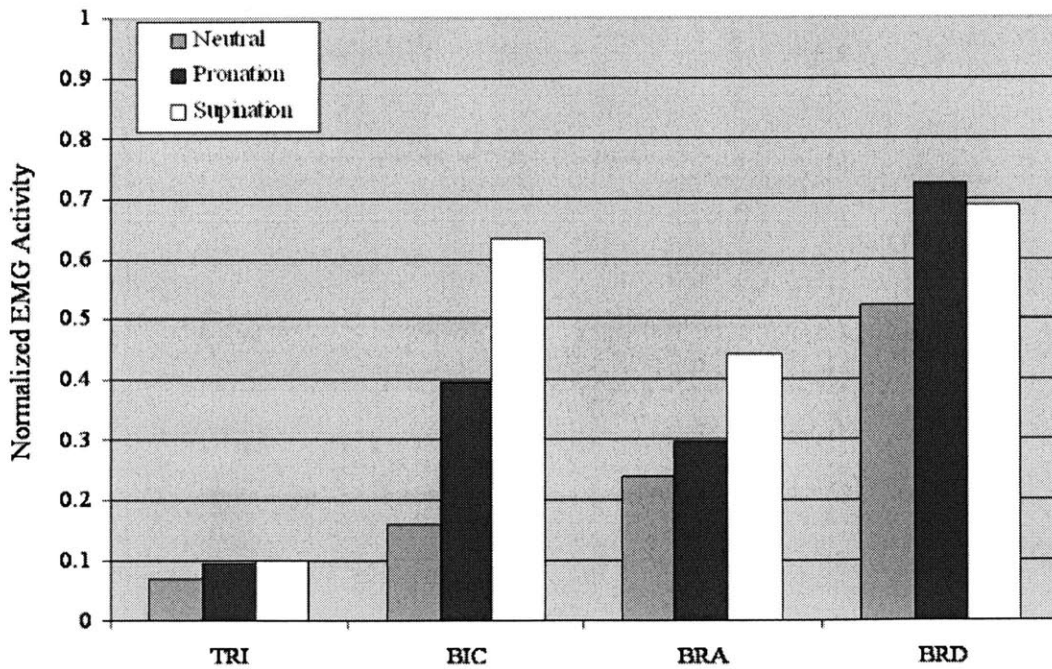
Figure C-15. Normalized Data, Subject 1, Resisted Flexion, Right Arm
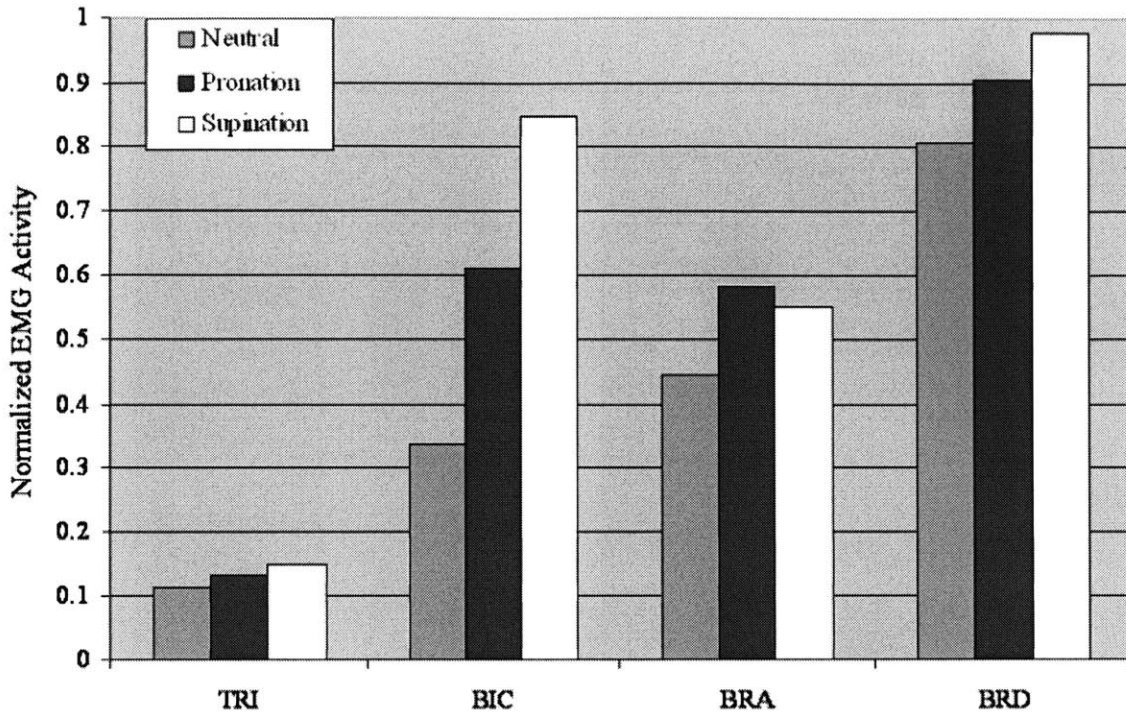
Figure C-16. Normalized Data, Subject 2, Resisted Flexion, Left Arm
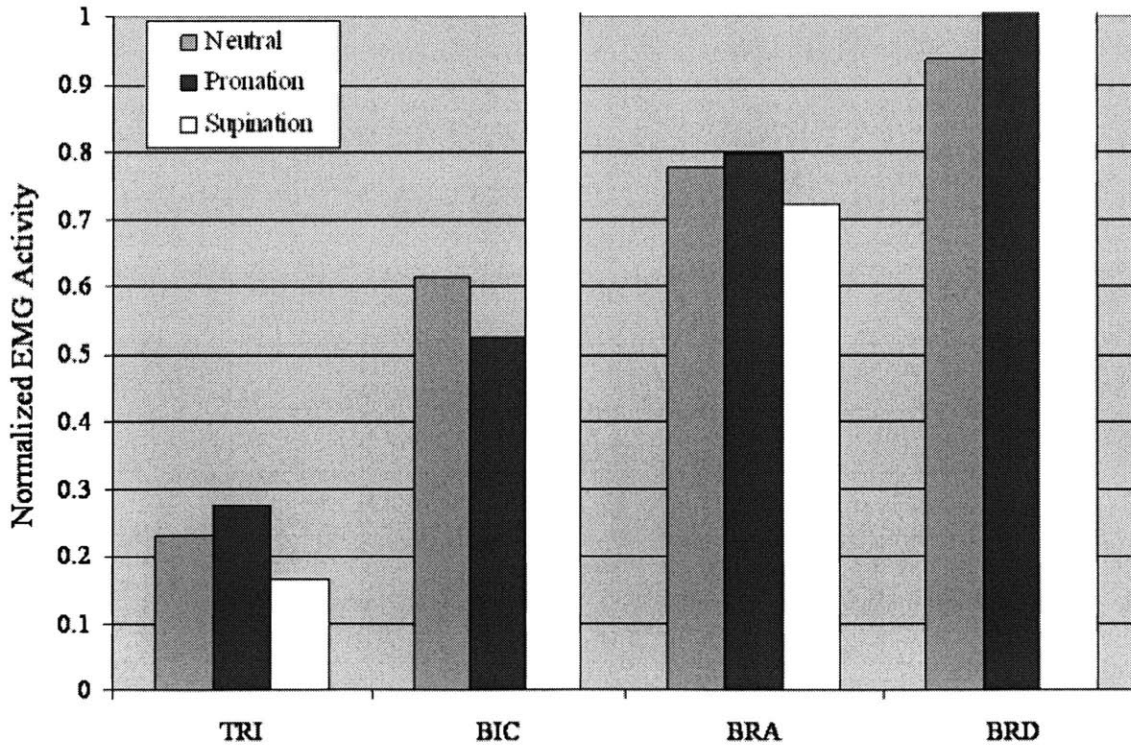
Figure C-17. Normalized Data, Subject 2, Resisted Flexion, Right Arm
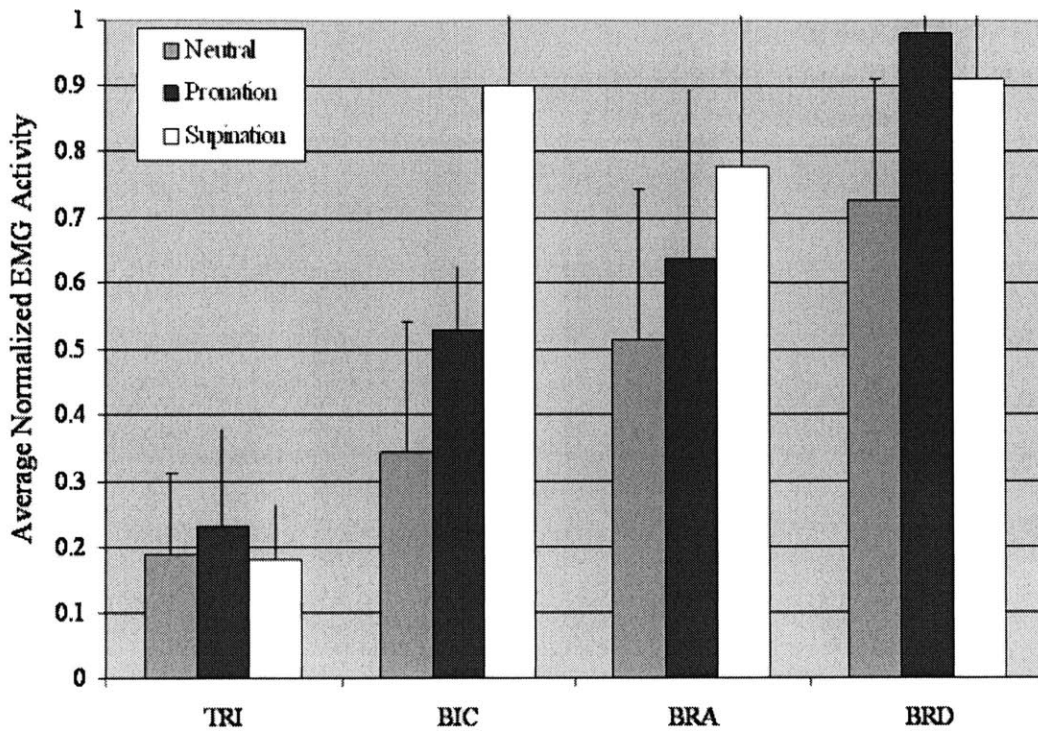
Figure C-18. Average EMG activity during flexion tests, averaged over two subjects (four arms) for the <u>passive and resisted</u> flexion tests.
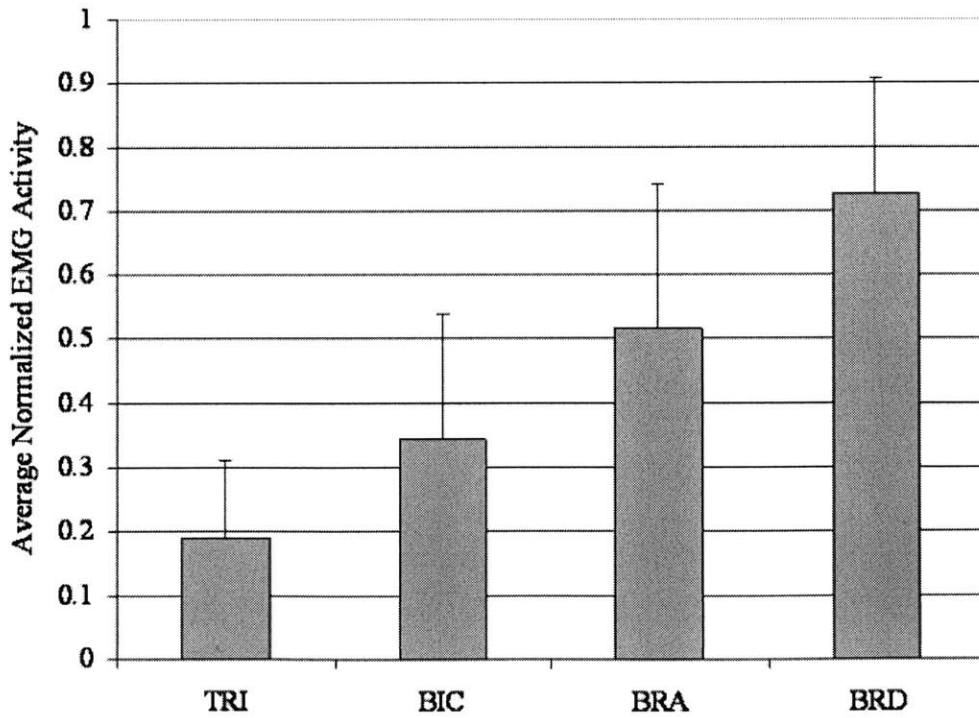
Figure C-19. Average EMG activity for the neutral forearm position, averaged over two subjects (four arms), and recorded while performing the <u>resisted</u> flexion test.

126

C.4 MATLAB® Codes

MATLAB® (The MathWorks, Inc., Natick MA) was used to process the EMG data. The three main codes used in this procedure can be found below.

C.4.1 MVC Value Determination

This code (RMSprocessorMAX.m) processed the data from the MVC tests and generated data files of RMS-averaged MVC values for use in data normalization (Section C.3).

```
%*******************************************************************%
% RMSprocessorMAX.m                                                 %
% Janine Pierce, MGH Bioengineering Laboratory                      %
%                                                                   %
% Processes MVC data obtained from EMG studies performed at the Motion    %
% Analysis Laboratory at Spaulding Rehabilitation Hospital (Boston, MA).  %
%*******************************************************************%

clear
pack
fc=1000;
Nchan=4; %The data was recorded using 4 channels.

[filename, pathname]=uigetfile('*.bin','OPEN FILE');
fin=fopen([pathname filename],'r');
offset=10;
fseek(fin,offset,'bof');
x=fread(fin,[Nchan,inf],'short');
fclose(fin);
x=5/2^15*x;
timeaxis=(1:length(x))/fc;

figure(1)
for i=1:Nchan
    subplot(Nchan,1,i),plot(timeaxis,x(i,:)),
        if i==1
            title(filename);
        end
        axis([min(timeaxis) max(timeaxis) -5 5]);
end

%Find the average MVC signal over the active signal collection time period

%--------------%Perform for each subject test file%---------------------%
%Define all time segments for each test file (changes for each test):
%--> manually look at raw data and determine the time segments
%over which the signal lasts (we did the neutral, pronation,
%supination, and extension MVC tests in the same order for each subject,
%but the time segments didn't align exactly from test to test).

%User can look at figure previously plotted and determine interval
%times for each of the tests (neutral, pronation, supination, extension)
prompt={'Neutral','Pronation','Supination','Extension'};
```

127

```matlab
def={'26','38','50', '63'};
dlgTitle='Input Start Times';
lineNo=[1,10];
answer=inputdlg(prompt,dlgTitle,lineNo,def);
startvals = str2double(answer)*fc;

prompt={'Neutral','Pronation','Supination', 'Extension'};
def={'27','39','51', '65'};
dlgTitle='Input End Times';
lineNo=[1,10];
answer=inputdlg(prompt,dlgTitle,lineNo,def);
endvals = str2double(answer)*fc;

t1 = startvals(1,1); t2 = endvals(1,1); %neutral flexion range
t3 = t1; t4 = t2; %neutral max activity range
t5 = startvals(2,1); t6 = endvals(2,1); %pronated flexion range
t7 = t5; t8 = t6; %pronated max activity range
t9 = startvals(3,1); t10 = endvals(3,1); %supinated flexion range
t11 = t9; t12 = t10; %supinated max activity range
t13 = startvals(4,1); t14 = endvals(4,1); %extension range
t15 = t13; t16 = t14; %extension max activity range

%Here we used the RMS averaging method:
%Calculated the RMS (root mean square) value of the EMG signal
%by summing the squared values of the raw EMG signal, determining
%the mean of the sum, and taking the square root of the mean, so
%in other words, RMS = Sqrt[(1/T)*integral(t --> t+T){EMG(t)^2 dt}],
%or RMS = Sqrt[(1/N)*sum(EMG(t)^2)] for t=t-->t+T, and N=T.

 %---Neutral Flexion---%
 %Neutral RMS (root mean square) average
 for i=1:Nchan
     t = t3; %time to start rms average: rms = sqrt[(1/N)*summation(x^2)]
     sumxsq = 0; %initialize variable
     N = t4-t3; %number of points used, for calculating average
     for t=t3:t4
         sumxsq = sumxsq + x(i,t)^2;
         t = t+1;
     end
  neutral_rms(i) = sqrt(sumxsq/N)
 end

 %---Pronated Flexion---%
 %Pronated RMS average
 for i=1:Nchan
     t = t7; %time to start rms average: rms = sqrt[(1/N)*summation(x^2)]
     sumxsq = 0; %initialize variable
     N = t8-t7; %number of points to average
     for t=t7:t8
         sumxsq = sumxsq + x(i,t)^2;
         t = t+1;
     end
     pronated_rms(i) = sqrt(sumxsq/N);
 end

 %---Supinated Flexion---%
 %Supinated RMS average
```

128

```
for i=1:Nchan
    t = t11; %time to start rms average: rms = sqrt[(1/N)*summation(x^2)]
    sumxsq = 0; %initialize variable
    N = t12-t11; %number of points to average
    for t=t11:t12
        sumxsq = sumxsq + x(i,t)^2;
        t = t+1;
    end
    supinated_rms(i) = sqrt(sumxsq/N);
end

%---Neutral Extension---%
%Extension RMS average
for i=1:Nchan
    t = t15; %time to start rms average: rms = sqrt[(1/N)*summation(x^2)]
    sumxsq = 0; %initialize variable
    N = t16-t15; %number of points to average
    for t=t15:t16
        sumxsq = sumxsq + x(i,t)^2;
        t = t+1;
    end
    extension_rms(i) = sqrt(sumxsq/N);
end

%*********************************************************************%
%Define Max RMS datafile (user defines filename in prompt)
[filename2, pathname] = uiputfile('RMSMAXfile.dat', 'Save Max RMS data as:')

%Write Max RMS values to a file (for input to normalization code)
fid = fopen(filename2,'w+');
fprintf(fid, '%f %f %f %f \n', neutral_rms);
fprintf(fid, '%f %f %f %f \n', pronated_rms);
fprintf(fid, '%f %f %f %f \n', supinated_rms);
fprintf(fid, '%f %f %f %f \n', extension_rms);
fclose(fid);
```

C.4.2 Calculate RMS of Test Data

Almost identical to the code above, this code (RMSprocessor.m) processed the data from the passive and resisted flexion tests and generated data files of RMS-averaged values, which were then normalized as described in Section C.3.

```
%*********************************************************************%
% RMSprocessor.m                                                     %
% Janine Pierce, MGH Bioengineering Laboratory                       %
%                                                                    %
% Processes data obtained from EMG studies performed at the Motion Analysis %
% Laboratory at Spaulding Rehabilitation Hospital (Boston, MA).      %
%*********************************************************************%

clear
pack
fc=1000;
Nchan=4; %The data was recorded using 4 channels.
```

129

```
[filename, pathname]=uigetfile('*.bin','OPEN FILE');
fin=fopen([pathname filename],'r');
offset=10;
fseek(fin,offset,'bof');
x=fread(fin,[Nchan,inf],'short');
fclose(fin);
x=5/2^15*x;
timeaxis=(1:length(x))/fc;

figure(1)
for i=1:Nchan
    subplot(Nchan,1,i),plot(timeaxis,x(i,:)),
      if i==1
          title(filename);
      end
      axis([min(timeaxis) max(timeaxis) -5 5]);
end

%Find the average signal over the active signal collection time period

%--------------%Perform for each subject test file%----------------------%
%Define all time segments for each test file (changes for each test):
%--> manually look at raw data and determine the time segments
%over which the signal lasts (we did the neutral, pronation,
%supination tests in the same order for each subject, but the time
%segments don't align exactly from test to test).

%User can look at figure previously plotted and determine interval
%times for each of the tests (neutral, pronation, supination)
prompt={'Neutral','Pronation','Supination'};
def={'26','38','50'};
dlgTitle='Input Start Times';
lineNo=[1,10];
answer=inputdlg(prompt,dlgTitle,lineNo,def);
startvals = str2double(answer)*fc;

prompt={'Neutral','Pronation','Supination'};
def={'27','39','51'};
dlgTitle='Input End Times';
lineNo=[1,10];
answer=inputdlg(prompt,dlgTitle,lineNo,def);
endvals = str2double(answer)*fc;

t1 = startvals(1,1); t2 = endvals(1,1); %neutral flexion range
t3 = t1; t4 = t2; %neutral max activity range
t5 = startvals(2,1); t6 = endvals(2,1); %pronated flexion range
t7 = t5; t8 = t6; %pronated max activity range
t9 = startvals(3,1); t10 = endvals(3,1); %supinated flexion range
t11 = t9; t12 = t10; %supinated max activity range

%Here we used the RMS averaging method:
%Calculated the RMS (root mean square) value of the EMG signal
%by summing the squared values of the raw EMG signal, determining
%the mean of the sum, and taking the square root of the mean, so
%in other words, RMS = Sqrt[(1/T)*integral(t --> t+T){EMG(t)^2 dt}],
%or RMS = Sqrt[(1/N)*sum(EMG(t)^2)] for t=t-->t+T, and N=T.
```

130

```
%---Neutral Flexion---%
%Neutral RMS (root mean square) average
for i=1:Nchan
    t = t3; %time to start rms average: rms = sqrt[(1/N)*summation(x^2)]
    sumxsq = 0; %initialize variable
    N = t4-t3; %number of points used, for calculating average
    for t=t3:t4
        sumxsq = sumxsq + x(i,t)^2;
        t = t+1;
    end
    neutral_rms(i) = sqrt(sumxsq/N)
end


 %---Pronated Flexion---%
 %Pronated RMS average
 for i=1:Nchan
    t = t7; %time to start rms average: rms = sqrt[(1/N)*summation(x^2)]
    sumxsq = 0; %initialize variable
    N = t8-t7; %number of points to average
    for t=t7:t8
        sumxsq = sumxsq + x(i,t)^2;
        t = t+1;
    end
    pronated_rms(i) = sqrt(sumxsq/N);
 end


 %---Supinated Flexion---%
 %Supinated RMS average
 for i=1:Nchan
    t = t11; %time to start rms average: rms = sqrt[(1/N)*summation(x^2)]
    sumxsq = 0; %initialize variable
    N = t12-t11; %number of points to average
    for t=t11:t12
        sumxsq = sumxsq + x(i,t)^2;
        t = t+1;
    end
    supinated_rms(i) = sqrt(sumxsq/N);
 end

 %Write RMS data to file (user defines filename in prompt)
 [filename2, pathname] = uiputfile('myfile.dat', 'Save RMS data as:')

 %Write RMS averages to a file (for input to normalization code)
 fid = fopen(filename2,'w+');
 fprintf(fid, '%f %f %f %f \n', neutral_rms);
 fprintf(fid, '%f %f %f %f \n', pronated_rms);
 fprintf(fid, '%f %f %f %f \n', supinated_rms);
 fclose(fid);
```

C.4.3 Normalize Data

Below is the generic code (Normalization.m) used to normalize both the passive and resisted flexion test data with respect to the MVC data, all RMS-averaged from the previously described codes.

```
%**********************************************************************%
% Normalization.m                                                      %
% Normalizes data obtained from EMG studies.                           %
% After being processed using RMSprocessor.m, all data is normalized   %
% against Maximum Voluntary Contraction (MVC) data, also normalized using %
% RMSprocessorMAX.m.  The user will be prompted to select the MVC datafile %
% of interest, as well as the original raw data file to be normalized.  %
%**********************************************************************%

clear
pack
fc=1000;
Nchan=4; %The new data was recorded using 4 channels, the old was 6 channels.

[filename1, pathname1]=uigetfile('*.dat','OPEN FILE: Choose Raw Data File');
rawdata = load ([pathname1 filename1]);
brd = rawdata(:,1); tri = rawdata(:,2);
bic = rawdata(:,3); bra = rawdata(:,4);

%Read in MVC (Max Voluntary Contraction) values and use to normalize
[filename2, pathname2]=uigetfile('*.dat','OPEN FILE: Choose MVC Data File');
mvcdata = load ([pathname2 filename2]);
mvcbrd = mvcdata(:,1); mvctri = mvcdata(:,2);
mvcbic = mvcdata(:,3); mvcbra = mvcdata(:,4);

%Normalize the data
normdata(1,:) = (brd/max(mvcbrd))';
normdata(2,:) = (tri/max(mvctri))';
normdata(3,:) = (bic/max(mvcbic))';
normdata(4,:) = (bra/max(mvcbra))';

%Print normalized data to file
[filename3, pathname] = uiputfile(filename1, 'Save RMS data as:')
fid = fopen(filename3,'w+');
fprintf(fid,'%f %f %f %f\n',normdata);
fclose(fid);
```

Appendix D: Optimization Program

The code (3dManual.nb) found below, written in Mathematica© (Wolfram Research, Inc., Champaign, IL) programming software, was used to predict the muscle and joint loads for the elbow joint model, while varying the y-coordinate of the joint center along the flexion-extension axis. A slightly modified version of this code was used to "automatically" estimate the y-coordinate of the joint center location.

```
(*Suppresses spelling error notifications*)
Off[General::spell1];
Off[General::spell];

(*changes tolerance and max iterations inside NMinimize*)
tol = 0.001;
maxits = 2000;
```

132

```
(*$RecursionLimit = 500;
  $IterationLimit = 7500;
  *)

For[l = 4, l < 5, l++,
If[l==1,datafile={"00N.prn","00P.prn","00S.prn"}; forearmposition=00;];
  If[l==2,datafile={"30N.prn","30P.prn","30S.prn"}; forearmposition=30;];
  If[l==3,datafile={"60N.prn","60P.prn","60S.prn"}; forearmposition=60;];
  If[l==4,datafile={"90N.prn","90P.prn","90S.prn"}; forearmposition=90;];
  If[l==5,datafile={"120N.prn","120P.prn","120S.prn"}; forearmposition=120;];
  NeuProSupin = {Neutral, Pronation, Supination};

(*Change Loading Conditions*)
(*Variable Moment*)
(*Moment = {-5, -4, -3, -2, -1, 0, 1, 2, 3, 4, 5};*)
(*Constant Moment*)
Mapp = {0, 0, 0};

(*Comment out the "m" loop if there is no variable moment*)
(*For[m = 1, m < 12, m++,
AppliedMoment = Moment[[m]];
      Mapp = {AppliedMoment, 0, 0}; (*Applied moment about the x axis*)
      Print[Mapp];
      *)

(*Change "k" loop to look at only neutral, only pronation, etc. *)
For[k = 1, k < 2, k++, (*loop through neutral, pronation, and supination*)

(*Use "j" loop to manually loop through y values. *)
For [j = -15, j < 16, j++, (*loop through different y axis origin positions*)
neworigin = {0, j, 0};
file = datafile[[k]];
NeuProSup = NeuProSupin[[k]];
position = forearmposition;
(*Set directory*)
mydirectory = "C:\Janine\Forearm\SpecimenStudy092903\0";
SetDirectory[mydirectory];

(*Set Initial Guesses (for optimization)*)
      F1guess=0;(*Tricep*) F2guess=50;(*Bicep*) F3guess=50;(*Brach*)
F4guess=50;(*BrachRad*) F5guess=10;(*Anconeus*)
F6guess=10;(*Pronator Teres*)
(*Define Muscle Physiological Cross - Sectional Area [cm^2]*)
      Atri=18.8; Abic=4.6; Abra=7.0; Abrd=1.5; Aanc=2.5; Aprt=3.4;

(*Max Physiological Muscle Stress [N/cm^2]*)
sigma = 100;  (*ranges 9.8 N/cm^2 to 150 N/cm^2 in literature*)

(*Initialize input variables*)
distradius={0,0,0}; bicep={0,0,0}; bicepeff={0,0,0}; bicep1s={0,0,0};
bicep1e={0,0,0}; bicep2s={0,0,0}; bicep2e={0,0,0}; bicep3s={0,0,0};
bicep3e={0,0,0}; tricep={0,0,0}; tricep1s={0,0,0}; tricep1e={0,0,0};
... AND SO FORTH

(*Read input data from Rhino*)
(*Set the directory and filename, locate point of interest (e.g."brach") *)
```

133

```
(*read in the data points after the "junk" *)

(*Don't forget to convert Rhino data points from mm to m so that *)
(*forces can be calculated in N*)

(*Distradius*)
data1 = OpenRead[file];
junk = Find[data1, "distradius "];
StringLength[junk];
posstream = StreamPosition[data1];
SetStreamPosition[data1, posstream - StringLength[junk]];
Read[data1, {Word, Word}];
distradius[[1]] = Read[data1, Number]; dummy = Read[data1, Character];
      distradius[[2]] = Read[data1, Number]; dummy = Read[data1, Character];
distradius[[3]] = Read[data1, Number]; dummy = Read[data1, Character];
Close[file];
(*The center of mass of the forearm is assumed to act at a distance "r",*)
(*where r = 0.677*length of forearm (used length of radius).*)
      L = Sqrt[distradius[[1]]^2 + distradius[[2]]^2 + distradius[[3]]^2];
      unitvecrad = {distradius[[1]]/L, distradius[[2]]/L, distradius[[3]]/L};
      forearmcg = 0.677*L*unitvecrad;  (*equation obtained from literature*)
(*Now that we have defined a constant location of the forearm center of *)
(*gravity, which will not change as we change the origin centerpoint, we *)
(*can find the new value of the moment arm from the new origin to the *)
(*distradius and to the forearmcg. *)
      distradius = (distradius - neworigin)/1000;  (*convert to m from mm*)
      forearmcg = (forearmcg - neworigin)/1000;


(*Tricep*)
data1 = OpenRead[file];
junk = Find[data1, "tricep "];
StringLength[junk];
posstream = StreamPosition[data1];
SetStreamPosition[data1, posstream - StringLength[junk]];
Read[data1, {Word, Word}];
      tricep[[1]] = Read[data1, Number]; dummy = Read[data1, Character];
      tricep[[2]] = Read[data1, Number]; dummy = Read[data1, Character];
      tricep[[3]] = Read[data1, Number]; dummy = Read[data1, Character];
      tricep = (tricep - neworigin)/1000;  (*convert to m from mm*)
      Close[file];
... DO THE SAME FOR THE REST OF THE DATAPOINTS IN THE FILE (BICEP, BRACHIALIS, ETC.)


(*Find unit vector for muscle force line of action*)
(*Line of action of muscle forces approx from digitized lines of *)
(*action given the start and end points of line of action curves *)
(*then approx as line and take average of the 2 or 3 lines*)

(*Specified Tricep Line of Action [from digitized line(s)]*)
      dx1=triceple[[1]]-tricep1s[[1]];
      dy1=triceple[[2]]-tricep1s[[2]];
      dz1=triceple[[3]]-tricep1s[[3]];
      L1=Sqrt[dx1^2 + dy1^2 + dz1^2];
      unitvec1 = {dx1/L1, dy1/L1, dz1/L1};
      a = unitvec1;
      If[tricep2e ≠ {0, 0, 0},
            dx2=tricep2e[[1]]-tricep2s[[1]];
            dy2=tricep2e[[2]]-tricep2s[[2]];
```

134

```
            dz2=tricep2e[[3]]-tricep2s[[3]];
            L2=Sqrt[dx2^2 + dy2^2 + dz2^2];
            unitvec2={dx2/L2, dy2/L2, dz2/L2};
            b=unitvec2;
            If[tricep3e ≠ {0, 0, 0},
                    dx3=tricep3e[[1]]-tricep3s[[1]];
                    dy3=tricep3e[[2]]-tricep3s[[2]];
                    dz3=tricep3e[[3]]-tricep3s[[3]];
                    L3=Sqrt[dx3^2 + dy3^2 + dz3^2];
                    unitvec3={dx3/L3, dy3/L3, dz3/L3};
                    c=unitvec3;
                    d = a + b + c;
                    unitvectri = d/Sqrt[d[[1]]^2 + d[[2]]^2 + d[[3]]^2];,
            d = a + b;
            unitvectri = d/Sqrt[d[[1]]^2 + d[[2]]^2 + d[[3]]^2];],
        unitvectri = a;];
```

... *DO SAME THING FOR BICEPS AND BRACHIALIS LINES OF ACTION*

```
(*Specified Brachioradialis Line of Action*)
      dx1=brdorigindist[[1]]-brachrad[[1]];
      dy1=brdorigindist[[2]]-brachrad[[2]];
      dz1=brdorigindist[[3]]-brachrad[[3]];
      (*brachrad is the insertion on the distal radius, *)
      (*brachradeff is the insertion on the proximal radius*)
      (*brdorigin is the centroid of the digitized origin, *)
      (*brdoriginprox is the proximal tip of the digitized origin, and *)
      (*brdorigindist is the distal tip of the digitized origin site.*)
      L1=Sqrt[dx1^2 + dy1^2 + dz1^2];
      If[brachrad=={0,0,0},
            unitvecbrd={0,0,0};,
      unitvecbrd={dx1/L1, dy1/L1, dz1/L1};];
(*Specified Anconeus Line of Action*)
      dx1=anconeusorigin[[1]]-anconeus[[1]];
      dy1=anconeusorigin[[2]]-anconeus[[2]];
      dz1=anconeusorigin[[3]]-anconeus[[3]];
      L1=Sqrt[dx1^2 + dy1^2 + dz1^2];
      If[anconeus=={0,0,0},
            unitvecanc={0,0,0};,
      unitvecanc={dx1/L1, dy1/L1, dz1/L1};];
(*Specified Pronator Teres Line of Action*)
      dx1=proterorigineff[[1]]-proter[[1]];
      dy1=proterorigineff[[2]]-proter[[2]];
      dz1=proterorigineff[[3]]-proter[[3]];
      L1=Sqrt[dx1^2 + dy1^2 + dz1^2];
      If[proter=={0,0,0},
            unitvecprt={0,0,0};,
      unitvecprt={dx1/L1,dy1/L1,dz1/L1};];


(*Define Force and Distance Variables*)
(*z - axis : roughly parallel to fixed axis of humerus*)
(*y - axis : centroid of line passing through trochlea*)
(*joint center:{0,0,0} defined as the midpoint of the elbow flex axis*)


(*Muscle Forces*)
      (*Ftri = Triceps Brachii muscle force*)
      (*Fbic = Biceps Brachii muscle force*)
      (*Fbra = Brachialis muscle force*)
```

135

```
    (*Fbrd = Brachioradialis force*)
    (*Fanc = Anconeus force*)
    (*Fprt = Pronator Teres force*)

    (*Other forces*)
    (*J = Joint reaction force*)
    (*Wapp = Applied Load at end of radius*)
    (*Warm = Weight of arm (N) - assume 1kg*gravity*)

    (*Distances*)
    (*Distance from force/load application to joint center {0, j, 0}*)
    (*Dtri = Distance from joint center to tricep insertion point*)
    (*Dbic = Distance from joint center to bicep insertion point*)
    (*Dbra = Distance from joint center to brachialis insertion point*)
    (*Dbrd = Distance from joint center to brachioradialis insertion pt*)
    (*Danc = Distance from joint center to anconeus insertion point*)
    (*Dprt = Distance from joint center to pronator teres insertion point*)
    (*Dapp = Distance from joint center to point of load application*)
    (*Darm = Distance from joint center to forearm center of gravity*)

(*Define other variables.*)
    (*Applied Load at distal radius in direction of gravity*)
    g = 9.81; (* gravitational acceleration *)
    Wappmag = 5*g; (* magnitude of force usually set to 5*g = ~50N *)
    unitvecapp = {0, 0, -1};
    Wapp = Wappmag*unitvecapp;

    (*Applied Load at distal radius along radius*)
    Wappmag2 = 0;
    unitvecapp2 = -1*
    unitvecrad;(*unitvector along radius, defined previously*)
    Wapp2 = Wappmag2*unitvecapp2;

    (*Weight of the arm acting at the centroid of the forearm *)
(*in the direction of gravity*)
    Warmmag = 1*g; (*Weight=mass*acceleration of grav=1kg*9.81m/s2~10N *)
    unitvecarm = {0, 0, -1};
    Warm = Warmmag*unitvecarm;

    (*Define distances from origins to insertions*)
    Dtri = tricep;
    Dbic = bicep;
    Dbra = brach;
    Dbrd = brachrad;
    Danc = anconeus;
    Dprt = proter;
    Dapp = distradius;
    Darm = forearmcg ;
    Ftri = F1*unitvectri;
    Fbic = F2*unitvecbic;
    Fbra = F3*unitvecbra;
    Fbrd = F4*unitvecbrd;
    Fanc = F5*unitvecanc;
    Fprt = F6*unitvecprt;
    J = {Jx, Jy, Jz};

(*Define Moment Arm Magnitudes*)
```

136

```
        Rtri = Cross[Dtri, unitvectri];
        Rtrimag = Sqrt[Rtri[[1]]^2 + Rtri[[2]]^2 + Rtri[[3]]^2];
        Rbic = Cross[Dbic, unitvecbic];
        Rbicmag = Sqrt[Rbic[[1]]^2 + Rbic[[2]]^2 + Rbic[[3]]^2];
        Rbra = Cross[Dbra, unitvecbra];
        Rbramag = Sqrt[Rbra[[1]]^2 + Rbra[[2]]^2 + Rbra[[3]]^2];
        Rbrd = Cross[Dbrd, unitvecbrd];
        Rbrdmag = Sqrt[Rbrd[[1]]^2 + Rbrd[[2]]^2 + Rbrd[[3]]^2];
        Ranc = Cross[Danc, unitvecanc];
        Rancmag = Sqrt[Ranc[[1]]^2 + Ranc[[2]]^2 + Ranc[[3]]^2];
        Rprt = Cross[Dprt, unitvecprt];
        Rprtmag = Sqrt[Rprt[[1]]^2 + Rprt[[2]]^2 + Rprt[[3]]^2];
        Rarm = Cross[Darm, unitvecarm];
        Rarmmag = Sqrt[Rarm[[1]]^2 + Rarm[[2]]^2 + Rarm[[3]]^2];
        Rapp = Cross[Dapp, unitvecapp];
        Rappmag = Sqrt[Rapp[[1]]^2 + Rapp[[2]]^2 + Rapp[[3]]^2];

(*OPTIMIZATION*)
(*Write out static equilibrium equations for forces and moments.*)
SumF=Ftri+Fbic+Fbra+Fbrd+Fanc+Fprt+Warm+Wapp+Wapp2+J;
        SumM=Cross[Dtri,Ftri]+Cross[Dbic,Fbic]+Cross[Dbra,Fbra]+
        Cross[Dbrd,Fbrd]+Cross[Danc,Fanc]+Cross[Dprt,Fprt]+
        Cross[Darm,Warm]+Cross[Dapp,Wapp]+Cross[Dapp,Wapp2]+Mapp;
        Mx = SumM[[1]];
        My = SumM[[2]];
        Mz = SumM[[3]];
(*Define objective function, f, as the sum of the cubic muscle stresses.*)
        f[F1_,F2_,F3_,F4_,F5_,F6_]=(F1/Atri)^3+(F2/Abic)^3+(F3/Abra)^3+
(F4/Abrd)^3+(F5/Aanc)^3+(F6/Aprt)^3;
(*Minimize the objective function with the following constraints and *)
(*solve for F1, F2, F3, F4, F5, F6 (muscle force magnitudes).*)
(*1. Muscle forces are always positive (can only act in tension)*)
(*2. Muscle stress (Fi/PCSAi) must be less than the maximum *)
(*physiological muscle stress*)
(*3. Moment equilibrium equations satisfied (Mx=0, My=0, Mz=0) *)

(*Use NMinimize to minimize objective function with given constraints *)
output1=NMinimize[{f[F1,F2,F3,F4,F5,F6],{F1≥0, F2≥0, F3≥0, F4≥0, F5≥0, F6≥0,
(sigma-F1/Atri)≥0, (sigma-F2/Abic)≥0, (sigma-F3/Abra)≥0, (sigma-F4/Abrd)≥0,
(sigma-F5/Aanc)≥0, (sigma-F6/Aprt)≥0, Mx==0, My==0,
Mz==0}},{F1,F2,F3,F4,F5,F6}, MaxIterations->maxits, Tolerance->tol,
Method->{"Automatic", "InitialPoints"->{{F1guess,F2guess,F3guess,F4guess,
F5guess, F6guess}}}];

Print[output1];

checkerror=Check[NMinimize[SAME AS ABOVE], "failed"];
checkerror2=Check[NMinimize[SAME AS ABOVE],"failed2",
NMinimize::outofregineq, NMinimize::outofregeq, NMinimize::nsol,
NMinimize::incst];

(* Check to see if NMinimize satisfied all constraints and produced a *)
(* valid result ... .. *)
If[ checkerror === "failed",
If[checkerror2 === "failed2",
(* If NMinimize failed to satisfy constraints: *)
Print["Failed."];
```

```
                (*Print all results to an array*)
                Residual = output1[[1]];
                F1 = output1[[2, 1, 2]];
                F2 = output1[[2, 2, 2]];
                F3 = output1[[2, 3, 2]];
                F4 = output1[[2, 4, 2]];
                F5 = output1[[2, 5, 2]];
                F6 = output1[[2, 6, 2]];
                y = j;
(*Find the joint contact force components using the force static*)
(*equilibrium equation, previously defined as SumF.*)
                output2 = Solve[{SumF == {0, 0, 0}}, {Jx, Jy, Jz}];
                Jx = output2[[1, 1, 2]];
                Jy = output2[[1, 2, 2]];
                Jz = output2[[1, 3, 2]];
                Array[results, 17];
                results[1] = NeuProSup;
                results[2] = position;
                results[3] = Mapp[[1]];
                results[4] = Mapp[[2]];
                results[5] = Mapp[[3]];
                results[6] = "failed";
                results[7] = y;(*location of new origin y coordinate*)
                results[8] = Residual;
                results[9] = F1;
                results[10] = F2;
                results[11] = F3;
                results[12] = F4;
                results[13] = F5;
                results[14] = F6;
                results[15] = Jx;
                results[16] = Jy;
                results[17] = Jz;,
(*If NMinimize produced an error that was not constraint-related:*)
                Print["Maybe."];
(*Print all results to an array*)
                Residual = output1[[1]];
                F1 = output1[[2, 1, 2]];
                F2 = output1[[2, 2, 2]];
                F3 = output1[[2, 3, 2]];
                F4 = output1[[2, 4, 2]];
                F5 = output1[[2, 5, 2]];
                F6 = output1[[2, 6, 2]];
                y = j;
(*Find the joint contact force components using the force static*)
(*equilibrium equation, previously defined as SumF.*)
                output2 = Solve[{SumF == {0, 0, 0}}, {Jx, Jy, Jz}];
                Jx = output2[[1, 1, 2]];
                Jy = output2[[1, 2, 2]];
                Jz = output2[[1, 3, 2]];
(*Print all results to an array*)
                Array[results, 17];
                results[1] = NeuProSup;
                results[2] = position;
                results[3] = Mapp[[1]];
                results[4] = Mapp[[2]];
                results[5] = Mapp[[3]];
```

138

```
            results[6] = "maybe";
            results[7] = y;(*location of new origin y coordinate*)
            results[8] = Residual;
            results[9] = F1;
            results[10] = F2;
            results[11] = F3;
            results[12] = F4;
            results[13] = F5;
            results[14] = F6;
            results[15] = Jx;
            results[16] = Jy;
            results[17] = Jz;
(*Reset muscle force guesses and force variables*)
            F1guess = F1;
            F2guess = F2;
            F3guess = F3;
            F4guess = F4;
            F5guess = F5;
            F6guess = F6;
            ];,
(* If NMinimize Produced Valid Result: *)
        Print["Yes Yes Yes !"];
(*Print all results to an array*)
        Residual = output1[[1]];
        F1 = output1[[2, 1, 2]];
        F2 = output1[[2, 2, 2]];
        F3 = output1[[2, 3, 2]];
        F4 = output1[[2, 4, 2]];
        F5 = output1[[2, 5, 2]];
        F6 = output1[[2, 6, 2]];
        y = j;
(*Find the joint contact force components using the force static*)
(*equilibrium equation, previously defined as SumF.*)
        output2 = Solve[{SumF == {0, 0, 0}}, {Jx, Jy, Jz}];
        Jx = output2[[1, 1, 2]];
        Jy = output2[[1, 2, 2]];
        Jz = output2[[1, 3, 2]];
        (*Print all results to an array*)
        Array[results, 17];
        results[1] = NeuProSup;
        results[2] = position;
        results[3] = Mapp[[1]];
        results[4] = Mapp[[2]];
        results[5] = Mapp[[3]];
        results[6] = "converged";
        results[7] = y;(*location of new origin y coordinate*)
        results[8] = Residual;
        results[9] = F1;
        results[10] = F2;
        results[11] = F3;
        results[12] = F4;
        results[13] = F5;
        results[14] = F6;
        results[15] = Jx;
        results[16] = Jy;
        results[17] = Jz;
        (*Reset muscle force guesses and force variables*)
```

```
        F1guess = F1;
        F2guess = F2;
        F3guess = F3;
        F4guess = F4;
        F5guess = F5;
        F6guess = F6;
        ];

(*Write results array to a file (output.csv)*)
        myfile = OpenAppend["retest00m.csv"];
        Export[myfile,{{results[1],results[2],results[3],results[4],
        results[5],results[6],results[7],results[8],results[9],
        results[10],results[11],results[12],results[13],results[14],
        results[15],results[16],results[17]}, ""}, "List"];
        Close[myfile];

(*Reset variables*)
        Clear[F1, F2, F3, F4, F5, F6, Jx, Jy, Jz];
        ]; (*End of "j" For loop which looped through y coordinate *)
     ]; (*End of "k" For loop which looped through positions, Neu/Pro/Sup *)
   ]; (*End of "l" For loop which looped through various flexion angles *)
(*]; (*End of "m" loop that changes applied moment*)*)
Print["I am done."];
```

References

References

1. Amis, A.A., D. Dowson, and V. Wright, 1980. *Analysis of elbow forces due to high-speed forearm movements.* Journal of Biomechanics, 13(10): p. 825-831.

2. Amis, A.A., D. Dowson, and V. Wright, 1980. *Elbow joint force predictions for some strenuous isometric actions.* Journal of Biomechanics, 13(9): p. 765-775.

3. An, K.N., et al., 1984. *Determination of muscle and joint forces: A new technique to solve the indeterminate problem.* Journal of Biomechanical Engineering, 106(4): p. 364-367.

4. Andrews, J.G. and Y. Youm, 1979. *A biomechanical investigation of wrist kinematics.* Journal of Biomechanics, 12(1): p. 83-93.

5. An, K.N., et al., 1981. *Muscles across the elbow joint: A biomechanical analysis.* Journal of Biomechanics, 14(10): p. 659-669.

6. Arvikar, R.J. and A. Seireg, 1978. *Evaluation of upper extremity joint forces during exercise,* in *Advances in bioengineering,* ed. ASME, 71-73.

7. Barbenel, J.C., 1972. *The biomechanics of the temporomandibular joint: A theoretical study.* Journal of Biomechanics, 5(3): p. 251-256.

8. Brumbaugh, R.B., et al., 1982. *An in-vivo study of normal wrist kinematics.* Journal of Biomechanical Engineering, 104(3): p. 176-181.

9. Chadwick, E.K. and A.C. Nicol, 2000. *Elbow and wrist joint contact forces during occupational pick and place activities.* Journal of Biomechanics, 33(5): p. 591-600.

10. Crowninshield, R.D., et al., 1978. *A biomechanical investigation of the human hip.* Journal of Biomechanics, 11(1-2): p. 75-85.

11. Crowninshield, R.D., 1978. *Use of optimization techniques to predict muscle forces,* in *Advances in bioengineering,* ed. ASME.

12. Crowninshield, R.D. and R.A. Brand, 1981. *A physiologically based criterion of muscle force prediction in locomotion.* Journal of Biomechanics, 14(11): p. 793-801.

13. Forster, E., et al., 2004. *Extension of a state-of-the-art optimization criterion to predict co-contraction.* Journal of Biomechanics, 37(4): p. 577-581.

14. Freund, J. and E.P. Takala, 2001. *A dynamic model of the forearm including fatigue.* Journal of Biomechanics, 34(5): p. 597-605.

15. Glitsch, U. and W. Baumann, 1997. *The three-dimensional determination of internal loads in the lower extremity.* Journal of Biomechanics, 30(11-12): p. 1123-1131.

16. Happee, R. and F.C. van der Helm, 1995. *The control of shoulder muscles during goal directed movements, an inverse dynamic analysis.* Journal of Biomechanics, 28(10): p. 1179-1191.

17. Hardt, D.E., 1978. *Determining muscle forces in the leg during normal human walking - an application and evaluation of optimization methods.* Journal of Biomechanical Engineering, 100: p. 72-78.

18. Hatze, H., 1981. *A comprehensive model for human motion simulation and its application to the take-off phase of the long jump.* Journal of Biomechanics, 14(3): p. 135-142.

19. Herzog, W., 1996. *Force-sharing among synergistic muscles: Theoretical considerations and experimental approaches.* Exercise and Sport Sciences Reviews, 24: p. 173-202.

20. Kaufman, K.R., 1988. *A mathematical model of muscle and joint forces in the knee during isokinetic exercise.* Ph.D. Thesis. North Dakota State University.

21. Kaufman, K.R., et al., 1991. *Physiological prediction of muscle forces--ii. Application to isokinetic exercise.* Neuroscience, **40**(3): p. 793-804.

22. Kaufman, K.R., et al., 1991. *Dynamic joint forces during knee isokinetic exercise.* The American Journal of Sports Medicine, **19**(3): p. 305-316.

23. Kaufman, K.R., et al., 1991. *Physiological prediction of muscle forces--i. Theoretical formulation.* Neuroscience, **40**(3): p. 781-792.

24. Lemay, M.A. and P.E. Crago, 1996. *A dynamic model for simulating movements of the elbow, forearm, and wrist.* Journal of Biomechanics, **29**(10): p. 1319-1330.

25. Li, G., et al., 1998. *Prediction of muscle recruitment and its effect on joint reaction forces during knee exercises.* Annals of Biomedical Engineering, **26**(4): p. 725-733.

26. Li, G., et al., 1999. *Prediction of antagonistic muscle forces using inverse dynamic optimization during flexion/extension of the knee.* Journal of Biomechanical Engineering, **121**(3): p. 316-322.

27. Nussbaum, M.A., D.B. Chaffin, and C.J. Rechtien, 1995. *Muscle lines-of-action affect predicted forces in optimization-based spine muscle modeling.* Journal of Biomechanics, **28**(4): p. 401-409.

28. Oizumi, N., et. al., 2003. *Numerical analysis of cooperative abduction muscle force in a human glenohumeral joint.* in *Summer Bioengineering Conference*. Key Biscayne, Florida.

29. Patriarco, A.G., et al., 1981. *An evaluation of the approaches of optimization models in the prediction of muscle forces during human gait.* Journal of Biomechanics, **14**: p. 513-525.

30. Pedotti, A., V.V. Krishnan, and L. Stark, 1978. *Optimization of the muscle force sequencing in human locomotion.* Mathematical Biosciences, **38**: p. 57-76.

31. Poppen, N.K. and P.S. Walker, 1978. *Forces at the glenohumeral joint in abduction.* Clinical Orthopaedics and Related Research, (135): p. 165-170.

32. Raikova, R., 1996. *A model of the flexion-extension motion in the elbow joint some problems concerning muscle forces modeling and computation.* Journal of Biomechanics, **29**(6): p. 763-772.

33. Raikova, R.T. and B.I. Prilutsky, 2001. *Sensitivity of predicted muscle forces to parameters of the optimization-based human leg model revealed by analytical and numerical analyses.* Journal of Biomechanics, **34**(10): p. 1243-1255.

34. Reuleaux, F., 1963. *Kinematics of machinery: Outlines of a theory of machines*, ed. A.B. Kennedy. Dover, New York. pp. 56-80.

35. Seireg, A. and R.J. Arvikar, 1973. *A mathematical model for evaluation of forces in lower extremities of the musculoskeletal system.* Journal of Biomechanics, **6**(3): p. 313-326.

36. Seireg, A. and R.J. Arvikar, 1975. *The prediction of muscular load bearing and joint forces in the lower extremities during walking.* Journal of Biomechanics, **8**(2): p. 89-102.

37. Tsirakos, D., V. Baltzopoulos, and R. Bartlett, 1997. *Inverse optimization: Functional and physiological considerations related to the force-sharing problem.* Critical Reviews in Biomedical Engineering, **25**(4-5): p. 371-407.

38. Veeger, H.E., et al., 1997. *Parameters for modeling the upper extremity.* Journal of Biomechanics, **30**(6): p. 647-652.

39. Wuelker, N., et al., 1995. *A dynamic shoulder model: Reliability testing and muscle force study.* Journal of Biomechanics, **28**(5): p. 489-499.

40. Yoshihuku, Y. and W. Herzog, 1990. *Optimal design parameters of the bicycle-rider system for maximal muscle power output.* Journal of Biomechanics, **23**(10): p. 1069-1079.

41. Youm, Y. and Y.S. Yoon, 1979. *Analytical development in investigation of wrist kinematics.* Journal of Biomechanics, **12**(8): p. 613-621.

42. London, J.T., 1981. *Kinematics of the elbow.* Journal of Bone and Joint Surgery [Am], **63**(4): p. 529-535.

43. Collins, J.J., 1995. *The redundant nature of locomotor optimization laws.* Journal of Biomechanics, **28**(3): p. 251-267.

44. Yeo, B.P., 1976. *Investigations concerning the principle of minimal total muscular force.* Journal of Biomechanics, **9**(6): p. 413-416.

45. An, K.N., K.R. Kaufman, and E.Y. Chao, 1989. *Physiological considerations of muscle force through the elbow joint.* Journal of Biomechanics, **22**(11-12): p. 1249-1256.

46. Bedford, A. and W. Fowler, 1995. *Engineering mechanics: Dynamics.* Addison-Wesley, Reading.

47. Weber, W.E. and E.F.W. Weber, 1836. *Ueber die mechanik der menschlichen gehwerkzeuge.* J. Springer, Berlin.

48. Saunders, J.B., V.T. Inman, and H.D. Eberhart, 1953. *The major determinants in normal and pathological gait.* Journal of Bone and Joint Surgery [Am], **35-A**(3): p. 543-558.

49. MacConnaill, M.A., 1967. *The ergonomic aspects of articular mechanics.* Studies of the anatomy and function of bones and joints, ed. F.G. Evans. Springer, Berlin.

50. Happee, R., 1994. *Inverse dynamic optimization including muscular dynamics, a new simulation method applied to goal directed movements.* Journal of Biomechanics, **27**(7): p. 953-960.

51. Hardt, D.E., 1978. *A minimum energy solution for muscle force control during walking.* Ph.D. dissertation Thesis. Massachusetts Institute of Technology, Cambridge, MA. p.

52. Basmajian, J.V. and A. Latif, 1957. *Integrated actions and functions of the chief flexors of the elbow: A detailed electromyographic analysis.* Journal of Bone and Joint Surgery [Am], **39-A**(5): p. 1106-1118.

53. Bean, J.C., D.B. Chaffin, and A.B. Schultz, 1988. *Biomechanical model calculation of muscle contraction forces: A double linear programming method.* Journal of Biomechanics, **21**(1): p. 59-66.

54. Gracovetsky, S., H.F. Farfan, and C. Lamy, 1977. *A mathematical model of the lumbar spine using an optimized system to control muscles and ligaments.* The Orthopedic Clinics of North America, **8**(1): p. 135-153.

55. Grosse-Lordemann, H. and E. Muller, 1937. *Der einfluss der leistung und der arbeitsgeschwindigkeit auf das arbeitsmaximum und den wirkungsgrad beim radfahren.* Arbeitsphysiologie, **9**: p. 454-475.

56. Epstein, M. and W. Herzog, 1998. *Theoretical models of skeletal muscle.* John Wiley & Sons, Chichester.

57. Hill, A.V., 1953. *The mechanics of active muscle.* Proceedings of the Royal Society of London. Series B. Biological sciences., **141**(902): p. 104-117.

58. Morrison, J., 1967. *The forces transmitted by the human knee joint during activity.* Ph.D. dissertation Thesis. University of Strathclyde, U.K. p.

59.   Paul, J.P., 1965. *Bioengineering studies of forces transmitted by joints (ii)*, in *Engineering analysis in biomechanics and related bio-engineering topics*, ed. R.M. Kenedi. Pergamon Press, Oxford. p. 369-380.

60.   Herzog, W., 1987. *Individual muscle force estimations using a non-linear optimal design.* Journal of Neuroscience Methods, **21**(2-4): p. 167-179.

61.   Bartel, D.L., D.T. Davy, and T.M. Keaveny, 2001. *Mechanics and design in musculoskeletal systems*, in *Course reading material for me c176 (uc berkeley, fall 2001)*, ed. T.M. Keaveny. Copy Central, Berkeley. p.

62.   Johnson, J.A., et al., 2000. *Simulation of elbow and forearm motion in vitro using a load controlled testing apparatus.* Journal of Biomechanics, **33**(5): p. 635-639.

63.   Dunning, C.E., et al., 2001. *Simulated active control produces repeatable motion pathways of the elbow in an in vitro testing system.* Journal of Biomechanics, **34**(8): p. 1039-1048.

64.   Nicol, A.C., 1977. *Elbow joint prosthesis design: Biomechanical aspects.* Ph.D. Thesis. University of Strathclyde, Glasgow. p.

65.   Simpson, D., 1975. *An examination of the design of an endoprosthesis for the elbow.* M.Sc. Thesis. University of Strathclyde, Glasgow. p.

66.   Debski, R.E., et al., 1995. *A new dynamic testing apparatus to study glenohumeral joint motion.* Journal of Biomechanics, **28**(7): p. 869-874.

67.   Bernstein, A.D., et al., 2000. *Elbow joint biomechanics: Basic science and clinical applications.* Orthopedics, **23**(12): p. 1293-1301.

68.   Maurel, W., 1996. *Anatomical analysis of the human upper limb.* Electronic Source. LIG/DI/EPFL Charm Project.

69.   Gray, H., ed. 1918. *Anatomy of the human body.* 20 ed., ed. W.H. Lewis. Lea & Febiger, Philadelphia.

70.   Morrey, B.F. and E.Y. Chao, 1976. *Passive motion of the elbow joint.* Journal of Bone and Joint Surgery [Am], **58**(4): p. 501-508.

71.   Bottlang, M., et al., 2000. *Assessment of elbow joint kinematics in passive motion by electromagnetic motion tracking.* Journal of Orthopaedic Research, **18**(2): p. 195-202.

72.   Murray, W.M., T.S. Buchanan, and S.L. Delp, 2002. *Scaling of peak moment arms of elbow muscles with upper extremity bone dimensions.* Journal of Biomechanics, **35**(1): p. 19-26.

73.   Fick, R., 1910. *Handbuch der anatomie des menschen.* Vol. 2. Gustav Fischer, Stuttgart.

74.   Brand, P.W., R.B. Beach, and D.E. Thompson, 1981. *Relative tension and potential excursion of muscles in the forearm and hand.* The Journal of Hand Surgery, **6**(3): p. 209-219.

75.   Chao, E.Y. and K.N. An, 1978. *Graphical interpretation of the solution to the redundant problem in biomechanics.* Journal of Biomechanical Engineering, **100**: p. 159-167.

76.   Gans, C. and W. Bock, 1965. *The functional significance of muscle architecture - a theoretical analysis*, in *Ergebnisse der anatomie und entwicklungsgeschichte*, ed. Springer, Berlin. p. 115-142.

77.   Haxton, H., 1944. *Absolute muscle force in ankle flexors of man.* Journal of Physiology, **103**: p. 267.

78.   Ikai, M. and T. Fukunaga, 1968. *Calculation of muscle strength per unit cross-sectional area of human muscle by means of ultrasonic measurements.* Internationale Zeitschrift fur angewandte Physiologie, einschliesslich Arbeitsphysiologie, **26**: p. 26-32.

79. Inman, V.T. and H.J. Ralston, 1968. *Human limbs and their substitutes*, ed. P.E. Klopsteg and P.D. Wilson. McGraw-Hill, New York. 296-317.

80. Morris, C.B., 1948. *The measurements of the strength of muscle relative to the cross-section*. Current Topics in Radiation Research Quarterly, **19**: p. 295-303.

81. Yamada, H., 1970. *Strength of biological materials*, ed. Williams & Wilkins, Baltimore, MD. p. 93-97.

82. van den Bogert, A.J., K.G. Gerritsen, and G.K. Cole, 1998. *Human muscle modeling from a user's perspective*. Journal of Electromyography and Kinesiology, **8**(2): p. 119-124.

83. Wolfram, S., 2003. *Mathematica software documentation*. Wolfram Research, Inc., Champaign (IL).

84. Press, W.H., et al., 1992. *Numerical recipes in fortran*. Second ed. Cambridge University Press, New York.

85. Nelder, J.A. and R. Mead, 1965. *A simplex method for function minimization*. Computer Journal, **7**(4): p. 308-312.

86. Price, K. and R. Storn, 1997. *Differential evolution*. Dr. Dobb's Journal, **264**(April): p. 18-24, 78.

87. Pigeon, P., L. Yahia, and A.G. Feldman, 1996. *Moment arms and lengths of human upper limb muscles as functions of joint angles*. Journal of Biomechanics, **29**(10): p. 1365-1370.

88. Winters, J.M. and D.G. Kleweno, 1993. *Effect of initial upper-limb alignment on muscle contributions to isometric strength curves*. Journal of Biomechanics, **26**(2): p. 143-153.

89. Nigg, B.M. and W. Herzog, eds, 1999. *Biomechanics of the musculo-skeletal system*. Second ed. John Wiley & Sons, Chichester.

90. Deland, J.T., A. Garg, and P.S. Walker, 1987. *Biomechanical basis for elbow hinge-distractor design*. Clinical Orthopaedics and Related Research, **215**: p. 303-312.

91. Fischer, O., 1911. *Handbuch der anatomie und mechanik der gelenke, unter berucksichtigung der bewegenden muskeln*. Vol. 2. Verlag Gustav Fischer, Jena, Germany.

92. Ewald, F.C., 1975. *Total elbow replacement*. The Orthopedic Clinics of North America, **6**(3): p. 685-696.

93. Ishizuki, M., 1979. *Functional anatomy of the elbow joint and three-dimensional quantitative motion analysis of the elbow joint*. Nippon Seikeigeka Gakkai Zasshi, **53**(8): p. 989-996.

94. Li, G., et al., 2004. *Kinematics of the knee at high flexion angles: An in vitro investigation*. Journal of Orthopaedic Research, **22**(1): p. 90-95.

95. Li, G., T.H. Wuerz, and L.E. DeFrate, 2004. *Feasibility of using orthogonal fluoroscopic images to measure in vivo joint kinematics*. Journal of Biomechanical Engineering, **126**(2): p. 313-318.

96. Meriam, J.L. and L.G. Kraige, 1997. *Engineering mechanics: Dynamics*. Fourth Edition ed. Vol. 2. John Wiley & Sons, Inc., New York.